August 2018

Spatial and Temporal Variation of Phytoplankton Production in Lake Michigan

Katelyn Alexis Bockwoldt
University of Wisconsin-Milwaukee

SPATIAL AND TEMPORAL VARIATION OF PHYTOPLANKTON PRODUCTION IN LAKE MICHIGAN

by

Katelyn A. Bockwoldt

A Thesis Submitted in

Partial Fulfillment of the

Requirements for the Degree of

Master of Science

in Freshwater Sciences and Technology

at

The University of Wisconsin-Milwaukee

August 2018

ABSTRACT

SPATIAL AND TEMPORAL VARIATION OF
PHYTOPLANKTON PRODUCTION IN LAKE MICHIGAN

by

Katelyn A. Bockwoldt

The University of Wisconsin-Milwaukee, 2018
Under the Supervision of Professor Harvey A. Bootsma

Although many studies have documented decreases in phytoplankton production since the quagga mussel invasion, we currently have a limited understanding of the spatial variation and temporal dynamics of phytoplankton production in Lake Michigan. In this study, phytoplankton production and seston stoichiometry were measured bi-weekly near Milwaukee, three times at two northern basin sites, and along three nearshore-offshore transects from May to November 2017, as well as at 5-6 sites on three whole-lake surveys in 2016 and 2017. Estimates of growth rates were calculated from phytoplankton production and carbon measurements. In spring 2016 and 2017, growth estimates were similar across the lake and no single factor appeared to control production perhaps because temperature, light, and nutrients were all limiting. In summer 2017, production, biomass, and growth estimates all increased from south to north following the trend in decreasing nutrient limitation. Nearshore production was generally greater than offshore production, but nearshore-offshore patterns were highly dependent on upwelling. Temporally, areal production peaked in August and September with the warmest temperatures, and temperature was the only variable significantly related to production and growth estimates. Mean summer production in 2017 (473 mg C m^{-2} day^{-1}) was lower than the mean summer production from prior to the mussel

invasion in 1983 to 1987 (867 mg C m^{-2} day^{-1}; Fahnenstiel et al., 2010). Deep chlorophyll layer (DCL) production also decreased from 30% of total water column production in the 1980s (Fahnenstiel et al., 1987a) to 17.3% of measured total water column production in 2017. Phosphorus limitation, light harvesting capabilities, light saturated maximum photosynthetic rates, and growth estimates of DCL and epilimnetic phytoplankton have not changed since the mussel invasion despite decreasing total phosphorus concentrations, suggesting the decrease in phytoplankton production in Lake Michigan is due primarily to grazing by mussels rather than increased nutrient limitation.

TABLE OF CONTENTS

LIST OF FIGURES

LIST OF TABLES

ACKNOWLEDGEMENTS

I am incredibly grateful for my advisor, Dr. Harvey Bootsma, who provided me with this research opportunity and served as a wonderful mentor for the past two years. Without his expertise and encouragement, this research would not have been possible. I would also like to thank Dr. Erica Young and Dr. Laodong Guo for serving on my committee and providing thoughtful feedback on my research. I owe many thanks to all of the students and technicians in the Bootsma Lab, especially Will Stacy and Jeff Houghton, for their help in the lab and field. Randy Metzger and Gerald Becker from the SFS instrument shop were also "instrumental" during field season when I needed equipment fixed at the last minute. I am also grateful for the time of Pat Anderson, who was always ready to fix the isotope ratio mass spectrometer whenever I would have issues running samples. This research was funded by Wisconsin Sea Grant, and I am thankful for conference and scholarship funding from Wisconsin Sea Grant, University of Wisconsin-Milwaukee, Great Lakes Cruising Club, and BRP/Evinrude.

Chapter 1: Introduction and Background

The Lake Michigan ecosystem has endured a long history of environmental stressors, the most problematic of which have been cultural eutrophication and invasive species. In the mid-twentieth century, high phosphorus concentrations and algal blooms in Lakes Michigan, Huron, Erie, and Ontario caused significant water quality concerns. In response, the Great Lakes Water Quality Agreement (GLWQA) was passed in 1972 to reduce phosphorus loading and improve water quality in the Great Lakes. The efforts of the GLWQA in Lake Michigan have been successful, as total phosphorus (TP) loading has been significantly reduced in the last several decades and is currently well below the loading target (Dolan and Chapra, 2012). Phosphorus concentrations in Green Bay, however, remain high and the Bay experiences seasonal hypoxia (Klump et al., in press), so several phosphorus reduction programs are currently in effect in the Green Bay watershed. Offshore TP concentrations in Lake Michigan are currently less than 3 μg/L (Barbiero et al., 2018), which is well below the 7 μg/L spring TP target established by the GLWQA (Pauer et al., 2011). Even though TP loading to the northern and southern basins of Lake Michigan has not been decreasing since 1994 (Dolan and Chapra, 2012), offshore TP concentrations continue to decrease due to the influence of invasive species, and now low offshore productivity is a great concern for the Lake Michigan ecosystem.

Invasive species have had profound effects in Lake Michigan. Over 180 species have invaded the Great Lakes since the 1800s and 76 of these are found in Lake Michigan (Cuhel and Aguilar, 2013). Arguably, the most disruptive invasive species to the Lake Michigan food web has been the quagga mussel (*Dreissena rostriformis bugenis*). Quagga mussels were first noted in Lake Michigan in 1997 and, by 2010, had colonized nearly every nearshore and offshore habitat (Nalepa et al., 2014). Quagga mussels are prolific filter feeders, and mussel filtering has changed physical,

chemical, and biological processes in Lake Michigan (Cuhel and Aguilar, 2013; Madenjian et al., 2015). The inability to control this invasive species has greatly affected the lower food web of Lake Michigan (Bunnell et al., 2018), which has raised concerns about the sustainability of the lake's important commercial and recreational fisheries.

Physically, quagga mussels have increased water clarity, light penetration, and euphotic zone depth (Barbiero et al., 2012; Binding et al., 2015; Yousef et al., 2017) by their efficient removal of phytoplankton from the water column (Vanderploeg et al., 2010). Increased euphotic zone depth increases the area in which phytoplankton can photosynthesize, but also decreases the area in which zooplankton and preyfish can hide from their predators. Benthic algae, such as *Cladophora*, have benefited from increased light availability because more light is reaching the bottom of the lake in the nearshore zone (Auer et al., 2010; Bootsma et al., 2015). *Cladophora*, however, has become a nuisance alga in the Great Lakes because sloughed *Cladophora* can foul shorelines and clog water intake pipes. Quagga mussels have also physically altered the bottom of the lake, as their shells have increased the surface area for benthic invertebrate habitat and benthic algal attachment.

Chemically, quagga mussels have greatly affected phosphorus cycling. Dreissenid filtering clears a large proportion of particulate material from the water column (Vanderploeg et al., 2010), and the material is either invested in new biomass, excreted as dissolved soluble reactive phosphorus, or released as feces or pseudofeces, which is particulate phosphorus (Hecky et al., 2004; Mosley and Bootsma, 2015). As mussel filtering has the greatest effect in regions less than 50 m (Rowe et al., 2015), much of this phosphorus gets trapped in benthos close to shore and is no longer efficiently transported offshore, creating a "nearshore phosphorus shunt" (Hecky et al., 2004). Dreissenids, therefore, are hypothesized to have resulted in the oligotrophication of Lake

Michigan and the lower offshore TP concentrations than would be expected due to current phosphorus loading (Chapra and Dolan, 2012). Even though mussels have affected phosphorus transport to offshore regions, ecological modeling suggests the impact of nutrients excreted by dreissenids on phytoplankton in the nearshore zone may exceed the impact of nearshore dreissenid grazing, so mussels may be important "algal fertilizers" in shallow regions and during periods of isothermal mixing when nutrients excreted by mussels can be mixed throughout the water column (Zhang et al., 2011).

Due to both reductions in offshore TP and mussel filtering, phytoplankton production has decreased over the last several decades (Fahnenstiel et al., 2010, 2016; Warner and Lesht, 2015). Between 1983 to 1987 and 2007 to 2008, daily integral phytoplankton production decreased 78% and 22% during the spring isothermal mixing and mid-stratification periods, respectively, but there was no difference in daily integral production during the late stratification period (Fahnenstiel et al., 2010). Other studies have also illustrated decreases in both spring and summer productivity, although the range of production estimates and magnitude of declines over time among studies varies (Fahnenstiel et al., 2016; Pothoven and Fahnenstiel, 2013; Warner and Lesht, 2015; Yousef et al., 2014). Differences in production declines among thermal periods are due to mussel access to the water column: during isothermal mixing, mussels have access to material in the entire water column; in the summer, mussels only have access to material that is recycled within the hypolimnion or that has settled or mixed down from upper thermal layers. Therefore, mussels have had a larger impact on spring production than any other thermal period.

Phytoplankton biomass and chlorophyll have also been declining since the 1980s. Chlorophyll has decreased across all depth regions of the lake since the mussel invasion (Fahnenstiel et al., 2010; Yousef et al., 2014), but chlorophyll closer to shore decreased faster from 1998 to 2010 than

offshore chlorophyll due to higher mussel densities less than 90 m (Nalepa et al., 2014; Yousef et al., 2014). Mussels have also resulted in a decrease in the magnitude of the summer deep chlorophyll layer (DCL), which is defined as the sub-epilimnetic region where chlorophyll concentrations exceed 2 mg m^{-3} (Fahnenstiel and Scavia, 1987b; Pothoven and Fahnenstiel, 2013). Historically, production within the DCL accounted for an average of 30% of total water column during the summer (Fahnenstiel and Scavia, 1987a). In some cases, the DCL accounted for up to 74% of total water column production. From 1995-2000 to 2007-2011, there was a 92% decrease in integrated DCL chlorophyll and a 56% decrease in the deep chlorophyll maximum (DCM) concentration, despite increases in water clarity (Pothoven and Fahnenstiel, 2013). Summer DCL size is strongly related to spring chlorophyll *a* concentrations (size of the spring bloom), so quagga mussel grazing on spring phytoplankton also has indirect effects on summer DCLs and summer production (Pothoven and Fahnenstiel, 2013).

Mussels have also affected phytoplankton community structure. Fahnenstiel et al. (2010) found that diatom abundance during the spring isothermal mixing period decreased from 29 mg C/m^3 in 1983-1987 to 1.6 mg C/m^3 in 2007-2008. Cryptophyceae, Chrysophyceae, and small flagellates also exhibited significantly lower spring abundance in 2007-2008, but a decrease was not observed for cyanobacteria and chlorophytes. Due to the decreases in other taxa, the relative abundance of cyanobacteria in the community has increased from 2% to 27%. During the mid-stratification period, cyanobacteria abundance increased from 2.9 mg C/m^3 to 6.1 mg C/m^3 from 1983-1987 to 2007-2008. The responses of each phytoplankton group in the summer were more variable and often did not respond in the same manner as spring isothermal mixing. Reavie et al. (2014) found similar changes in phytoplankton community composition from 2001-2011: spring diatom biovolume (μm^3/ml) significantly decreased in both the northern and southern basins of Lake

Michigan. During the summer, variable responses were observed, as in Fahnenstiel et al. (2010). The large decrease in diatom abundance is hypothesized to be the result of selective mussel filtering (Vanderploeg et al., 2001). Dreissenid mussels prefer to consume nutritious diatoms and microzooplankton over less nutritious phytoplankton groups, such as cyanobacteria (Nalepa and Schloesser, 2014). As a result, the phytoplankton community in Lake Michigan has shifted away from diatoms and towards cyanobacteria.

The observed change in phytoplankton community composition is closely related to phytoplankton size. Diatoms and dinoflagellates are the largest phytoplankton, classified as microplankton (> 20 μm; Wetzel, 2001). Nanoplankton (2-20 μm) often include chrysophytes, cryptophytes, and haptophytes, while picoplankton (< 2 μm) typically include small cyanobacteria and eukaryotes (Carrick et al., 2015). Engevold et al. (2015) found a significant decrease in chlorophyll *a* for the > 53 μm and 10-53 μm size fractions of phytoplankton from 1988-1992 to 2007-2009 in southwestern Lake Michigan. The smallest size fraction (< 10 μm) of chlorophyll *a* did not change over the study period. Carrick et al. (2015) illustrated a decline in picoplankton and microplankton abundances in southern Lake Michigan from 1987 to 2012, but a two-fold increase in the percent contribution of picoplankton to the community. Considering these size patterns and changes in community composition, there has been a shift from microplankton to picoplankton in Lake Michigan.

Reduced phytoplankton production and altered phytoplankton community composition have implications for higher trophic levels due to bottom-up control (Menge, 2000). Reduced phytoplankton production and biomass equates to fewer food resources for zooplankton, which can limit zooplankton growth, biomass, and reproduction (Wetzel, 2001). Size shifts in the phytoplankton community may also affect trophic efficiency because picoplankton are generally

more difficult to graze and less nutritious for zooplankton than larger phytoplankton (Wetzel, 2001; Lampert, 1987). Total offshore zooplankton abundance has declined significantly in the last several decades as phytoplankton production has declined, and the greatest decreases have occurred in cyclopoids and herbivorous cladocerans (Engevold et al., 2015; Vanderploeg et al., 2012). These changes, however, may not only be due to resource limitation but also due to increased direct predation by predatory cladocerans (Vanderploeg et al., 2012). Since the 1990s, total prey fish biomass in Lake Michigan has also declined, but these changes are also likely due to both top-down and bottom-up causes (Bunnell et al., 2014; Madenjian et al., 2015). Although the mechanisms behind food web changes in Lake Michigan are not always clear, the apparent relationship between declining primary production and declining zooplankton and preyfish abundance has raised concerns about the sustainability of Lake Michigan's salmonid fisheries.

Due to the potential bottom-up effects of reduced primary production on fisheries production, a thorough understanding of phytoplankton production in Lake Michigan is needed. An accurate understanding of the spatial and temporal variability of phytoplankton production is important because it represents the spatial and temporal distribution of food resources available for higher trophic levels, which is necessary for lake managers to understand in order to effectively manage the changing Lake Michigan ecosystem. Although many studies have documented decreases in phytoplankton production since the quagga mussel invasion, we have a limited understanding of the current spatial variation and temporal dynamics of phytoplankton production in Lake Michigan.

Our current understanding of the spatial variability of phytoplankton production in Lake Michigan comes from remote sensing (Fahnenstiel et al., 2016). Although remote sensing can provide high spatial and temporal resolution, it has many limitations estimating primary production

from surface chlorophyll (Lee et al., 2015), so remote sensing-based production estimates may not always be accurate and require frequent validation with direct measurements of production. Temporally, our understanding of phytoplankton production in Lake Michigan comes from an in-depth series of studies from the 1980s (Fahnenstiel et al., 1989; Fahnenstiel and Carrick, 1988; Fahnenstiel and Scavia, 1987; Scavia et al., 1988; Scavia and Fahnenstiel, 1987). These studies determined the many factors controlling phytoplankton dynamics, including temporal variation in growth rates, nutrient supply, zooplankton grazing, and algal sedimentation, but the Lake Michigan ecosystem has undergone many physical, chemical, and biological changes since the 1980s, and there have been few detailed studies of changes to temporal dynamics of phytoplankton production.

The objective of this study was to investigate the current spatial and temporal variability of phytoplankton production in Lake Michigan. Spatially, I was most interested in comparing northern versus southern basin production and nearshore versus offshore production, as these regions are physically, chemically, and biologically distinct (Barbiero et al., 2012; Cai and Reavie, 2018; Warren et al., 2017; Yurista et al., 2015). I directly measured phytoplankton production and seston stoichiometry at 5-6 sites on three whole-lake surveys in 2016 and 2017, at three sites on three nearshore-offshore transects in southwestern Lake Michigan in 2017, and at three 75 m sites from different regions of the lake in 2017. Spatial variation is discussed in Chapter 2. Temporally, I was most interested in determining the vertical distribution of production throughout the year and which environmental factors have the greatest influence on temporal phytoplankton dynamics. I directly measured production and seston stoichiometry approximately bi-weekly from May to November 2017 at one 75 m site in southwestern Lake Michigan, and also measured several environmental variables in order to determine the main drivers of phytoplankton dynamics in Lake

Michigan. Temporal variation is discussed in Chapter 3. Chapter 4 of this thesis serves as a summation of the previous chapters and provides suggestions for future research.

Chapter 2: Spatial variation of phytoplankton production in Lake Michigan

Introduction

In Lake Michigan, reductions in external phosphorus loading and invasive quagga mussel (*Dreissena rostriformis bugensis*) filtering have increased water clarity (Binding et al., 2015; Yousef et al., 2017), altered phosphorus cycling (Chapra and Dolan, 2012; Hecky et al., 2004; Lin and Guo, 2016), and reduced phytoplankton biomass and production (Fahnenstiel et al., 2010). Although many studies have documented recent decreases in production (Fahnenstiel et al., 2010, 2016; Pothoven and Fahnenstiel, 2013; Warner and Lesht, 2015), we currently have a limited understanding of the spatial variability of phytoplankton production in Lake Michigan. As phytoplankton dynamics are controlled by biogeochemical conditions (Scavia and Fahnenstiel, 1987) and the lake is physically and biologically heterogeneous (Cai and Reavie, 2018; Rao and Schwab, 2007), spatial variation in production may reveal the mechanisms controlling production in Lake Michigan, which may have changed since the last assessments of phytoplankton dynamics (Cuhel and Aguilar, 2003; Scavia and Fahnenstiel, 1987) due to recent changes in ecosystem structure (Madenjian et al., 2015). Understanding the distribution of primary production is also important because it reflects the distribution of resources available for higher trophic levels, which is of increasing interest because reductions in offshore primary productivity correlate with reductions in prey fish abundance (Bunnell et al., 2014), raising concerns about the sustainability of Lake Michigan's commercially and recreationally important salmonid fisheries.

Our current understanding of the spatial variability of phytoplankton production in Lake Michigan is from remote sensing production estimates and not direct production measurements (Fahnenstiel et al., 2016). Fahnenstiel et al. (2010) directly measured phytoplankton production in 2007 and 2008, but their study was limited to two 100 m offshore stations in the southeastern

region of the lake. Fahnenstiel et al. (2016) used remote sensing to compare phytoplankton production and chlorophyll in the northern and southern basins and shallow (< 30 m), mid-depth (30-90 m), and deep (> 90 m) regions of Lake Michigan from 2010 to 2013. Fahnenstiel et al. (2016) found significantly higher chlorophyll in the northern basin than southern basin, but no differences in mean annual production between basins. They also found no significant differences in chlorophyll among depth zones, but significantly lower production in the shallow region compared to mid-depth and deep regions.

Although remote sensing can provide high spatial and temporal resolution, it has several limitations estimating phytoplankton production from surface chlorophyll (Lee et al., 2015). Bottom reflectance and complex optical properties nearshore make it difficult to accurately resolve nearshore parameters, and surface measurements cannot account for deep chlorophyll layer (DCL) production, which has historically been a large component of total water column production in Lake Michigan (Fahnenstiel and Scavia, 1987a). Due to these limitations, remote sensing-based production estimates require frequent validation with direct measurements of production, and any direct measurements of production along nearshore-offshore and south-north gradients will be a valuable contribution to our understanding of the spatial variation of phytoplankton production in Lake Michigan.

The northern and southern basins of Lake Michigan are physically, chemically, and biologically different (Cai and Reavie, 2017; Barbiero et al., 2012; Dolan and Chapra, 2012; Nalepa et al., 2014). The phytoplankton community composition of the northern and southern basins differs (Cai and Reavie, 2018; Reavie et al., 2014), which may be a reflection of differences in physical and chemical conditions. Depths in southern basin are shallower than depths in the northern basin basin, which causes warmer temperatures in the southern basin (Barbiero et al., 2002). Total

phosphorus loading to the northern basin of Lake Michigan is lower than the southern basin due to different watershed characteristics (Dolan and Chapra, 2012; Kult et al., 2014), but the northern basin has 12% higher total phosphorus and 47% higher chlorophyll concentrations than the southern basin (Cai and Reavie, 2018). Nitrate, total dissolved nitrogen, dissolved inorganic phosphorus, and dissolved organic carbon are also all higher in the northern basin near Green Bay in 2013 (Guo et al., unpub. data), suggesting there may be nutrient influence from Green Bay in the northern basin. Lower external phosphorus loading but higher in-lake phosphorus concentrations in the northern basin also suggests there may be greater internal nutrient recycling in the northern basin. As mussel filtering reduces phytoplankton biomass (Fahnenstiel et al., 2010) and decreases the residence time of phosphorus in the water column by sequestering phosphorus in the hypolimnion and benthos during stratification (Moseley and Bootsma, 2015), lower offshore mussel densities with greater depths in the northern basin (Nalepa et al., 2014) may reduce the effects of mussels on phytoplankton production in the north. Therefore, we may expect to observe differences in phytoplankton production between the northern and southern basins of Lake Michigan, but we currently have few direct comparisons of northern and southern basin production.

Phytoplankton production may also be expected to differ along nearshore-offshore gradients in Lake Michigan. The nearshore region of Lake Michigan is highly variable due to the influence of external nutrient loading, upwelling, sediment resuspension, and complex currents nearshore (Eadie et al., 2002; Plattner et al., 2006; Yurista et al., 2015). Fee (1973a) found nearshore production to be 62% higher than offshore production, while Schelske and Callender (1970) found nearshore production to be greater than offshore production by as much as 90%. Since the mussel invasion, however, nearshore-offshore dynamics have changed. Mussel densities differ among

depth zones and substratum (Nalepa et al., 2014), and mussel grazing has a greater effect on phytoplankton biomass and chlorophyll nearshore where mixing delivers more phytoplankton to the benthic boundary layer where mussels filter (Yousef et al., 2014; Zhang et al., 2011). Although mussel grazing has larger effects on phytoplankton biomass nearshore than offshore, mussels trap and recycle phosphorus in the nearshore zone (Hecky et al., 2004; Zhang et al., 2011), resulting in higher phosphorus concentrations nearshore than offshore (Bunnell et al., 2018; Marko et al., 2013; Yurista et al., 2015). Therefore, the effects of mussel nutrient excretion may be greater than the impacts of mussel grazing on nearshore phytoplankton (Zhang et al., 2011), and we may expect to observe differences in phytoplankton production in the nearshore and offshore regions of Lake Michigan, but we currently have few direct measurements of production along nearshore-offshore gradients.

To address the need for greater spatial resolution in direct phytoplankton production measurements, the objective of this study was to directly measure phytoplankton production along nearshore-offshore and south-north gradients in Lake Michigan. I directly measured phytoplankton production and seston stoichiometry and estimated growth rates at several sites in the northern and southern basins of Lake Michigan to investigate basin differences. I also measured production along three nearshore-offshore transects in southwestern Lake Michigan to investigate how production varies along nutrient and mussel impact gradients. Spatial comparisons incorporated a seasonal component, as spatial patterns were assessed during spring, summer, and fall. I hypothesized that northern basin production would be higher than southern basin production due to higher in-lake nutrient concentrations and chlorophyll in the northern basin and that nearshore production would be higher than offshore production due to higher nutrient concentrations nearshore.

Methods

Spatial sampling

All sampling for this study occurred in 2016 and 2017. The greatest spatial coverage was gained through three whole-lake surveys on the EPA's R/V Lake Guardian. To compare northern and southern basin production, five sites were sampled in March 2016, and six sites were sampled in March and August 2017 (Figure 2.1; Table 2.1). "MI" stations are representative of offshore water quality conditions in Lake Michigan (Barbiero et al., 2012; Cai and Reavie, 2018), and GB1 was added in 2017 to quantify production near the mouth of Green Bay.

To facilitate further comparisons of northern and southern basin production, three 75 m depth stations from different regions of the lake were sampled in 2017. AW75 (44.098, -87.718; Figure 2.1) near Milwaukee, Wisconsin was sampled approximately bi-weekly from May to November. Due to the average southward longshore current near Milwaukee (Rao and Schwab, 2007), AW75 is upstream of riverine influence and expected to be representative of offshore water quality conditions in southwestern Lake Michigan. DC75 (44.894, -87.052; Figure 2.1) was sampled twice in June 2017 and once in August 2017 to measure primary production at a potential production "hot spot" off Door county identified by remote sensing (B.M. Lesht, unpub. data). MT75 (45.084, -85.893; Figure 2.1) in northeastern Lake Michigan was sampled once in June, July, and October 2017. Northwestern Michigan is less agriculturally developed and urbanized than eastern Wisconsin and characterized by more forest cover (Kult et al., 2014), suggesting external nutrient loading, internal nutrient concentrations, and production may be lower in this region of the lake. Comparing MT75 and two western sites may also reveal whether production on the western shore is higher due to more frequent upwelling (Plattner et al., 2006; Yurista et al., 2015).

Nearshore-offshore transects near Milwaukee at AW15 (43.0958, -87.8611; Figure 2.1), AW45 (43.0980, -87.7840; Figure 2.1), and AW75 were sampled in July, September, and October 2017. 15 m and 45 m depth sites were chosen to match depths sampled in earlier Lake Michigan studies (Carrick et al., 2015; Pothoven and Fahnenstiel, 2015; Rowe et al., 2017). Warren et al. (2017) used remotely-sensed chlorophyll to define the Lake Michigan nearshore zone as 4.8 to 6.3 km wide (corresponding to depths of 12.9 m to 16 m), meaning AW15 is within the nearshore zone, while AW45 is close to the nearshore-offshore boundary, and AW75 is offshore. By Rao and Schwab (2007) definitions, AW15, AW45, and AW75 (1 km, 7 km, and 12 km from shore, respectively) are within the generalized nearshore zone, coastal boundary layer, and offshore zone, respectively. Therefore, the transect sites used in this study capture a range of physical conditions in Lake Michigan.

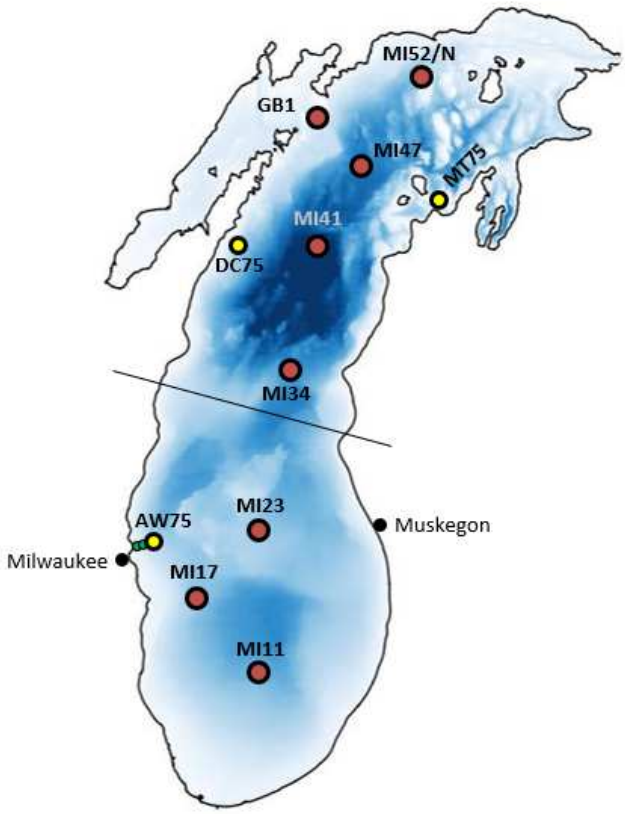

Figure 2.1. Map of sampling sites used in this study. Red points: Lake Guardian sites. Yellow points: 75 m site regional comparisons. Green points: 15 m and 45 m nearshore-offshore transect sites. Black line indicates the northern and southern basin distinction from Barbiero et al. (2012).

Table 2.1. Station sampling times and station bottom depths from whole-lake surveys. Bold indicates samples collected at night.

Spring 2016				Spring 2017				Summer 2017			
Site	Date	Time	Depth	Site	Date	Time	Depth	Site	Date	Time	Depth
MI17	Mar 26	11:56	100 m	MI11	Mar 26	**19:39**	128 m	MI11	Aug 2	17:55	128 m
MI23	Mar 27	**05:22**	88 m	MI23	Mar 27	**05:53**	88 m	MI23	Aug 3	13:38	88 m
MI34	Mar 27	12:21	160 m	MI34	Mar 27	13:05	160 m	MI34	Aug 5	19:12	160 m
MI47	Mar 28	14:52	186 m	MI41	Mar 28	**02:30**	250 m	MI41	Aug 6	08:07	250 m
MI-N	Mar 28	**20:33**	38 m	GB1	Mar 28	**19:48**	40 m	GB1	Aug 7	**01:03**	40 m
-	-	-	-	MI52	Mar 29	**03:00**	54 m	MI52	Aug 7	10:55	54 m

Field operations

At each site, a calibrated SeaBird CTD was used to determine vertical profiles of temperature, conductivity, chlorophyll *a* fluorescence, beam attenuation, beam transmission, pH, dissolved oxygen, and underwater photosynthetically active radiation (PAR). All data were binned into 0.5 m intervals and downcast data were used in analyses.

At 75 m depth and transect sites, discrete water samples from two depths were collected for photosynthesis experiments and nutrient analyses. Samples were collected between 08:00 and 11:00 using a Niskin bottle and stored in a dark cooler for no longer than three hours before photosynthesis experiments or filtering. 5 m was sampled on every occasion to represent the epilimnion (Carrick et al., 2015). When the water column was unstratified, 25 or 35 m was chosen as the second depth to characterize phytoplankton at mid-depth. From June to September, the depth at which the fluorescence maximum occurred was the second depth sampled. At AW75 on October 9, the second sample collected was from the base of the epilimnion. At AW75 on October 23, the second depth sampled was the dissolved oxygen percent saturation maximum to sample the metalimnetic oxygen peak.

At whole-lake survey sites, discrete water samples were collected using a Rosette sampler with 12 Niskin bottles. During the spring 2016 survey, 2 m and station mid-depth were sampled. During the spring 2017 survey, 2 m and 35 m samples were integrated into one sample for experiments because the water column was well mixed. During the summer 2017 survey, 5 m or mid-epilimnion and the DCL were sampled. Samples were collected during both day and night (Table 2.1) because the ship operates 24 hours per day, and experiments began immediately after sample collection.

Fluorescence Profile Corrections

Chlorophyll *a* fluorescence profiles were converted to chlorophyll *a* profiles by correcting for quenching (decrease in fluorescence yield at high light intensities due to photo-protective processes) and then to extracted chlorophyll *a*. As fluorescence quenching varies with light intensity, temperature, nutrient status, and phytoplankton community composition (Harrison and Smith, 2013; Muller et al., 2001), quenching was corrected using relationships between surface water chlorophyll *a* fluorescence and surface PAR measured continuously during day and night across physical and biological gradients on whole-lake surveys:

$$\text{CTD quench corrected fluor.} = \text{CTD measured fluor.} \bullet (a \bullet \text{UPAR}^2 + b \bullet \text{UPAR} + 1)$$

where *a* and *b* are survey-specific regression coefficients and UPAR refers to underwater PAR measured by CTD. This correction was derived in five steps: (1) natural log-transformed measured surface chlorophyll fluorescence was regressed against measured surface PAR to determine the relationship between fluorescence and irradiance, (2) the quadratic relationship from (1) was applied over the range of measured irradiance to determine the relationship between quenching and irradiance, (3) quenched fluorescence from (2) was divided by fluorescence at surface PAR = 0 where there is no quenching effect to create quenching correction factors over the range of measured irradiance, (4) quenching correction factors were regressed against surface PAR to determine the relationship between quenching corrections and irradiance, and *a* and *b* were determined as the coefficients of this quadratic relationship, (5) to determine quench corrected CTD fluorescence profiles, measured CTD fluorescence was multiplied by the relationship between quenching corrections and irradiance for each survey using underwater irradiance as measured by the CTD. Surface PAR data was only available at night and for two daylight hours in

spring 2017, so the spring 2016 equation (a = -5.0 x 10^{-7}, b = 0.0022) was used to correct spring 2017 CTD profiles. The summer 2017 correction equation (a = -1.0 x 10^{-7}, b = 0.0013) was used for all CTD profiles from May to November 2017.

After chlorophyll fluorescence profiles had been corrected for quenching, chlorophyll fluorescence was converted to chlorophyll *a* using linear relationships between extracted chlorophyll *a* and fluorescence from depths greater than 20 m where quenching was minimal. As quench- and extract-corrected profiles did not perfectly match extracted chlorophyll *a* on all sites and dates (extracted chlorophyll *a* = 0.90(quench- & extract-corrected chlorophyll) + 0.04; r^2 = 0.82), some regions of some profiles were manually corrected to extracted chlorophyll *a*. Manual corrections were performed by constraining certain regions of chlorophyll profiles to pass through extracted chlorophyll *a* points where necessary.

Nutrient analyses

Water from each depth sampled for photosynthesis experiments was filtered onto pre-combusted 0.7 µm Whatman GF/F filters for chlorophyll, particulate phosphorus (PP), particulate carbon (PC), and particulate nitrogen (PN) analyses. Filters were rinsed several times with deionized (DI) water. PC and PN samples were not rinsed with dilute HCl, as this may leach organic matter (Peterson, 1980). Chlorophyll filters were stored in a dark freezer until analysis. Chlorophyll was extracted using a 68% methanol, 27% acetone, and 5% DI water solution for 24 hours and fluorescence was measured on a calibrated fluorometer (Turner Designs 10-000 R). Filters for PP, PC, and PN analyses were stored in a desiccator at room temperature until analysis. PP samples were analyzed using the method of Stainton et al. (1977). PC and PN were measured

on an elemental analyzer (Costech Instruments ECS 4010 CHNSO Analyzer) using acetanilide as a standard.

Photosynthesis experiments

Phytoplankton photosynthesis was measured using the particulate ^{13}C tracer technique (Hama et al., 1983). The ^{13}C method produces results similar to the ^{14}C method (Hama et al., 1983; Steemann Nielsen, 1952), but the stable isotope is safer and easier to use. For each depth sampled, 5 L of unfiltered lake water was spiked with 80-90 mg of ^{13}C-labeled sodium bicarbonate ($NaH^{13}CO_3$) to produce 9-10% inorganic carbon enrichment. Spiked water was separated into one dark and 7 transparent 600 mL polycarbonate bottles, and bottles were incubated under a light gradient (0 to 1000 μmol photons m^{-2} s^{-1}) created using a series of mesh filters in a bench-top incubator. Light at each bottle position was measured using a quantum scalar radiometer (Biospherical Instruments). Bottles were incubated for a period of 4 hours, kept within 2 degrees of *in situ* temperature from sampling depth, and gently inverted at least once every 30 minutes to prevent phytoplankton from settling. After incubation, bottles were filtered on to 0.7 μm GF/F glass fiber filters and rinsed several times with DI water to remove inorganic carbon. Filters were dried in a desiccator at room temperature until further analysis.

Dissolved inorganic carbon (DIC) for each sample depth was calculated using measured CTD pH and relationships within the inorganic carbon system (Millero, 2007), assuming a constant average Lake Michigan alkalinity (2148 μeq L^{-1}; Cai and Reavie, 2018). Mean calculated DIC from all sites and depths sampled in this study was 2138.7 ± 39.1 μmol L^{-1}. The ^{13}C:^{12}C ratio of particulate organic carbon for each incubated sample and ambient background sample was measured on an isotope ratio mass spectrometer (Thermo Scientific DELTA V IRMS) using

acetanilide as a standard. The photosynthetic rate of each incubated sample was then calculated as (Hama et al., 1983):

$$P = \frac{C(a_{is} - a_{ns})}{t(a_{ic} - a_{ns})} \bullet 1.025$$

where P = photosynthetic rate (mg m^{-3} hr^{-1}), C = POC concentration of the incubated sample (mg m^{-3}), a_{is} is the ^{13}C atom % of incubated POC, a_{ns} is the ^{13}C atom % of ambient background POC, a_{ic} is the ^{13}C atom % of DIC after the ^{13}C spike, and t is time (hr). The multiplication factor of 1.025 corrects for isotopic discrimination (Hama et al., 1983). Dark bottle results were subtracted from each light bottle to account for the anaplerotic fixation of $^{13}CO_2$ (Geider and Osborne, 1992; Williams and Lefèvre, 2008). The ^{13}C tracer results are interpreted as net primary production in this study, but there is considerable debate on whether carbon isotope tracer methods measure gross photosynthesis, net photosynthesis, or something in between (Peterson, 1980; Marra, 2009).

Areal production calculations

Daily areal production (mg C m^{-2} day^{-1}) was calculated using the approach of Fee (1973b), which has been widely used in the Great Lakes (Fahnenstiel et al., 1989, 2010, 2016; Lang and Fahnenstiel, 1996). This approach requires four components: (1) photosynthesis irradiance (P-I) curve, (2) distribution of photosynthetically active radiation (PAR) over the day, (3) underwater PAR extinction coefficient (k_{PAR}), and (4) chlorophyll profile.

Photosynthetic rates normalized to chlorophyll were fit to the P-I model of Platt et al. (1980):

$$P^B = P_S^B \bullet (1 - e^{-\alpha I / P_S^B}) \bullet e^{-\beta I / P_S^B}$$

where P^B = specific photosynthetic rate normalized to biomass (mg C mg chl^{-1} hr^{-1}), P_S^B = maximum photosynthetic output if there was no photoinhibition in the curve (same units as P^B), α = initial linear slope (mg C mg chl^{-1} mol $photons^{-1}$ m^2), I = irradiance (mol photons m^{-2} hr^{-1}), and

β = negative linear slope at high irradiances representing photoinhibition (same units as α). Chlorophyll-normalized P-I parameters are responsive to environmental conditions and can be indicators of phytoplankton physiological status. α^B, the initial linear slope of the light-limited region of the curve normalized to chlorophyll, characterizes the photochemical reactions of photosynthesis and is dependent on light history and availability, nutrient availability, and community structure (Edwards et al., 2015; Platt and Jassby, 1976; Talling, 1957; Welschmeyer and Lorenzen, 1981). Higher α^B indicates more efficient use of low light. P_S^B is a scaling parameter with little biological significance, but P_M^B is physiologically meaningful and represents the maximum photosynthetic rate at light saturation normalized to biomass. P_M^B is calculated from other P-I parameters as:

$$P_M^B = P_S^B \bullet \left[\frac{\alpha}{\alpha+\beta}\right] \bullet \left[\frac{\beta}{\alpha+\beta}\right]^{\frac{\beta}{\alpha}} .$$

P_M^B is a function of the enzymatic reactions of photosynthesis and dependent on temperature, nutrient availability, light history, and community composition (Fahnenstiel et al., 1989; Geider and Osborne, 1992; Harding et al., 1987; Senft, 1978; Talling, 1957).

The Platt equation was fit to experimental data using the 'fitPGH' function in the 'phytotools' package in R (Silsbe and Malkin, 2015). PORT model optimization routines (Gay, 1990) were used to fit the model because it consistently provided the best fit to data and most successful convergence on model parameters. When there is no photoinhibition in the P-I curve, β = 0, $P_M^B = P_S^B$, and the two-parameter model of Webb et al. (1974) can be used:

$$P^B = P_M^B \bullet (1 - e^{-\alpha I/P_M^B}).$$

If the 95% confidence interval for β included zero, then β was not included in the model and the 'fitWebb' function was used (Fahnenstiel et al., 1989; Silsbe and Malkin, 2015), unless

photoinhibition was clearly evident in the P-I curve. In cases where model fitting error was high, β was excluded, and P_M^B and α were calculated manually as the maximum measured photosynthetic rate and the slope of the line between the first two points of the curve, respectively.

For each day of sampling, k_{PAR} was calculated as the negative slope of natural log-transformed PAR versus depth, excluding irradiance measurements from the upper 2 meters. In several cases during the summer, k_{PAR} varied with depth. The euphotic depth, defined as the depth where underwater irradiance was 0.5% of surface irradiance (Fee, 1990), was calculated as $5.3/k_{PAR}$. When k_{PAR} was variable, the upper k_{PAR} value was used because the distinction between multiple k_{PAR} values often occurred between the euphotic and aphotic zone. For stations sampled at night and stations sampled during the day without an underwater PAR sensor, k_{PAR} was calculated from beam attenuation and Secchi depth, respectively (Bukata et al., 1988). The conversion from beam attenuation to k_{PAR} was developed using mean 10-20 m beam attenuation values and the 10-20 m k_{PAR} from sites sampled during daytime ($k_{PAR} = 0.21(\text{beam}) + 0.08$, $r^2 = 0.36$). Secchi depth was converted to k_{PAR} using the relationship between inverse secchi depth and the 10-20 m k_{PAR} ($k_{PAR} = 0.55(S^{-1}) + 0.07$, $r^2 = 0.42$). Only spring 2016 and spring 2017 whole-lake survey data were used to develop these relationships because there is less vertical variation in water clarity during the spring. While the r^2 values of our empirical relationships are low, the slope and intercept of our two equations are similar to those from Bukata et al. (1988).

To eliminate the effects of variation in cloud cover on areal photosynthetic rates and facilitate spatial comparisons, surface PAR for each site and date was simulated at 30-minute intervals using the 'incident' function from the 'phytotools' package (Silsbe and Malkin, 2015). Cloud-free atmospheric turbidity factors, which quantify the attenuation of solar radiation due to gaseous water vapor and aerosols in the atmosphere, were entered for each month and site to account for

the seasonal and spatial variability of atmospheric turbidity (http://www.soda-is.com/linke/linke_helioserve.html). On average from May to October 2017, cloud cover reduced daily mean surface irradiance measured on a 20 m buoy near Milwaukee (43.100, -87.850) by 26.5% in 2017, so all simulated PAR was multiplied by a constant 0.735 to account for cloud cover. Surface reflectance was calculated for each site and day using the 'reflectance' function in the 'phytotools' package (Silsbe and Malkin, 2015). Irradiance at depth was then calculated using the Beer-Lambert law:

$$I_z = (1 - r) \bullet I_s \bullet e^{-k_{PAR} * z}$$

where I_z is PAR at depth z (mol photons m^{-2} hr^{-1}), r is surface reflectance, I_s is surface PAR measured in air (same units as I_z), and z is depth (m).

To facilitate spatial comparisons among whole-lake survey sites sampled across multiple days, surface PAR for each date and location was simulated using the middle day of the survey. To facilitate comparisons among the 75 m sites from different regions of the lake not sampled on the same day, simulated PAR for the 15th day of each month at each site was used. As a result, differences among sites were due to spatial variability in P-I parameters, k_{PAR}, chlorophyll, atmospheric turbidity, and the distribution of solar irradiance due to latitude, but not cloud cover. For each nearshore-offshore comparison, simulated PAR from AW75 was used at all sites. Therefore, differences in areal production at AW15, AW45, and AW75 during each day are due to differences in P-I parameters, k_{PAR}, and chlorophyll.

To calculate daily areal production, the 'phytoprod' function in the 'phytotools' package was modified to incorporate two k_{PAR} values and two sets of P-I parameters (Fee, 1973b; Silsbe and Malkin, 2015). For depths where P-I parameters were not measured, linear interpolation was used to estimate parameters. Photosynthesis for every 0.1 m interval was calculated using interpolated

P-I parameters and irradiance at depth. Photosynthetic rates were then multiplied by the biomass profile to result in volumetric estimates of photosynthesis (mg C m^{-3} h^{-1}). Instantaneous areal photosynthesis was obtained by integrating photosynthesis over the euphotic zone, and this process was repeated for every 30-minute simulated PAR interval to obtain instantaneous depth integrals. Areal production (mg C m^{-2} day^{-1}) was calculated as the integral of instantaneous depth integrals over the entire day (Fee, 1990).

Data analysis

All data analysis was performed using R version 3.4.4 (R Core Team, 2018). Production to biomass (P:B) ratios for epilimnetic samples were calculated by dividing volumetric production (mg C m^{-3} day^{-1}) by the phytoplankton carbon concentration (mg C m^{-3}) to obtain an estimate of phytoplankton growth rate (day^{-1}). Phytoplankton carbon was calculated from seston carbon assuming a maximum 40% of seston carbon is live phytoplankton (Hessen et al., 2003). Assuming the maximum percent of seston carbon is live phytoplankton provided a conservative estimate of growth rates, as growth rates may actually be higher if the phytoplankton contribution to seston carbon is lower than 40%.

Seston stoichiometry (molar C:P, C:N, and N:P) was used to evaluate phytoplankton nutrient status (Hecky et al., 1993). C:P, C:N, and N:P were analyzed according to the nutrient deficiency criteria from Healy and Hendzel (1980). Nutrient deficiency as revealed by seston stoichiometry has agreed with physiological methods for measuring nutrient deficiency (Hecky et al., 1993), so seston stoichiometry is a relatively simple and useful indicator of phytoplankton nutrient status. Physical, chemical, and biological parameters measured along south-north and nearshore-offshore gradients in this study were mainly analyzed as spatial trends rather than statistical differences.

When comparing 75 m depth site replicates from different regions, a Student two-sample t test was performed and $\alpha = 0.05$ was used. The 'interp' function from the 'akima' package was used to perform spline interpolation of temperature, chlorophyll, and production between sampling sites along nearshore-offshore transects (Akima and Gebhardt, 2016). Mean irradiance in the mixed layer was calculated using Equation 3 from Fahnenstiel et al. (2000).

Results

Whole-lake surveys

Spring 2016

Surface temperature was similar at all sites (~3.5ºC) except MI-N where temperature was 1ºC lower (Figure 2.2a). Mean percent surface irradiance in the mixed layer was lowest at MI34 and MI47, the deepest sites, and highest at MI-N, the shallowest site (Figure 2.2b; Table 2.1). Seston C:P and N:P decreased from south to north, indicating less phosphorus limitation in the northern basin (Figure 2.2c-d). Seston C:P revealed severe phosphorus deficiency at MI17, and seston C:N was also highest at MI17 (Figure 2.2c-e). No measurements of seston stoichiometry were available at MI47 due to elemental analyzer error. Chlorophyll was highest at MI23, lowest at MI-N, and similar at all other sites (Figure 2.2f). P_M^B increased from south to north (Figure 2.2g), following the trend in decreasing phosphorus limitation. The lowest P:B, areal production, P_M^B , and α^B were found at MI17 where nutrient limitation was greatest (Figure 2.2g-j). Spatial patterns in production and P:B generally agreed except at MI23 where production was high and the P:B was similar to all other sites, excluding MI17 (Figure 2.2i-j). High production at MI23 (Figure 2.2i) corresponded to the highest chlorophyll concentration (Figure 2.2f), which was 30% higher than the mean of all

other sites. Production generally followed the trend in chlorophyll, excluding MI-N (Figure 2.2f, i).

Spring 2017

All temperatures were below 4ºC and temperature generally decreased from south to north (Figure 2.3a). Some ice was present around Green Bay. Mean percent surface irradiance in the mixed layer was again greatest at the shallowest sites and lowest at the deepest sites (Figure 2.3b; Table 2.1). Seston C:P and N:P were highest at MI23, GB1, and MI52 (Figure 2.3c-d) and seston C:N was highest at MI11, GB1, and MI52 (Figure 2.3e), suggesting greater nutrient limitation at the coldest sites. Chlorophyll and α^B decreased from south to north following the trend in temperature (Figure 2.3f, h), but P_M^B was highest at the deepest sites (Figure 2.3g). Areal production followed the decreasing trend in temperature and chlorophyll (Figure 2.3i), but not the trends in P-I parameters or nutrient limitation (Figure 2.3c-e, g-h). P:B did not follow the trend in production or vary much spatially, but P:B was lowest at the three northernmost sites and highest at MI34 (Figure 2.3j).

Summer 2017

Temperatures in the northern basin (19 ºC) were 3-4ºC cooler than the southern basin (22-23ºC; Figure 2.4a), and mean percent surface irradiance within the surface mixed layer decreased from south to north (Figure 2.4b), as k_{PAR} increased (data not shown). Seston C:P was highest at MI23 and MI34 and phosphorus deficiency was severe, but all other sites were only moderately

phosphorus deficient (Figure 2.4c). Seston C:P and N:P were lowest at GB1 and MI52, and N:P revealed no phosphorus deficiency at these sites while all other sites were phosphorus deficient (Figure 2.4c-d). Seston C:N was similar at all sites but was slightly higher GB1 and MI52 (Figure 2.4e). α^B and P_M^B were similar at all sites except MI23 where P_M^B was twice as high as the P_M^B of all other sites (Figure 2.4g-h). High P_M^B at MI23 does not appear to be related to more favorable nutrient, temperature, or light conditions (Figure 2.4a-e). Chlorophyll, areal production, and P:B increased from south to north and were highest at GB1 and MI52 (Figure 2.4f, i-j), corresponding to the lowest phosphorus limitation (Figure 2.4c-d).

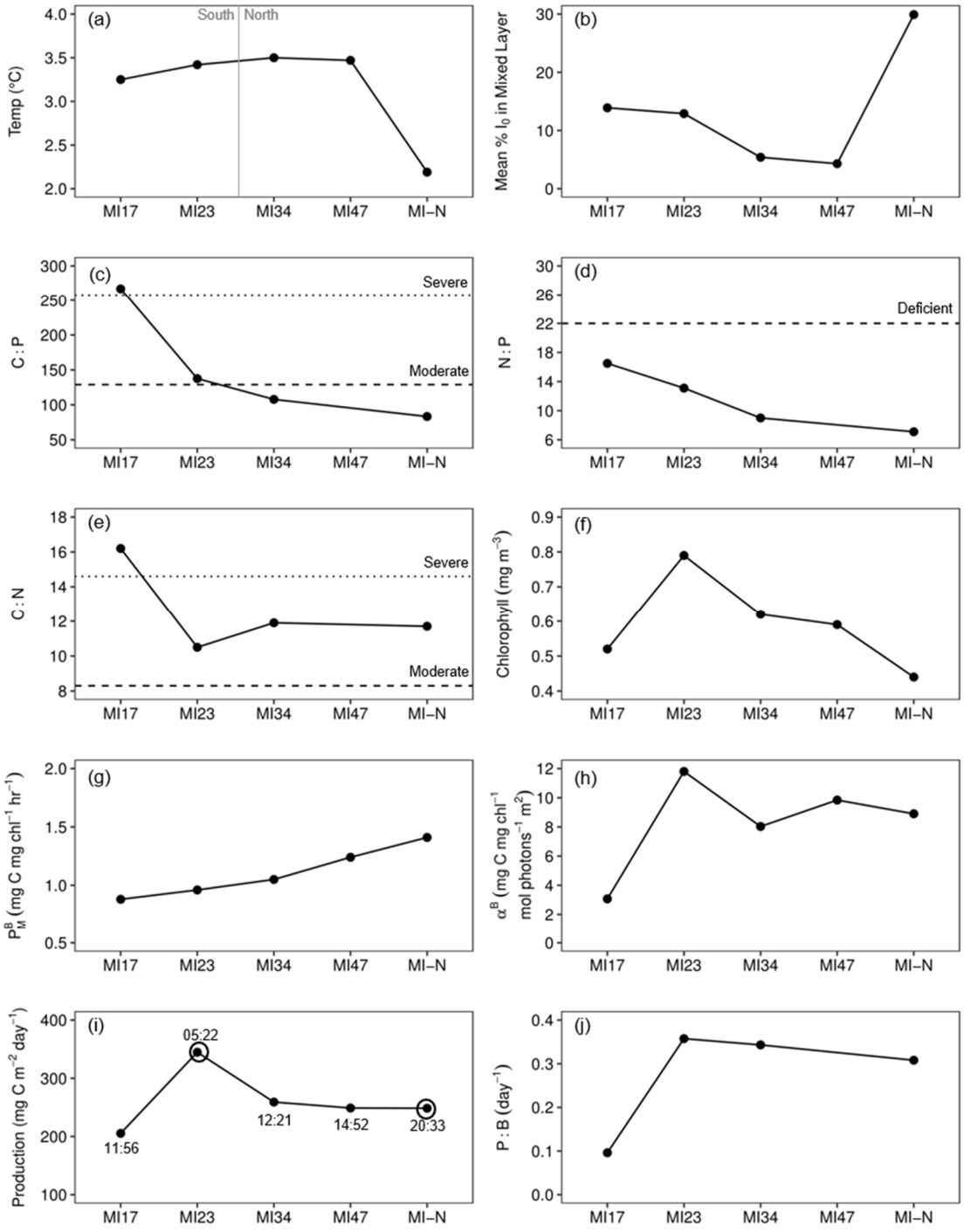

Figure 2.2. Spring 2016 areal production, mean percent surface irradiance (I_0) in mixed layer, and 2 m temperature, seston stoichiometry, chlorophyll, P_M^B, α, and P:B. Production measurements from night samples are outlined with black circles, and sampling times are presented next to each measurement. Dotted lines indicate nutrient deficiency criteria from Healy and Hendzel (1980).

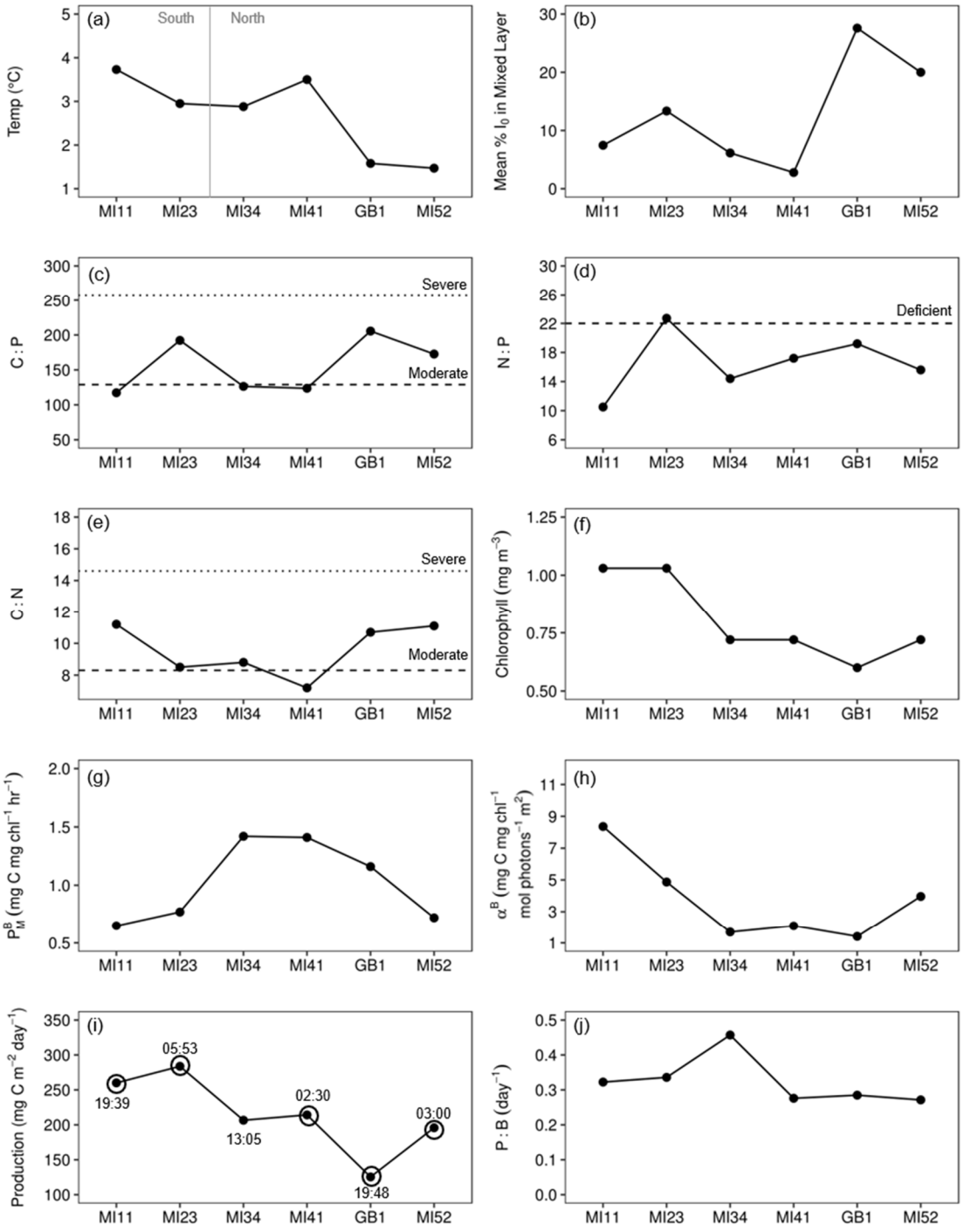

Figure 2.3. Spring 2017 areal production, mean percent surface irradiance (I_0) in mixed layer, and 2 m temperature, seston stoichiometry, chlorophyll, P_M^B, α, and P:B. Symbols and lines as in Figure 2.2.

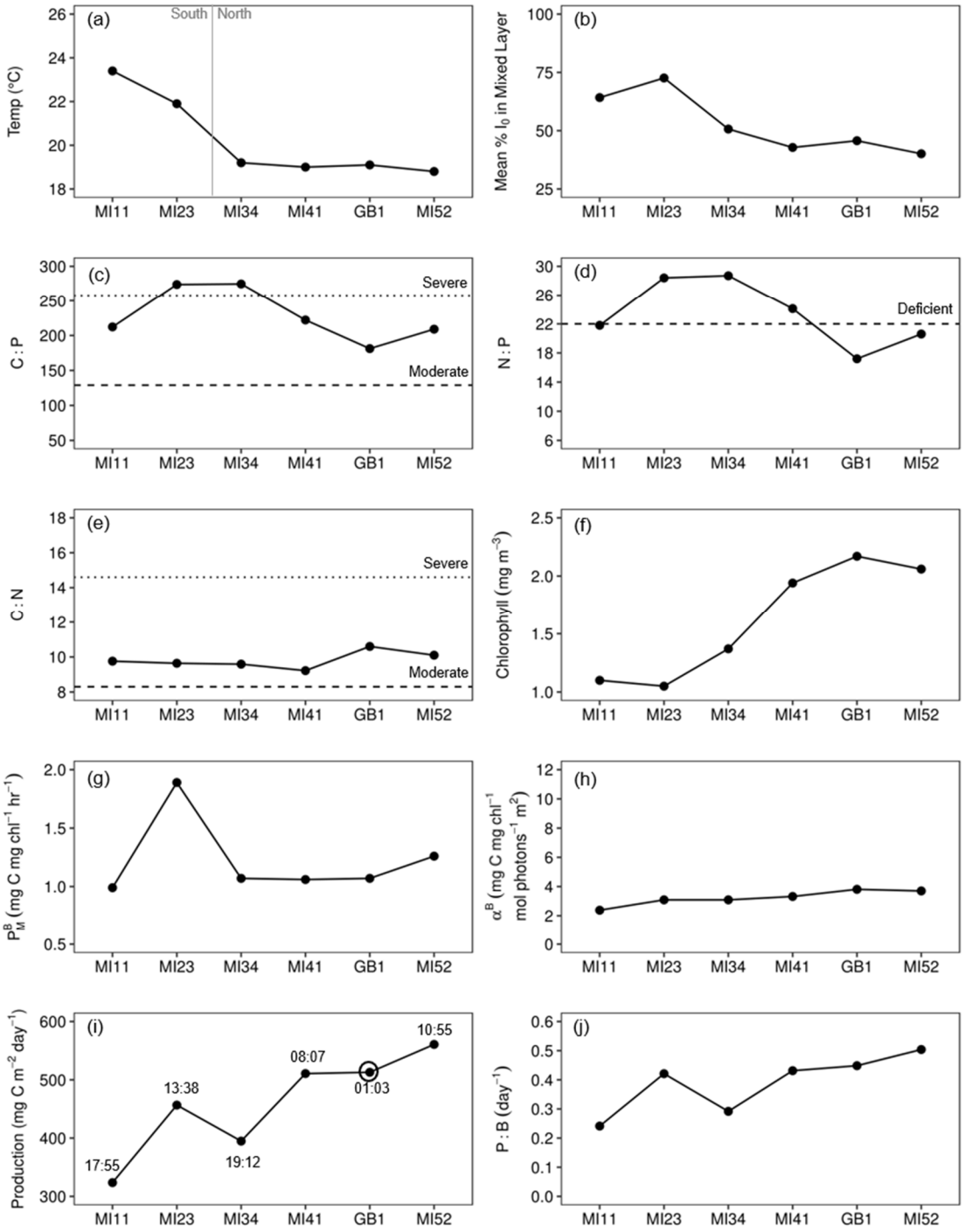

Figure 2.4. Summer 2017 areal production, mean percent surface irradiance (I_0) in mixed layer, and mid-epilimnetic temperature, seston stoichiometry, chlorophyll, P_M^B, α, and P:B. Symbols and lines as in Figure 2.2.

75 m site comparisons

There do not appear to be any consistent differences in production at 75 m sites from different regions (Table 2.2). In June, mean production at AW75 was not significantly different from DC75 (Student two sample t-test, $p = 0.33$), and production at MT75 and DC75 was similar. In July, production was 21.0% higher at MT75 than at AW75, but only one measurement was available at MT75. AW75 production was 18.8% higher than DC75 production in August, but only one measurement was available from DC75. In October, production was higher at AW75 than at MT75 unlike in July, but only one measurement was available at MT75. Limited replication at the northern basin sites limits our ability to make spatial comparisons.

Table 2.2. Regional measured areal production (mg C m^{-2} day^{-1}) comparisons calculated using mid-month simulated PAR (26.5% cloud cover) at each site. For months with multiple sampling dates, mean measured production ± 1 SD is presented.

Site	June	July	August	October
DC75	340.7 ± 88.2	-	539.3	-
MT75	364.8	482.9	-	420.9
AW75	449.1 ± 83.7	382.0 ± 62.9	663.8 ± 114.4	473.4 ± 108.8

Nearshore-offshore comparisons

July 11, 2017

The water column was more strongly stratified offshore than nearshore (Figure 2.5a), and remote sensing revealed strong upwelling along the western shore of Lake Michigan on July 8 and re-warming of the lake on the day of sampling (http://www.greatlakesremotesensing.org/). A DCL was present at AW45 and AW75, but the DCL at AW75 was 8 m deeper (Figure 2.5b). Epilimnetic chlorophyll, P:B, and production were greatest nearshore and decreased offshore (Figure 2.5b-c, Table 2.3). Maximum volumetric production rates at AW15, AW45, and AW75 were 210.5, 31.9, and 15.0 mg C m^{-3} day^{-1}, respectively. Most production was concentrated in the epilimnion despite the presence of a DCL. Seston C:P and N:P revealed the greatest phosphorus deficiency at AW15, where biomass, growth rates, and production were highest (Table 2.3). The lowest seston C:P, C:N, and N:P were observed at AW45, indicating the lowest nutrient limitation in the mid-depth region.

September 12, 2017

The water column was strongly stratified, and surface temperatures were similar among sites (Figure 2.6a). Remote sensing revealed no evidence of upwelling or downwelling from September 10 to September 13 (incomplete map September 12). Epilimnetic chlorophyll was highest at AW15 and AW45, and production and P:B decreased from nearshore to offshore (Figure 2.6b-c, Table 2.3). Maximum volumetric production rates at AW15, AW45, and AW75 were 161.0, 50.8, and 33.0 mg C m^{-3} day^{-1}, respectively. Seston C:P was lowest at AW15, where production and growth rates were highest, and increased from nearshore to offshore (Table 2.3). The greatest phosphorus

deficiency was observed offshore at AW75, where production and growth rates were lowest. Seston C:N was highest in the mid-depth region at AW45.

October 9, 2017

Temperature, chlorophyll, growth rates, and production were greatest offshore, and remote sensing revealed strong upwelling nearshore from October 5-9 (Figure 2.7a-c; Table 2.3). Maximum volumetric production rates at AW15, AW45, and AW75 were 23.5, 19.0, and 36.2 mg C m^{-3} day^{-1}, respectively. Although areal production at AW45 was higher than at AW15, volumetric production and growth rates were higher at AW15 (Figure 2.7c; Table 2.3). Volumetric production at AW75 peaked below the surface from 4 to 8 m (Figure 2.7c). Seston C:P was lowest at AW15 where production was lowest and highest at AW75 where production and growth rates were highest (Table 2.3). The lowest seston C:N was also found offshore at AW75, but no N measurements were available for AW15 due to elemental analyzer error.

Table 2.3. Nearshore-offshore transect areal production and epilimnetic chlorophyll, seston stoichiometry, and P:B. Bold indicates no phosphorus deficiency for C:P and N:P and no nitrogen deficiency for C:N. Normal font indicates moderate phosphorus deficiency for C:P and moderate nitrogen deficiency for C:N. For N:P, normal font indicates phosphorus deficiency. Nutrient deficiency criteria from Healy and Hendzel (1980).

Date	Site	Production (mg C m^{-2} day^{-1})	Chlorophyll (mg m^{-3})	C:P (molar)	C:N (molar)	N:P (molar)	P:B (day^{-1})
11 Jul	AW15	1215.5	4.01	229.8	11.0	**20.8**	0.346
	AW45	415.7	1.37	**121.2**	8.56	**14.2**	0.172
	AW75	340.6	0.91	224.0	13.0	**17.2**	0.148
12 Sep	AW15	1175.9	2.28	**116.4**	8.98	**13.0**	0.636
	AW45	895.2	2.28	193.5	10.5	**18.4**	0.289
	AW75	650.8	1.60	192.9	8.43	22.9	0.199
09 Oct	AW15	176.3	0.38	**94.5**	-	-	0.125
	AW45	283.2	0.92	150.0	9.29	**16.2**	0.105
	AW75	414.6	0.89	215.4	**7.40**	29.1	0.203

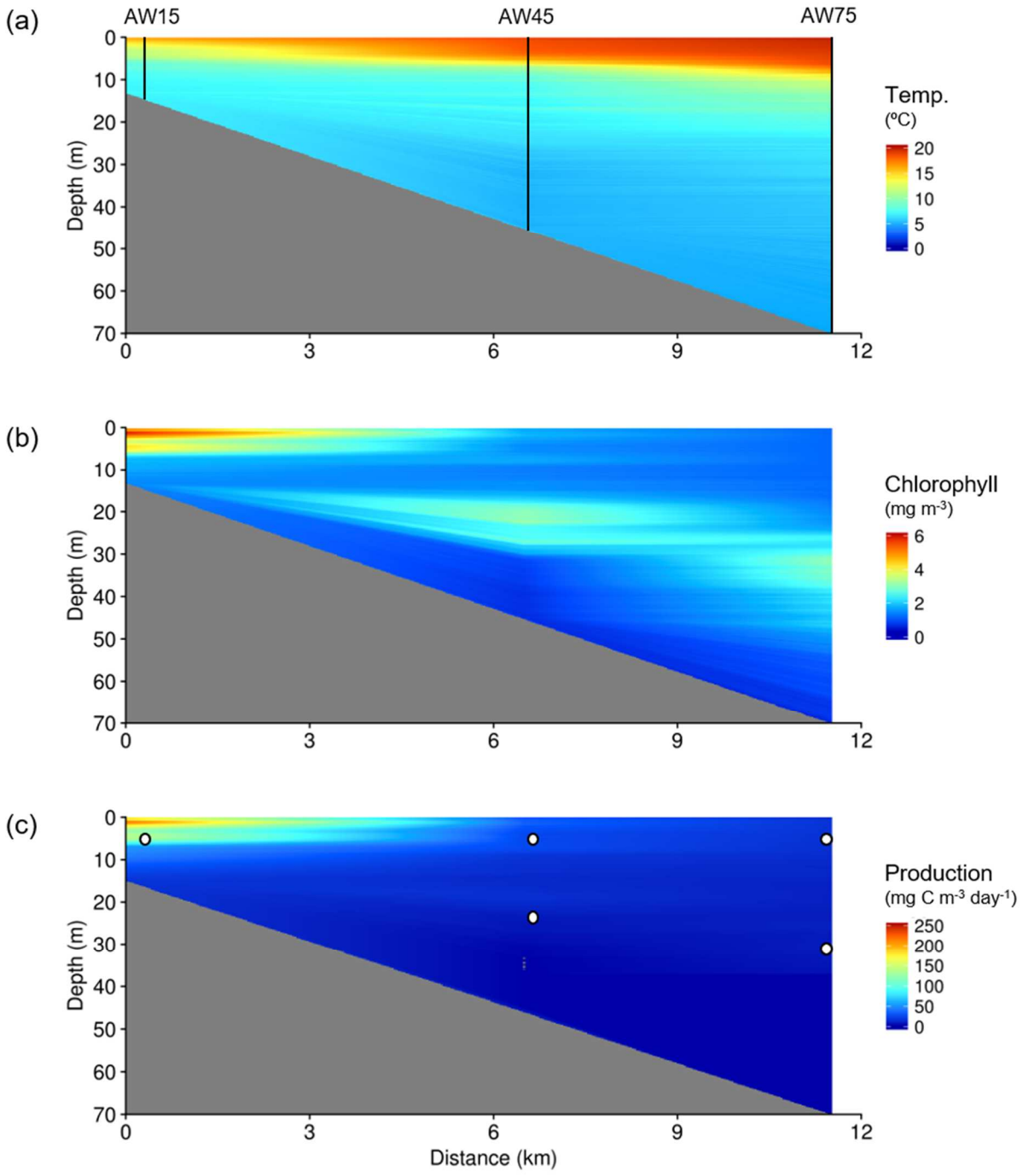

Figure 2.5. Nearshore to offshore vertical structure of temperature, corrected CTD chlorophyll, and phytoplankton production on July 11, 2017. Spline interpolation was used between sampling sites. White points represent discrete sampling points for photosynthesis measurements.

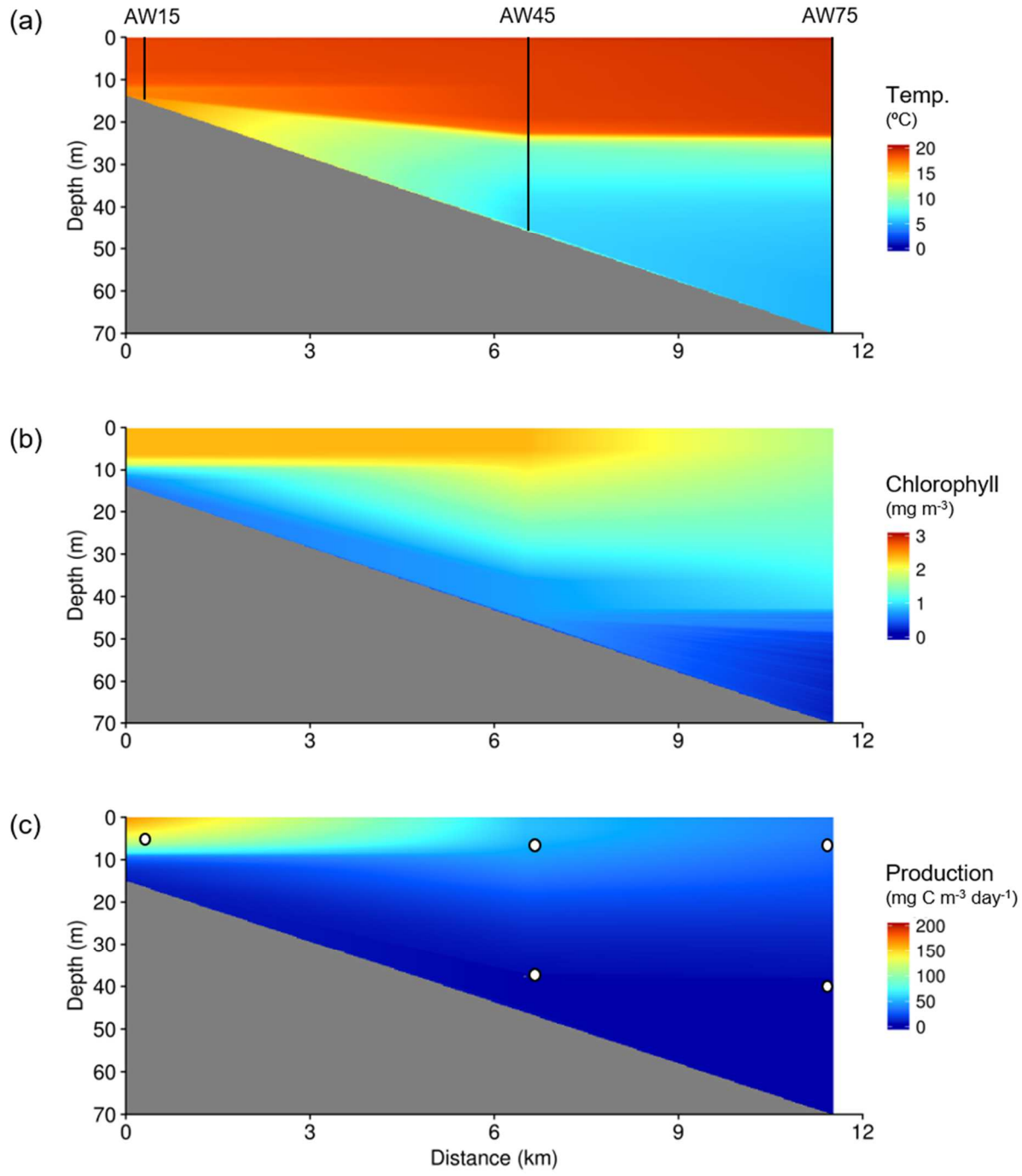

Figure 2.6. Nearshore to offshore vertical structure of temperature, corrected CTD chlorophyll, and phytoplankton production on Sep 12, 2017. Symbols as in Figure 2.5.

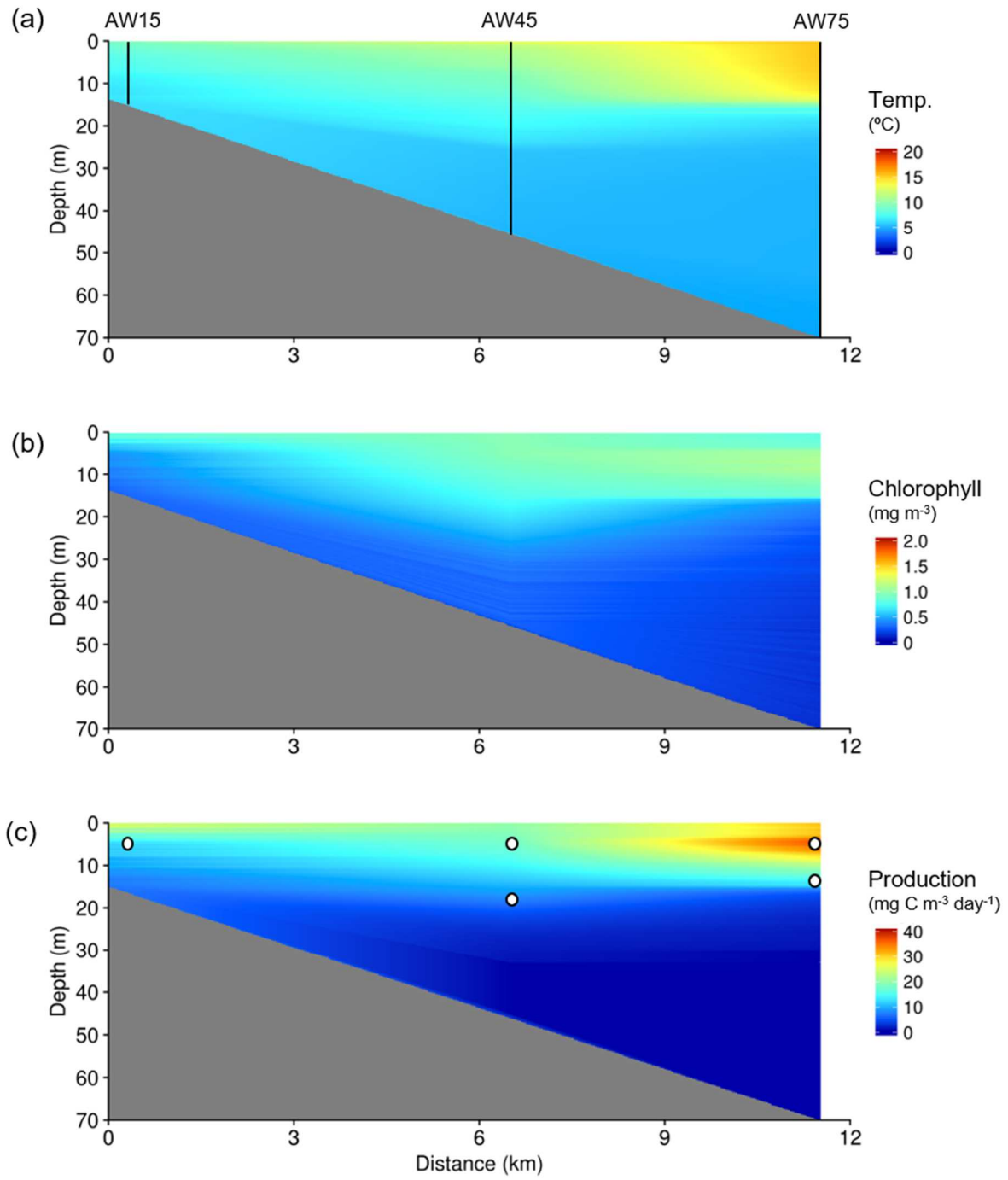

Figure 2.7. Nearshore to offshore vertical structure of temperature, corrected CTD chlorophyll, and phytoplankton production on Oct 9, 2017. Symbols as in Figure 2.5.

Discussion

This study revealed spatial variability of phytoplankton production, growth rate estimates, and seston stoichiometry along south-north and nearshore-offshore gradients in Lake Michigan. South-north patterns varied seasonally and among years, and nearshore-offshore patterns varied with season and upwelling. Limited replication at the 75 m northern basin sites hindered our conclusions regarding regional differences. Spatial variation in phytoplankton growth rates reflects the biogeochemical conditions controlling phytoplankton dynamics, while the spatial variability of phytoplankton production illustrates the balance between growth and loss processes and reveals the spatial variability of resources available for higher trophic levels. Seston stoichiometry can be used alongside production to also indicate the quality of food resources available for higher trophic levels, including zooplankton, preyfish, and piscivores.

North-south comparisons

Regional production comparisons based on the three 75 m sites in Lake Michigan were not as robust as basin comparisons from whole-lake surveys. Production did not appear to differ among the three sites in a consistent manner despite different watershed characteristics and upwelling frequency. WI hypothesized that production at DC75 in northwestern Lake Michigan would be higher than production at MT75 and AW75 Lake Michigan due to nutrient influence from Green Bay, but DC75 production was similar to or lower than production at the other 75 m sites. I also hypothesized that MT75 would have the lowest production because the eastern shore of Lake Michigan does not experience as frequent upwelling as the western shore (Plattner et al., 2006), and increased forest cover in northern Michigan should result in less external nutrient loading and lower in-lake nutrient concentrations, but production at MT75 was not consistently lower than

other sites. In general, my hypotheses were not supported and limited replication in the northern basin limited my ability to detect spatial trends.

Some 75 m site comparisons, however, do support past research on the spatial variability of water quality in Lake Michigan. Through continuous survey of the 20 m depth contour with a towed instrument package in 2010, Yurista et al. (2014) identified different coastal water quality regions of Lake Michigan and attributed these differences to different landscape characteristics. Yurista et al. (2014) found the northwestern region near DC75 and the northeastern region near MT75 to be similar to each other and distinct from southwestern Lake Michigan near AW75. When all three 75 m sites were sampled in June 2017, production at DC75 (341 mg C m^{-2} day^{-1}) and MT75 (365 mg C m^{-2} day^{-1}) was similar and lower than production at AW75 (449 mg C m^{-2} day^{-1}), perhaps supporting the coastal cluster analysis from Yurista et al., (2014). Our sites, however, were 55 m deeper than the 20 m contour sampled by Yurista et al. (2014) and the offshore region was identified as distinct from the nearshore region in their study, but Cai and Reavie (2018) found the offshore region in the northern basin to be distinct from the southern offshore region. As our replication of northern basin sites was limited, future studies should continue to investigate similarities and differences among near-coastal regions in Lake Michigan in order to gain a better understanding of how landscape characteristics may influence the coastal regions of Lake Michigan.

Spatial patterns in offshore phytoplankton production, growth rate estimates, and seston stoichiometry differed among all three whole-lake surveys. In spring 2016, nutrient limitation decreased from south to north, and P_M^B, α^B, growth estimates, and areal production were lowest at MI17 where C:P, N:P, and C:N were highest. High seston C:P and C:N at MI17 compared to the other sites suggests that a greater proportion of seston at MI17 was non-living phytoplankton. As

MI17 was closer to shore than all other sites sampled in spring 2016, high nutrient limitation and low growth estimates may be due to late winter-early spring sediment resuspension close to shore, which can increase suspended organic carbon concentrations and turbidity, and decrease light availability and phytoplankton production (Eadie et al., 1984; Eadie et al., 2002; Lohrenz et al., 2004).

Areal production and growth estimates in spring 2016 were similar at sites except MI17. Spring isothermal mixing in Lake Michigan is characterized by suboptimal nutrient, light, and temperature conditions for phytoplankton growth (Fahnenstiel et al., 2000). Using nutrient enrichment experiments with spring phytoplankton from Lake Ontario, Fahnenstiel et al. (2000) found higher growth rates in treatments with both increased nutrient and light availability than treatments with increased nutrient or light availability alone, suggesting nutrients and light both limit spring phytoplankton growth rates. Temperature limitation of spring phytoplankton growth was not directly assessed in their study, but suboptimal temperatures during spring isothermal mixing may also constrain phytoplankton growth rates (Fahnenstiel et al., 2000). These multiple limiting factors may explain why spring growth estimates were similar at nearly all sites in Lake Michigan in spring 2016.

There was greater spatial variability in phytoplankton production and seston stoichiometry than growth rates in spring 2016. Production and biomass at MI23 were higher than in the northern basin despite similar growth estimates, suggesting phytoplankton loss processes varied across the lake and there may have been reduced grazing or sedimentation loss at MI23 relative to other sites (Scavia and Fahnenstiel, 1987). Although production was highest at MI23, higher quality food resources for consumers, as indicated by lower C:P, were found in the northern basin of the lake. Consumers, such as zooplankton, require P for growth and reproduction, so lower C:P results in

higher food quality and is associated with more efficient energy transfer (Sterner et al., 1997; Sterner and Hessen, 1994). Under nutrient limitation, consumers assimilate available nutrients to meet their nutrient demands and excrete excess nutrients, such as carbon, thus resulting in inefficiencies in energy transfer (Olsen et al. 1986; Urabe 1994). Therefore, lower C:P in the northern basin suggests more efficient energy transfer in the north, although greater phytoplankton biomass (chlorophyll) was found at MI23.

In spring 2017, spatial trends in biomass appeared to be most strongly related to temperature, and production appeared to be most strongly related to biomass. Temperature, biomass, and production all decreased from south to north, and some ice was present close to shore in the northern basin during the survey. There were no consistent spatial patterns in nutrient limitation in spring 2017, but it appears that nutrient limitation was generally higher at GB1 and MI52 where temperatures were coolest. Ice and reverse stratification can limit the delivery of nutrients from the watershed and reduce the upward mixing of nutrients (Wetzel, 2001), perhaps explaining why generally higher nutrient limitation and the lowest biomass and production were observed at the coldest sites.

Spatial patterns in production and biomass, however, were not due entirely to temperature because low production and biomass were also found at MI34 and MI41 where temperatures were warmer. Lower production at these sites may be related to light limitation associated with greater mixed layer depths at deeper sites. When temperatures are close to 4ºC, mixing occurs throughout the entire water column and phytoplankton spend more time in the aphotic zone. Therefore, deeper sites have a deeper aphotic zone, phytoplankton are exposed to a lower average irradiance, and biomass may be lower because of light limitation (Rowe et al., 2017). P-I parameters, however, do not appear to be strongly related the trend in temperature or irradiance. P_M^B was highest at the

deepest sites where mean irradiance and nutrient limitation were lowest, suggesting nutrients played a more important role than irradiance. Spatial patterns in α^B are difficult to explain because they were lowest at the sites with lowest irradiance and highest nutrients, suggesting the influence of some factor not measured in this study.

Growth estimates in spring 2017 demonstrated less spatial variability than production and were generally similar across the lake. The highest growth estimate was calculated at MI34, which corresponded to low nutrient limitation and high P_M^B, but similar P_M^B, nutrient limitation, and temperatures were also found at MI41. MI41, however, is 90 m deeper than MI34, suggesting greater light availability at MI34 resulted in higher growth rates. As in spring 2016, multiple limiting factors (temperature, light, and nutrients) may explain why growth rates were similar across the lake.

Unlike spring 2016 and 2017, production, biomass, and growth rates in summer 2017 all exhibited similar spatial patterns. The mechanisms controlling summer epilimnetic phytoplankton in Lake Michigan are less complex than the mechanisms regulating spring isothermal mixing communities because nutrients are the main limiting factor during stratification (Fahnenstiel and Scavia, 1987a; Scavia and Fahnenstiel, 1987). In the northern basin, seston C:P and N:P decreased from south to north and chlorophyll, production, and growth rates increased with decreasing phosphorus limitation. Southern basin production, however, did not follow similar trends in phosphorus limitation, suggesting light availability, temperature, grazing, or differing community compositions controlled spatial patterns in the southern basin. Across the lake, P_M^B and α^B did not follow trends in phosphorus, temperature, or light conditions, so spatial patterns in production appear to be mostly due to trends growth rates, which in turn are related to phosphorus availability.

Lower seston C:P, production, growth rates, and biomass in the northern basin are likely due to higher total phosphorus concentrations in the north (Cai and Reavie, 2018), which may be due to nutrient influence from Green Bay and less mussel influence in the northern basin. Remote sensing production estimates suggest there are occasional areas of high production in the northern basin off the coast of Door County and near the mouth of Green Bay (B. Lesht, unpub. data). If this is due to upwelling on the western shoreline, production may be stimulated along the entire western shore (Rowe et al., 2017; Yurista et al., 2015), but this was not observed (B. Lesht, unpub data), suggesting more localized nutrient input. While Green Bay only represents 1.4% of the volume of Lake Michigan, it receives approximately one-third of the total nutrient loading to the lake, 70% of which arrives through the Fox River (Klump et al., 2009). Water exchange between Green Bay and Lake Michigan (Hamidi et al., 2012) may stimulate summer production in the main lake by supplying nutrients. If Green Bay nutrients are stimulating northern basin production, production should be highest closer to Green Bay where nutrients are most concentrated, and the highest production and growth estimates in this study were observed at the sites closest to Green Bay (MI41, GB1, MI52).

Greater production in the northern basin may also be related to reduced mussel impacts with greater depths. Most of the depths in the northern basin exceed 90 m, meaning there is less mussel biomass offshore in the northern basin than the southern basin, although northern basin biomass exceeds southern basin biomass at some shallow depth intervals (Nalepa et al., 2014; Rowe et al., 2015). As a result of lower offshore biomass, mussel filtering clears a smaller volume of the northern basin during isothermal mixing (Rowe et al., 2015). In much of the southern basin, dreissenid filter-feeding intensity in April exceeds the spring phytoplankton growth rate of 0.6 day^{-1} thus significantly reducing the spring phytoplankton bloom in the southern basin (Fahnenstiel et

al., 2010; Rowe et al., 2015). Reduction in the size of spring phytoplankton bloom is associated with lower whole water column chlorophyll and DCL size in the summer even though mussels do not have access to the entire water column during stratification (Pothoven and Fahnenstiel, 2013). Therefore, greater mussel clearing offshore in the southern basin during the spring may result in lower productivity during summer stratification compared to the northern basin (Pothoven and Fahnenstiel, 2013; Warner and Lesht, 2015).

Due to less mussel influence offshore, phosphorus in the northern basin may also be more efficiently recycled among primary producers, consumers, and the benthos. Less mussel biomass offshore means less P during stratification is sequestered in the hypolimnion and benthos in mussel biomass, feces, and pseudofeces (Hecky et al., 2004; Mosley and Bootsma, 2015). The benthic sequestration of nutrients by dreissenids can exceed passive sedimentation by 50%, which greatly reduces the residence time of P in the water column (Chapra and Dolan, 2012; Klerks et al., 1996; Mosley and Bootsma, 2015). The residence time of P in the northern basin, therefore, should be greater than the southern basin and more P should be available for uptake by phytoplankton. Lower C:P in the northern basin should also increase the efficiency of P recycling by consumers, as consumers can more efficiently regenerate consumed P if their P demands are met (Elser and Urabe, 1999). Considering nutrient influence from Green Bay and reduced mussel impacts in the northern basin, the northern basin appears to be more favorable for phytoplankton growth and production than the southern basin during stratification.

The potential productivity of aquatic food webs is related to nutrient supply and primary production, so higher food web production might be expected with higher primary production through bottom-up control (Menge, 2000). Satellite-derived surface chlorophyll concentrations have been strongly related to fish yield in other systems (Ware and Thomson, 2005), suggesting

we might expect to see higher food web production in the northern basin of Lake Michigan. In 2016, alewife, rainbow smelt, and bloater densities were generally higher in the northern basin compared to the southern basin (D. Warner, USGS, unpub. data), although preyfish abundance is related to many factors and not just primary production (Bunnell et al., 2018; Crowder et al., 1987; Madenjian et al., 2015). In 2010, catch per unit effort (CPUE) of Chinook salmon in Lake Michigan was greatest along the western shore near Door County (Clark et al., 2016), and chinook CPUE from 2012 to 2016 was highest in Green Bay and the main lake between GB1 and MI52 (M. Kornis, USFWS, unpub. data). Chinook salmon are highly mobile offshore piscivores, and their movement patterns are related to temperature and forage conditions (Adlerstein et al., 2008). Although some chinook salmon move north in the summer following favorable temperatures, higher CPUE in the northern basin may also be related to higher preyfish abundance, which might be related to the bottom-up effects of higher primary production. Lower C:P in the northern basin may enhance the effects of bottom-up control, as greater P is associated with more efficient energy transfer in aquatic food webs (Sterner et al., 1997; Sterner and Hessen, 1994). Although we did not investigate spatial trends in higher food web production in this study, the correlation between higher primary production and higher upper food web production in the northern basin is interesting and may require further investigation.

Summer growth estimates measured in this study were similar to summer growth estimates prior to the mussel invasion. Summer growth estimates in this study ranged from 0.24 to 0.50 day^{-1}, which is within the range of 0.06-0.60 day^{-1} reported by Fahnenstiel and Scavia (1987), who also estimated growth rates from model (^{14}C) photosynthesis experiments and phytoplankton carbon estimates. Spring growth estimates in this study ranged from 0.10 to 0.45 day^{-1}, which was higher than nearly all growth rate measurements (^{14}C labeling into chlorophyll a) of 0.03 to 0.13

day^{-1} reported by Fahnenstiel et al. (2000). While methodological differences between our studies may account for some differences with Fahnenstiel et al. (2000), the large difference between pre- and post-mussel spring growth estimates may be related to the light and nutrient effects of mussels.

As light is partially responsible for limiting phytoplankton growth during spring isotheral mixing in the Great Lakes (Fahnenstiel et al., 2000), increased water clarity caused by mussels may be expected to decrease light limitation and increase spring phytoplankton growth rates in Lake Michigan. Further, although mussel grazing during spring isothermal mixing decreases phytoplankton biomass and total phosphorus (dissolved + particulate), soluble reactive phosphorus (SRP) excretion by mussels is significant and can be well-mixed throughout the water column during the spring (Moseley and Bootsma, 2015), which may decrease spring phosphorus limitation. While spring particulate phosphorus has decreased since the mussel invasion in 2000, spring total dissolved phosphorus (TDP) has not decreased (Barbiero et al., 2018), suggesting decreases in total phosphorus are due to decreases in particulate phosphorus by mussel grazing and mussel nutrient excretion may be an important source of dissolved phosphorus. Increased spring SRP may explain higher spring growth rates after the mussel invasion, but SRP changes over time are difficult to measure, as SRP turnover in surface waters can be as fast as 5 minutes in the summer (Cuhel and Aguilar, 2003). Nonetheless, higher spring phytoplankton growth estimates after the mussel invasion may be evidence that the nutrient and light effects of mussels may offset the loss of phytoplankton to mussel grazing (Zhang et al., 2011).

It should be noted that our conclusions about north-south spatial patterns are limited due to the limited number of whole-lake surveys. Production varies over relatively short time periods in response to environmental conditions (Cuhel and Aguilar, 2003), so spatial patterns are likely to be highly variable through time. The large differences in spatial patterns observed in the two spring

cruises suggests that two years of measurements may not have been enough to generally characterize spatial patterns in spring productivity. We also had no summer replication, so we cannot conclusively say that northern basin production is always greater than southern basin production. Also, correlation between environmental variables and primary production does not imply causality, so caution must be taken in interpreting correlations between production and nutrients, light, and temperature.

Day and night sampling during whole-lake surveys may also have impacted our spatial production comparisons. Phytoplankton adjust photosynthetic machinery to varying light conditions, which can greatly affect photosynthetic parameters (Harding et al., 1987; Legendre et al., 1988). Diel variation in α^B and P_M^B depends greatly on the environment (marine vs. freshwater, oligotrophic vs. eutrophic) and phytoplankton community composition (Harding et al., 1987, 1982a; Fee, 1975; Kana et al., 1985; Marra et al., 1985; Reinke et al., 1970), making it difficult to draw definitive conclusions about diel oscillations in P-I parameters. Generally, in natural phytoplankton communities, P_M^B is lowest at night due phytoplankton circadian rhythms, peak photosynthetic activity can occur during morning, midday, or afternoon, α^B sometimes, but not always, exhibits periodicity with P_M^B, and diel variation in P-I parameters is sometimes, but not always, associated with variation in chlorophyll (Harding et al., 1982a, b; Erga and Skjoldal, 1990; Kana et al., 1985). Although there may be diel variation in both α and P_M^B, variation in P_M^B is expected to have a greater effect on areal photosynthetic rates in our study system because most production in Lake Michigan occurs at high irradiances in the epilimnion (see Chapter 3). α has a larger effect on photosynthetic rates at lower irradiances deeper in the water column, so diel variation in α should not cause large differences in our areal production estimates.

Although P-I parameters are known to vary throughout the day, we are most concerned about potential diel variation in areal production. In a marine system, Harding et al., (1982b) found that the application of mid-day P-I parameters from model experiments produced areal production results 13% lower to 25% higher than simulated *in situ* incubations, which naturally incorporate variation in P-I parameters throughout the day. However, errors associated with and without accounting for diel variation in the P-I relationship were within the natural range of errors of laboratory photosynthesis experiments (Harding et al., 1982b). Further, differences between actual daily production and production calculated with variable P-I parameters were similar to differences in production caused by the natural patchiness and variability of phytoplankton communities (Harding et al., 1982b; Platt, 1975; Fee, 1975). In an oligotrophic to mesotrophic freshwater system, Fee (1975) found incorporating diurnal variability into photosynthetic models only affected annual estimates by 5-11%, which is within the range of sampling and experimental error. In spatial surveys, biomass differences among sites may also help diminish the potential effect of P-I variability on areal photosynthesis. Overall, we may conclude that our whole-lake spatial comparisons are generally comparable despite potential diel oscillations in the P-I relationship.

Variable sampling times did not appear to affect our conclusions about spatial patterns in productivity. During the spring 2016 survey, MI23 and MI-N were sampled at night. If MI23 was sampled during the day, higher photosynthetic rates may be expected due to higher P_M^B during the day and MI23 would still have the highest production, so our conclusions would not be affected. If MI-N were sampled during the day, areal production may be higher, but growth estimates suggest MI-N is similar to MI34 sampled during the day and production was similar between these two sites. In spring 2017, all samples were collected at night except MI34 and removing MI34 does not change the general decrease in production from south to north. In summer 2017, all

samples were collected during the day except GB1. GB1 production may be biased low due to night sampling, so production may be even higher than measured and this does not affect our conclusions that production is highest in the northern basin. Therefore, it may be concluded that our whole-lake survey spatial comparisons are valid.

Overall, whole-lake surveys revealed south-north patterns in production and growth estimates during spring and summer. Nutrient, light, and temperature were likely all limiting phytoplankton growth in the spring, and there may have been sediment resuspension close to shore in spring 2016. Spatial patterns in growth, biomass, and production during the spring were not always equal, suggesting spatial variability in phytoplankton loss processes. During the summer, spatial patterns in growth, biomass, and production agreed, and higher production and growth in the northern basin were related to lower phosphorus limitation. Higher phytoplankton production in the northern basin may contribute to the greater biomass of higher trophic levels in that region, although many other factors are also responsible for controlling spatial patterns in preyfish and piscivores.

Nearshore-offshore comparisons

Patterns in production, biomass, growth rates, and seston stoichiometry from nearshore to offshore displayed significant variability. In July, there was evidence of strong upwelling during the week before sampling, and the lake was re-stratifying on our day of sampling. Production, growth estimates, and biomass were highest nearshore, suggesting nutrients from upwelling during the past week may have stimulated production on the day of sampling. C:P and N:P, however, were highest at AW15, suggesting carbon fixation was outpacing the ability of phytoplankton to build cellular components or hypolimnetic seston high in C (Pothoven and Fahnenstiel, 2013) was a significant contributor to nearshore seston. In October, upwelling was strong on the day of

sampling, as there was no stratification nearshore. Unlike July, nutrients from upwelling had not yet stimulated nearshore production, as the nearshore zone appeared to be composed of unproductive hypolimnetic water and chlorophyll, production, and growth rates were highest offshore. The effect of upwelling on nearshore production appeared to occur at least several days after the upwelling event when the lake began to re-stratify, but time series observations from before, during, and after upwelling are needed to better determine how phytoplankton communities respond to upwelling events in Lake Michigan.

In September, phosphorus limitation was lowest, and production, biomass, and growth estimates were highest nearshore and there was no evidence of upwelling or downwelling. In the absence of mussel grazing and upwelled nutrients nearshore, external nutrient loading and more efficient nutrient recycling due to less nutrient loss to sinking and burial nearshore would likely be the cause of higher nearshore production. External nutrient supplies may contribute some to higher nearshore production in September, but we did not quantify this. In the presence of mussels, however, higher nearshore production may be due to soluble reactive phosphorus (SRP) excretion by mussels, which has been shown to exceed the phosphorus loading rate of the Milwaukee River by a factor of four (Bootsma, 2009). Grazing by mussels, however, may result in lower biomass nearshore, as mussels have a greater effect on phytoplankton biomass in shallow areas where mixing delivers more phytoplankton to the boundary layer where mussels filter (Rowe et al., 2015; Yousef et al., 2014; Zhang et al., 2011). Although mussel grazing reduces phytoplankton biomass more in nearshore regions, the role of mussels as nutrient suppliers has been shown to exceed their impact as phytoplankton grazers (Zhang et al., 2011). Our results may support the hypothesis of mussels as "algal fertilizers" because phosphorus limitation was lowest, and growth, biomass, and production were highest nearshore in September where mussel influence was greatest.

In addition to generally higher production nearshore, phosphorus limitation was always lowest in the shallow and mid-depth region, suggesting higher food quantity and quality nearshore. Higher algal P content in this region may result in more efficient energy transfer to invertebrates because food quality, along with food quantity and water temperatures, are the most important factors controlling invertebrate production (Sterner and Hessen, 1994; Stockwell and Johannsson, 1997). From 2007 to 2012, volumetric zooplankton biomass in southeastern Lake Michigan was higher at 45 m than 110 m or 15 m (Pothoven and Fahnenstiel, 2015b), which may be due to reduced predation pressure or higher quality food resources at 45 m because the highest phytoplankton biomass was not observed at 45 m. This potential nearshore bottom-up effect may be beneficial for the many fish species, such as alewife and yellow perch, that spend part of their life cycles feeding in the nearshore zone of Lake Michigan (Withers et al., 2015).

Despite limited replication from only three transects, the data presented here indicate that production is generally higher nearshore and highly dependent on upwelling. Considering upwelling had a significant effect on nearshore production, and upwelling occurs on 58.6% of the days of the stratified season lake-wide (Plattner et al., 2006), it is possible that mean nearshore production may be lower than mean offshore production (Fahnenstiel et al., 2016). It appears, however, that this may not be due to the influence of mussels as grazers, as was supposed by Fahnenstiel et al. (2016), but rather to the influence of upwelling, although we cannot assess the relative importance of these two factors. The nearshore region of Lake Michigan is highly dynamic, and more frequent sampling is required in order to gain a better understanding of the mechanisms controlling nearshore-offshore production differences. More frequent empirical measurements of photosynthesis are especially important due to the limitations of remote sensing in the nearshore zone.

Summary & conclusions

In conclusion, this study highlights seasonal and interannual spatial variability in phytoplankton production, growth estimates, and seston stoichiometry in Lake Michigan. Spatial patterns in spring production and growth estimates differed between years, and no single factor appeared to control spring spatial patterns in production and growth perhaps because nutrients, temperature, and light are all suboptimal during the spring. During the summer, phytoplankton production and growth estimates were higher in the northern basin likely due to nutrient influence from Green Bay and reduced mussel impacts in the northern basin. Nearshore production was generally higher than offshore production, except during upwelling events. Analyzing seston stoichiometry along with primary production allowed us to not just draw conclusions about spatial variability in phytoplankton production, but also infer the variability of food quality available to consumers. The northern basin and nearshore zone of Lake Michigan generally appeared to be the most productive and provide the highest quality food resources to higher trophic levels. Spatial variation in production and food quality suggests variation in trophic efficiency in Lake Michigan, which has implications for fisheries management. Most importantly, our results suggest that the northern basin of Lake Michigan may have a higher carrying capacity than the southern basin due to higher summer production and seston food quality.

Chapter 3: Temporal dynamics of phytoplankton production in southwestern Lake Michigan

Introduction

Understanding the temporal dynamics of phytoplankton production is essential to understanding overall ecosystem dynamics (Wetzel, 2001). In the 1980s and 1990s, extensive research on the dynamics of Lake Michigan phytoplankton was conducted to understand the factors controlling phytoplankton dynamics following food web restructuring and reductions in phosphorus in the 1970s (Fahnenstiel and Scavia, 1987a; Fahnenstiel et al., 1989; Fahnenstiel and Carrick, 1992; Scavia and Fahnenstiel, 1987). Due to this extensive research, we gained a comprehensive understanding of phytoplankton dynamics in Lake Michigan and its relation to nutrient loading, zooplankton dynamics, and the top-down influence of planktivorous fishes (Scavia et al., 1988).

During spring mixing, temperature, nutrient, and light interact to control phytoplankton growth and production (Fahnenstiel et al., 2000). Diatoms were historically the dominant taxa of spring communities (Fahnenstiel and Scavia, 1987). As stratification develops, the supply of nutrients from the sediment and the hypolimnion to the epilimnion is reduced, and epilimnetic production is limited by nutrients, particularly phosphorus (Schelske and Stoermer, 1971; Fahnenstiel and Scavia, 1987b). External nutrient loading minimally affects offshore phytoplankton over the short term during the stratified period, so nutrient supplies within the epilimnion are controlled by internal recycling (Scavia, 1979). Epilimnetic nutrient recycling mainly results from the decomposition of organic material, phytoplankton nutrient excretion, and zooplankton nutrient excretion (Rigler, 1973), but zooplankton-driven nutrient recycling is the dominant component of epilimnetic nutrient recycling in the Great Lakes (Scavia, 1979; Scavia and Fahnenstiel, 1987;

Scavia et al., 1988). Below the thermocline, a deep chlorophyll layer (DCL) develops due to *in situ* growth, photo-acclimation (increased chlorophyll content per cell under low-light conditions), and the settling of algal cells (Fahnenstiel and Scavia, 1987a; Moll et al., 1984), and phytoplankton growth is controlled by nutrient-light interactions (Fahnenstiel et al., 1984) and zooplankton grazing (Fahnenstiel and Scavia, 1987a). Historically, production below the epilimnion accounted for 50% of total summer water column production, and 30% of total production was found within the DCL (Fahnenstiel and Scavia, 1987b). In the fall, stratification breaks down and phytoplankton production is again controlled by temperature-nutrient-light interactions during mixing (Scavia, 1979).

Most research on temporal phytoplankton dynamics in Lake Michigan occurred over three decades ago, and the Lake Michigan food web has undergone significant restructuring since the 1990s (Bunnell et al., 2014; Madenjian et al., 2015). Continued reductions in phosphorus (Barbiero et al., 2018) and invasive quagga mussel (*Dreissena rostriformis bugensis*) filtering (Nalepa et al., 2014; Rowe et al., 2015; Vanderploeg et al., 2010) combined have increased water clarity (Binding et al., 2015; Yousef et al., 2017), altered phosphorus cycling (Hecky et al., 2004), and dramatically affected the lower food web (Bunnell et al., 2018). More specifically, there have been significant reductions in phytoplankton production (Fahnenstiel et al., 2010, 2016) and shifts in phytoplankton community composition away from diatoms and towards smaller taxa, such as cyanobacteria (Carrick et al., 2015; Fahnenstiel et al., 2010). Integrated DCL chlorophyll concentrations (size of the DCL) and the deep chlorophyll maximum (DCM) concentration have also been reduced since the mussel invasion (Pothoven and Fahnenstiel, 2013). Offshore zooplankton abundance and biomass have also decreased since the 1990s due to both resource limitation and predation by

invasive cladocerans, and the community has shifted towards greater copepod dominance (Engevold et al., 2015; Vanderploeg et al., 2012).

Recent lower food web changes in Lake Michigan suggest some temporal dynamics of phytoplankton production may have changed, but there have been few detailed studies of these changes. Although many studies have documented decreases in primary production since the mussel invasion, we do not currently know if these reductions in production are due only to decreases in biomass caused by mussels or if reductions in production may also be due to lower phytoplankton growth rates caused by decreasing phosphorus concentrations (Mida et al., 2010). A thorough understanding of the factors controlling phytoplankton production is especially important now because reductions in lower food web production correlate with reductions in prey fish abundance (Bunnell et al., 2014), which has raised concerns about the sustainability of Lake Michigan's commercially and recreationally important fisheries. Accurate field measurements of phytoplankton production are also needed to assess the accuracy of remote sensing-based production estimates (Fahnenstiel et al., 2016; Shuchman et al., 2013; Warner and Lesht, 2015) and validate remote sensing models because remote sensing has several limitations in estimating primary production (Lee et al., 2015). In Lake Michigan, one of the greatest concerns is that remote sensing cannot estimate sub-epilimnetic production, which has historically been a significant component of total water column production (Fahnenstiel and Scavia, 1987b).

To address the need for a better understanding of post-dreissenid phytoplankton dynamics in Lake Michigan, the objective of this study was to investigate the temporal variation of phytoplankton production in Lake Michigan. I directly quantified phytoplankton production at one site in southwestern Lake Michigan from May to November 2017 and used measurements to estimate growth rates and annual production. To gain an understanding of the factors controlling

temporal variation in production, I related production, growth estimates, and photosynthetic parameters to seston stoichiometry and physical conditions. I also compared epilimnetic and sub-epilimnetic production, investigated the mechanisms controlling the DCL, quantified the contribution of the DCL to total water column production, and determined the relative importance of different phytoplankton size classes in the DCL. Finally, I compared current and historical photosynthetic parameters and growth estimates to assess how mussels may have affected phytoplankton production in Lake Michigan.

In general, I hypothesized that areal phytoplankton production, DCL production, growth estimates, and photosynthetic parameters will have decreased since the mussel invasion due to reductions in phytoplankton biomass and increasing phosphorus limitation. I also hypothesized that nutrient parameters will be the most strongly related to production, growth estimates, and photosynthetic parameters due to strong phosphorus limitation in Lake Michigan. Finally, I expected picoplankton to be the dominant contributors to DCL production due to the significant decreases in microplankton in Lake Michigan.

Methods

Field operations

A 75 m depth site (AW75; 43.098ºN, 87.719ºW; Figure 2.1) near Milwaukee, Wisconsin was sampled approximately biweekly from May to November 2017 (Table 3.1). AW75 is 16 km northeast of downtown Milwaukee and 11.5 km southwest of Fox Point, a well-studied 100 m pelagic station (Cuhel and Aguilar, 2003; Engevold et al., 2015). On each day of sampling, a calibrated SeaBird CTD was used to determine vertical profiles of temperature, conductivity, chlorophyll *a* fluorescence, water clarity (measured as beam attenuation), pH, dissolved oxygen

(DO), and photosynthetically active radiation (PAR). Data were binned into 0.5 m intervals and downcast data were used in analyses. CTD chlorophyll *a* fluorescence was converted to chlorophyll concentrations following the methods described in Chapter 2, and DO concentrations (mg/L) were converted to DO percent saturation using the equations from APHA (1998).

Discrete water samples from two depths were collected for photosynthesis experiments and nutrient analyses (Table 3.1). All sampling occurred between 08:00 and 11:00 using a Niskin bottle and samples were stored in a dark cooler for no longer than three hours before experiments. 5 m was sampled on every occasion to represent the epilimnion (Carrick et al., 2015). When the water column was unstratified in May and November, 25 or 35 m was chosen as the second depth to characterize phytoplankton at mid-depth. From June to September, the fluorescence maximum was the second depth sampled. On October 9, the second sample collected was from the base of the epilimnion. On October 23, the second depth sampled was the DO percent saturation maximum in the metalimnion.

Table 3.1. Epilimnetic and mid-depth depths sampled (m) for photosynthesis experiments and nutrient analyses.

	11 May	26 May	08 Jun	23 Jun	11 Jul	25 Jul	16 Aug	29 Aug	12 Sep	25 Sep	09 Oct	23 Oct	13 Nov
Epi.	5	5	5	5	5	5	5	5	5	5	5	5	5
Mid.	35	35	26	27	30	40	25	22	38	28	10	16	25

DCL definitions

Stratification was defined as the presence of a thermocline with a temperature gradient of at least 0.5ºC/m (Scofield et al., 2017), and the thermocline depth was defined as deepest depth with a temperature gradient of 0.5ºC/m. The DCL was defined as the region below the epilimnion where chlorophyll concentrations exceeded 2 mg m^{-3} (Fahnenstiel and Scavia, 1987a; Pothoven and Fahnenstiel, 2013), and the deep chlorophyll maximum (DCM) was the depth within the DCL with the greatest chlorophyll concentration. The beam attenuation (BAT) maximum was the depth where beam attenuation was greatest, and the dissolved oxygen (DO) percent saturation maximum was the depth below the epilimnion where DO percent saturation was highest. In addition to *in situ* production measurements, the DO percent saturation and BAT maxima were used to assess DCL productivity. If the DCL, DO maximum, and BAT maximum overlap and production is high, the DCL is assumed to be maintained by *in situ* growth due to increased particle concentrations and DO supersaturation (Scofield et al., 2017). If the depths do not overlap and production is low, the DCL may be due to photo-acclimation and/or the settling of senescent cells rather than *in situ* growth (Fahnenstiel and Scavia, 1987a).

Nutrient analyses

Chlorophyll *a*, particulate phosphorus (PP), particulate carbon (PC), and particulate nitrogen (PN) were analyzed according to the methods outlined in Chapter 2.

Photosynthesis experiments & calculations

Photosynthesis experiments and areal production calculations were performed following the methods described in Chapter 2. In this chapter, however, areal production was calculated using

measured PAR and simulated PAR. To facilitate comparisons across dates and eliminate the effects of variation in cloud cover (Figure 3.1, Table 3.2), surface PAR was simulated using the method outlined in Chapter 2. To calculate annual production, monthly averages (Figure 3.4), and daily variation (Figure 3.5), measured surface PAR was used in production calculations. Solar radiation (W/m^2) was measured in 30-minute intervals on a 20 m buoy near Milwaukee (43.100ºN, 87.850 ºW) from May to October. In November, no buoy data was available and solar radiation data was obtained from a National Weather Service station in Horicon, Wisconsin (43.571 ºN, -88.609 ºW; https://mesowest.utah.edu/). Solar radiation (W/m^2) was multiplied by 0.46, the estimated proportion of PAR in shortwave radiation, to calculate PAR (W/m^2), then PAR (W/m^2) was multiplied by 4.56 to achieve PAR fluence rate (µmol photons m^{-2} s^{-1}; Fahnenstiel et al., 2016; Malkin et al., 2008; Wetzel, 2001). PAR in µmol photons m^{-2} s^{-1} was converted to mol photons m^{-2} hr^{-1} for integrations (Lang and Fahnenstiel, 1996). To obtain daily production estimates for days not sampled, P-I parameters, k_{PAR}, and chlorophyll were linearly interpolated between dates (Fee, 1990).

Drivers of seasonal variation

Based on Fee (1973a, b)'s method for calculating areal production, temporal variation in areal production is due to variation in surface irradiance, chlorophyll, underwater light extinction, and P-I parameters. To determine the relative importance of various regulators of primary production at AW75, daily areal production was calculated by holding three variables constant and allowing the fourth to vary as observed empirically. For determining production variation due to chlorophyll, production was calculated using constant simulated surface irradiance, mean epilimnetic P-I parameters (surface P_S^B = 1.73, mid-depth P_S^B = 0.96; surface α = 6.75, mid-depth

$\alpha = 9.66$), mean k_{PAR} (0.137 m^{-1}), and measured chlorophyll profiles for all dates. Variation due to epilimnetic P-I parameters was calculated using constant surface irradiance, mean k_{PAR}, constant chlorophyll, and measured P-I parameters. Variation due to k_{PAR} was determined by using constant chlorophyll, mean epilimnetic P-I parameters, constant surface irradiance, and measured k_{PAR}. Variation due to surface irradiance was calculated using mean epilimnetic P-I parameters, mean k_{PAR}, constant chlorophyll, and measured surface PAR. Daily variation (Figure 3.5a-b) for each variable was calculated as:

$$\% \text{ deviation from mean} = \frac{\text{daily areal photosynthesis} - \text{mean areal photosynthesis}}{\text{mean areal photosynthesis}} \text{ x } 100\%.$$

Size fractionation

On three occasions during the stratifed period, seston analyses and photosynthesis experiments from the sub-thermocline chlorophyll *a* fluorescence maximum were separated into picoplankton (0.7-2 µm), nanoplankton (2-20 µm), and microplankton (20-200 µm) size classes (Carrick et al., 2015). Samples were first passed through a 200 µm mesh to remove larger zooplankton, after which the filtrate was passed through a 20 µm Nitex nylon mesh. Phytoplankton captured on the 20 µm mesh were back-flushed with a DI squirt bottle and filtered onto a 0.7 µm GF/F filter to collect microplankton. The filtrate from the 20 µm mesh was then filtered onto a 2 µm polycarbonate membrane filter, which was back-flushed and filtered onto a 0.7 µm GF/F to collect nanoplankton. Filtrate that passed through the 20 µm mesh was filtered onto a 0.7 µm GF/F to catch the remaining picoplankton. All GF/F filters were rinsed with DI and stored in a freezer or desiccator until analysis. For photosynthesis measurements, samples were size-fractionated after the incubation. Photosynthetic rates of bulk seston from the sub-thermocline chlorophyll *a* fluorescence maximum were not measured alongside size-fractioned experiments, so P-I

parameters from these depths were calculated as biomass weighted averages for areal production calculations.

Data Analysis

All data analysis was performed using R version 3.4.4 (R Core Team, 2018). Production to biomass (P:B) ratios for epilimnetic samples and molar seston stoichiometry (C:N, C:P, N:P) were calculated and analyzed according to the method outlined in Chapter 2. I_k (mol photons m^{-2} hr^{-1}), calculated as P_M^B / α^B, represents the onset of light saturated photosynthesis and was used as an index of low-light acclimation (lower I_k is indicative of greater low light acclimation). Phytoplankton C:Chl ratios (phytoplankton carbon calculated as 40% seston carbon) were also used to assess light acclimation, with lower ratios generally indicating greater low-light acclimation and better nutrient conditions (Geider et al., 1997). P_M^B and α^B un-normalized to chlorophyll (P_M and α, respectively) were used to assess the cumulative photosynthetic capabilities of the entire phytoplankton community. Linear regressions between environmental parameters and photosynthetic parameters, areal production, and growth estimates were performed using the 'lm' function in R (R Core Team, 2018). An F-test of overall significance was used to evaluate each regression, and significant relationships were defined as $p < 0.05$. Epilimnetic P-I parameters from this study were compared to epilimnetic P-I parameters from Fahnenstiel et al. (1989) using a Student two sample t-test when all assumptions were met, and a Welch two-sample t-test when data violated the homogeneity of variance assumption (R Core Team, 2018).

Results

Seasonal vertical structure

Stratification at AW75 occurred in mid-June and lasted until late October (Figure 3.1a). Following the onset of stratification, a DCL developed in the hypolimnion and progressed deeper into the water column until it reached the maximum in late July (Figure 3.1b). When the DCL was present, epilimnetic chlorophyll concentrations were low. From mid-August through November, no DCL was present and chlorophyll was higher in the upper water column, but chlorophyll concentrations were highly variable. Generally, surface chlorophyll decreased from August to October, then stratification broke down in November and surface chlorophyll increased.

Volumetric production was lowest in May and November when the water column was unstratified (Figure 3.1c). In early June, chlorophyll below 15 m did not meet the DCL criteria, but production below 15 m exceeded surface production. On June 23, 27% of total water column production was within epilimnion, 73% was below the epilimnion, 37% was below the thermocline depth, and 25% was within the DCL (Table 3.2). On July 11, production was similarly vertically distributed, but only 20.5% of production was within the DCL (Table 3.2). On July 25, 58% of total production was within the epilimnion, 42% was below the epilimnion, and production within the DCL and below the thermocline decreased to 7% and 14% of total water column production, respectively. When the DCL was measured in June and July, an average 17% of water column production occurred within the DCL.

The majority of total water column production after July was found within the epilimnion. Volumetric production was greatest in August and September within the upper 10 m, corresponding to the greatest epilimnetic temperatures and epilimnion depth (Figure 3.1a). During

the stratified period, an average of 61% of measured production occurred within the epilimnion and only 16% occurred below the thermocline (Table 3.2; Figure 3.1c). In October, stratification began to break down and peaks in production were observed below 5 m. Production decreased from October through November despite relatively high chlorophyll concentrations down to 50 m in November. On October 23, the metalimnetic oxygen peak and epilimnion were sampled, and higher production was found in the metalimnion.

The vertical structure of DO percent saturation did not exhibit much seasonal variation (Figure 3.1d). The entire water column was near or above saturation for the entire season. Following stratification in June, peaks in DO percent saturation occurred in the metalimnion. The greatest DO percent saturation maximum occurred on Sep 12 and corresponded to the steepest thermocline. When a DCL was present, the DO percent saturation maximum was always shallower than the DCL (Table 3.3).

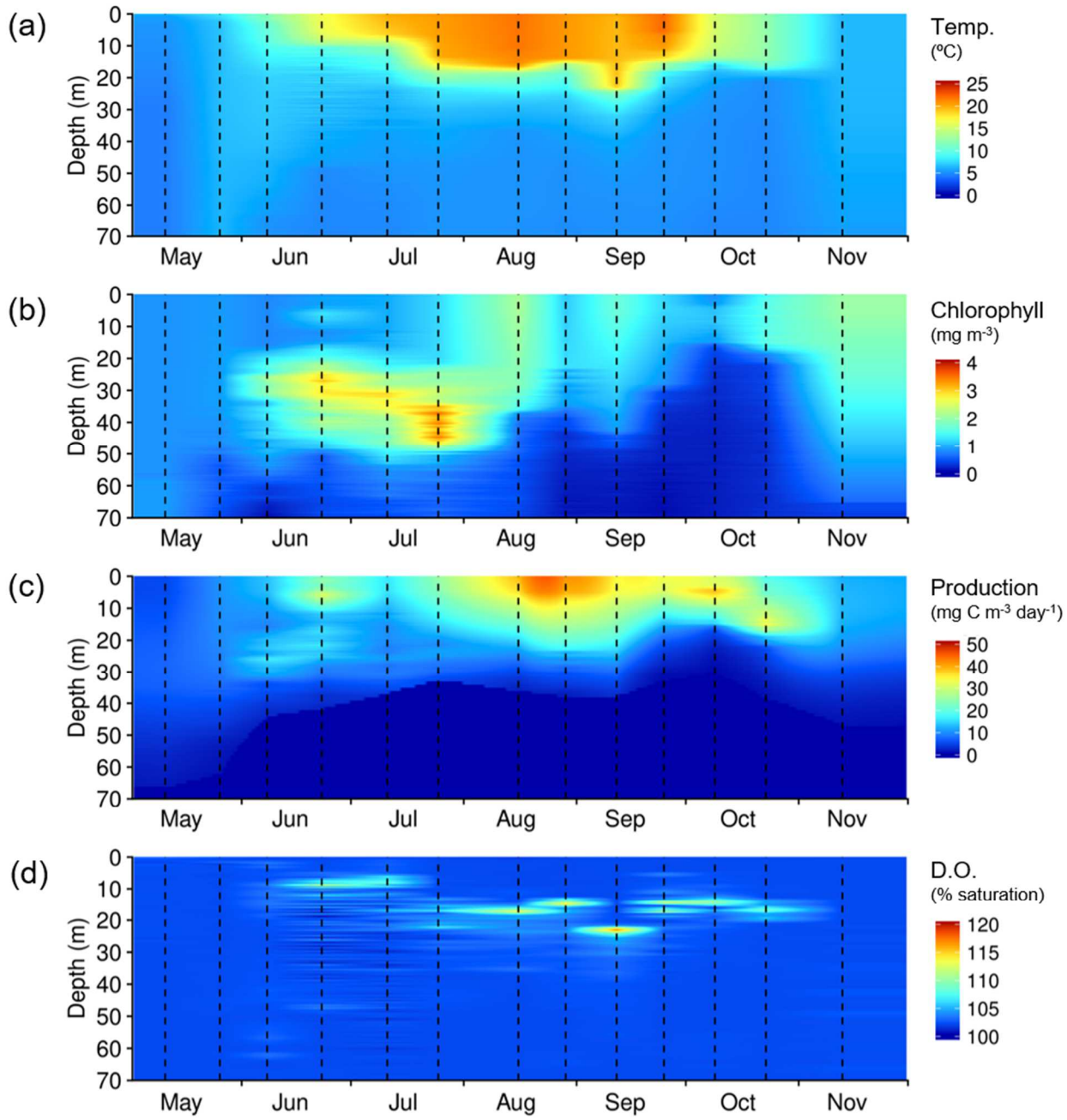

Figure 3.1. Seasonal vertical structure of temperature, chlorophyll, phytoplankton production, and dissolved oxygen percent saturation. Vertical lines indicate sampling dates. Linear interpolation was used between sampling dates for temperature, chlorophyll, and DO percent saturation. Production was calculated for each day using P-I parameters, k_{PAR}, and biomass linearly interpolated between dates and simulated PAR.

Table 3.2. Proportion of total water column production found within the epilimnion, below the epilimnion, and within the deep chlorophyll layer (DCL; chlorophyll > 2 mg m^{-3}) during the stratified period. Thermocline depth was defined as the deepest depth with a temperature gradient of 0.5ºC/m.

	Epi. Depth (m)	Therm. Depth (m)	% w/in Epi.	% below Epi.	% below Therm.	% w/in DCL
23 Jun	6	17	27.4	72.6	37.7	25.0
11 Jul	6	18	24.5	75.5	39.6	20.2
25 Jul	13	24	58.2	41.8	14.3	6.6
16 Aug	15	26	70.7	29.3	6.4	-
29 Aug	13	20	59.6	40.4	19.0	-
12 Sep	22	32	82.4	17.6	3.4	-
25 Sep	11	20	68.8	31.2	7.6	-
09 Oct	12	18	88.4	11.6	3.9	-
23 Oct	14	21	64.8	35.2	8.9	-
MEAN	12.4	21.8	60.5	39.5	15.6	17.3

Table 3.3. Comparisons of the measured deep chlorophyll layer (DCL) and deep chlorophyll maximum (DCM) with euphotic zone depth (Z_{eu}; 0.5% surface irradiance), beam attenuation maximum (BAT max) depth, and dissolved oxygen percent saturation maximum (DO max) depth.

	Z_{eu} Depth (m)	DCL Range (m)	DCM Depth (m)	BAT Max Depth (m)	DO Max Depth (m)
23 June	41	22-41	27	24	9
11 July	36	26-39	30	17	8
25 July	32	28-48	40	27	17

Characteristics of epilimnetic and mid-depth phytoplankton

Seston stoichiometry and phytoplankton growth estimates

Epilimnetic and mid-depth phytoplankton communities displayed seasonal patterns in chlorophyll, nutrient limitation, and growth rates (Figure 3.2a-f). Epilimnetic chlorophyll concentrations increased from May to August as temperatures increased, generally decreased from August to October, then increased again in late October and November with the breakdown in stratification (Figure 3.2a, 3.3f, 3.1b). Mid-depth chlorophyll was greatest in the DCL in late June and July and decreased throughout the rest of the season. Phosphorus deficiency was generally greater in epilimnetic phytoplankton (Figures 3.2e-f), but patterns in C:N between mid-depth and epilimnetic phytoplankton were more variable (Figure 3.2d). Epilimnetic C:P and C:N generally increased over time and as epilimnetic temperatures warmed but dropped in August and September during the warmest temperatures (Figure 3.2d-e, Figure 3.3f). Conversely, epilimnetic N:P dropped as temperatures warmed, but lows were also observed with the peak in temperature (Figure 3.2d, 3.3f). During the stratified period, mid-depth C:P and N:P were generally highest and C:N was generally lowest during the period of the DCL (Figurers 3.2e-f).

Epilimnetic phytoplankton generally displayed higher growth rate estimates (June-August mean = 0.48 day^{-1}) than mid-depth phytoplankton (June-August mean = 0.16 day^{-1}; Figure 3.2b). Epilimnetic growth rates increased from May to August and decreased from August to November, following the trend in temperature (Figure 3.3f). The highest epilimnetic growth rates in August corresponded to the highest temperatures and lowest C:P and N:P. Mid-depth growth rates were similar to epilimnetic growth rates during mixing periods, but lower than epilimnetic growth rates during the stratified period. Growth rates within the DCL decreased as the DCL moved deeper into

the water column (DCL mean = 0.13 day^{-1}). Epilimnetic phytoplankton C:Chl was lowest during the highest growth rates (Figure 3.2b-c). Mid-depth C:Chl was lowest during the DCL, but increased after the DCL dissipated. During the period of the DCL, phytoplankton C:Chl averaged 46 in the epilimnetic community, and 20 in the DCL community.

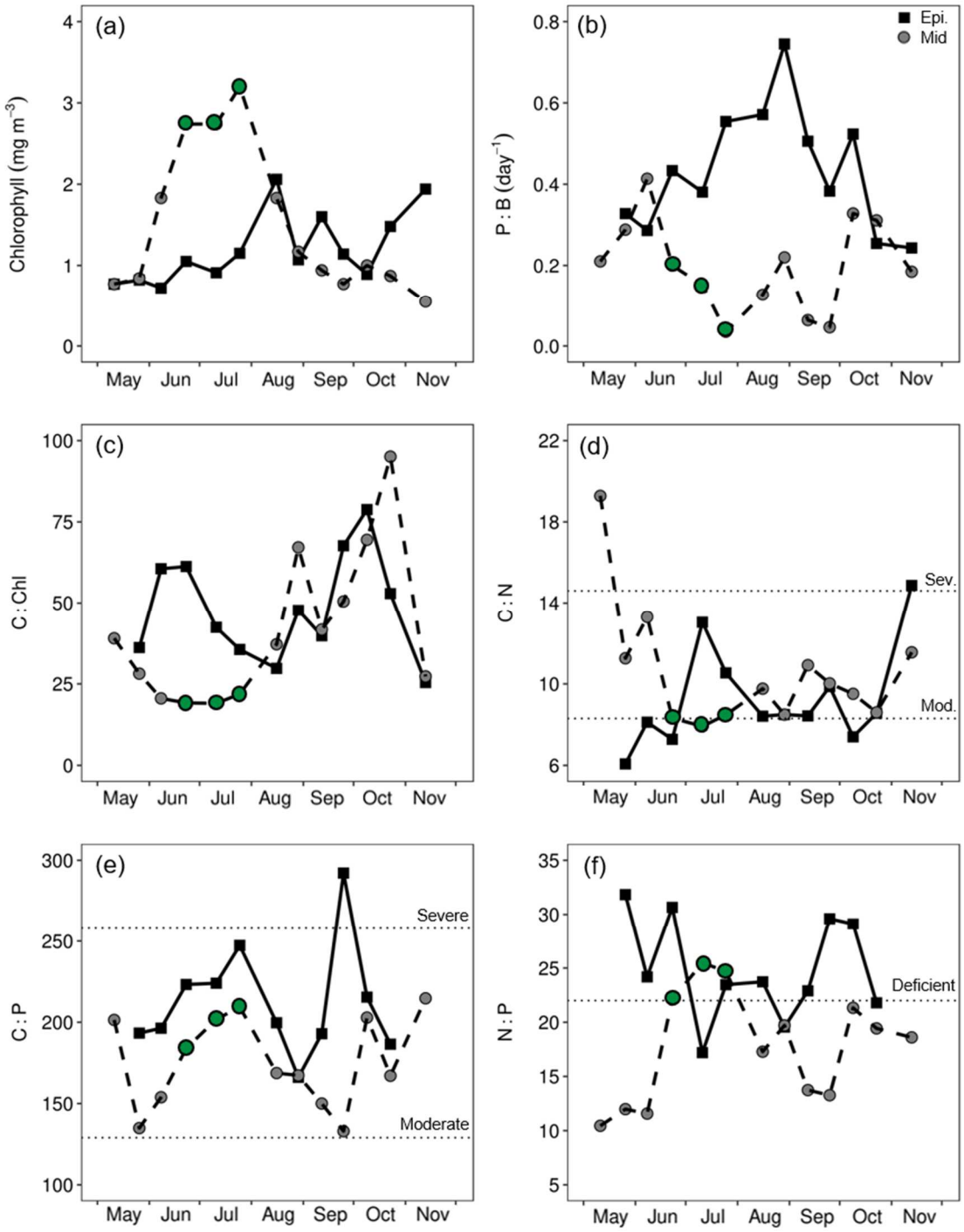

Figure 3.2. Seasonal variation in epilimnetic and mid-depth chlorophyll, growth rates, phytoplankton C:Chl, and seston stoichiometry. Large green points represent DCL. Dotted lines indicate nutrient deficiency criteria from Healy and Hendzel (1980).

P-I parameters

Epilimnetic and mid-depth phytoplankton displayed different photosynthetic characteristics (Figure 3.3a-e). P_M^B was higher in the epilimnion during the stratified period and increased from May to August following the increase in temperature (Figure 3.3a, f). The highest epilimnetic P_M^B values were measured on October 9 and August 29, corresponding to some of the lowest C:P and C:N during the stratified period and the highest growth rates (Figure 3.2b, d-e). Epilimnetic P_M followed the trend of epilimnetic temperature exactly except for a peak in June that corresponded to a peak in P_M^B (Figure 3.3a, c, f). Mid-depth P_M^B decreased from May to late June as the DCL formed, then increased as the DCL broke down. Low P_M^B in the DCL corresponded to high phosphorus limitation, low phytoplankton C:Chl, and low growth rates (Figure 3.2b, c, e). The highest mid-depth P_M^B occurred in October at the base of the epilimnion and in the metalimnetic oxygen maxima. Mean epilimnetic and mid-depth P_M^B from May to October were 1.73 and 1.12 mg C mg chl^{-1} hr^{-1}, respectively.

α^B and α were generally lower in epilimnetic phytoplankton (Figure 3.3b, d). Mean epilimnetic and mid-depth α^B from May to October were 6.75 and 9.65 mg C mg chl^{-1} mol $photons^{-1}$ m^2, respectively. Epilimnetic α^B and α decreased as the epilimnion warmed and phosphorus limitation increased, but increased in September with the decrease in phosphorus limitation (Figure 3f, 2c, e). Mid-depth α^B was variable throughout the season but showed a generally increasing trend and was highest in the metalimnetic oxygen maxima sample in October. Within the DCL, α^B and α increased as the DCL grew and moved deeper into the water column. Epilimnetic I_k generally increased from May to August following the increase in temperature and C:P, then decreased in late August and September when nutrient limitation decreased (Figure 3.3f, 3.2c-d). I_k was lower

in mid-depth phytoplankton than epilimnetic phytoplankton and decreased within the DCL over time (Figure 3.3e).

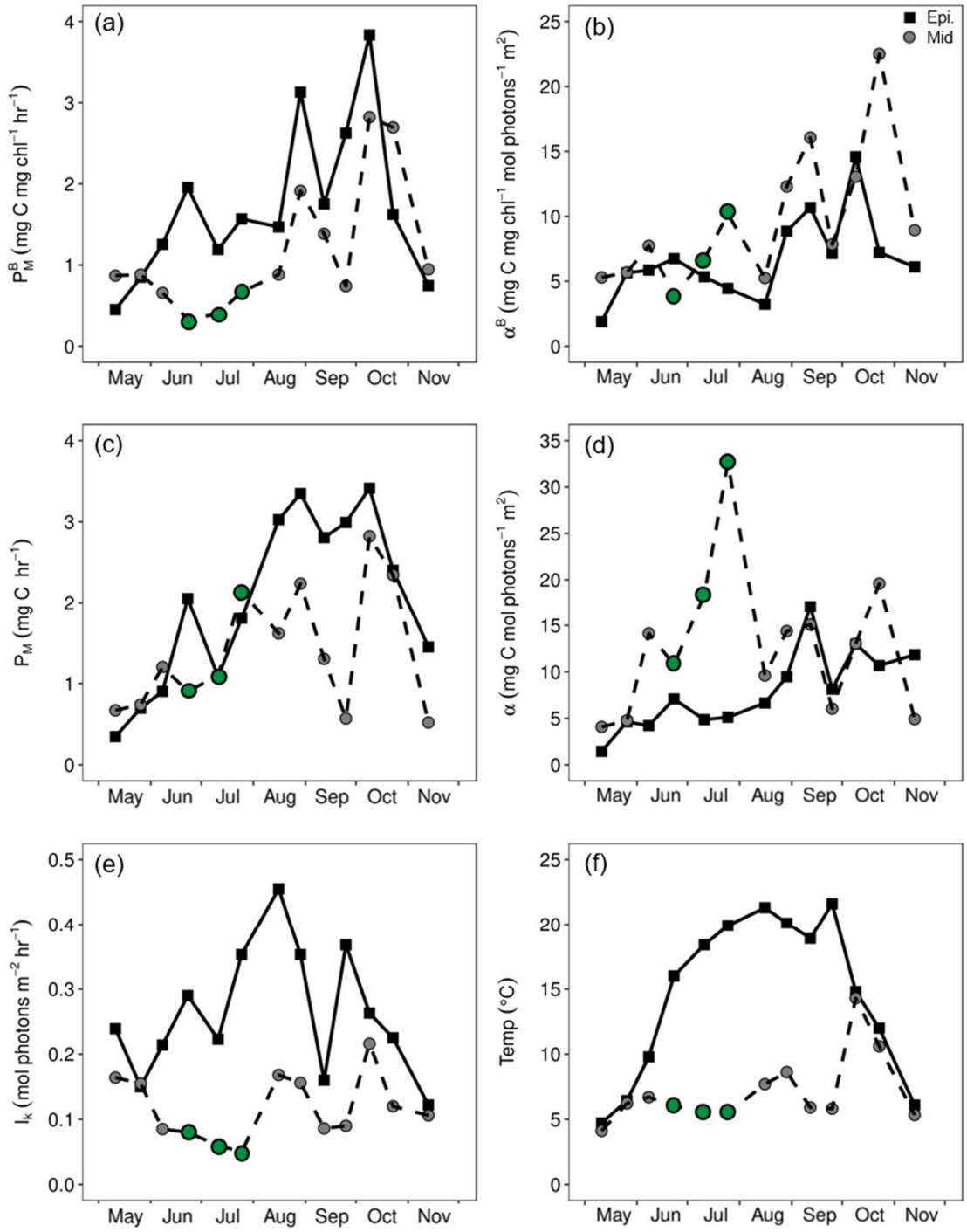

Figure 3.3. Seasonal variation in epilimnetic and mid-depth P-I parameters and temperature. Large green points represent DCL.

DCL structure

The entire DCL was always within the hypolimnion (Figure 3.1a-b). The DCM and most of the DCL were within the euphotic zone on June 23 and July 11 but were below the euphotic zone on July 25 (Table 3.3). The BAT maximum was near the top of the DCL on June 23, but the DCM, BAT maximum, and DO percent saturation maximum did not overlap during any DCL sampling date. Since the DO percent saturation maximum was always found within the metalimnion, the DO percent saturation maximum was always shallower than the DCM, DCL, and BAT maximum.

Mid-depth size-fractionated photosynthesis experiments revealed differences in chlorophyll and P-I parameters among phytoplankton size classes. When the DCL was present, chlorophyll was composed of 54% picoplankton (< 2 μm), 23-26% nanoplankton (2-20 μm), and 18-21% microplankton (20-200 μm; Table 3.4). Picoplankton displayed the highest P_M^B within the DCL, followed by nanoplankton then microplankton. The greatest low-light adaptation within the DCL, as revealed by higher α and lower I_k values, was also found in picoplankton. In late September, a DCL was not present and patterns among size classes differed. Picoplankton still made up the largest fraction of chlorophyll (46%), but microplankton (36%) were more abundant than nanoplankton (18%). Microplankton were the most low-light adapted in September, and nanoplankton displayed the highest P_M^B.

Table 3.4. Size-fractionated mid-depth photosynthetic parameters (± SE) and chlorophyll concentrations (mg m^{-3}). P_M^B and P_S^B = mg C mg chl^{-1} hr^{-1}. α^B = mg C mg chl^{-1} mol photons $^{-1}$ m^2. I_k = mol photons m^{-2} hr^{-1}. Bold indicates insignificant β parameter, but visible photoinhibition in the P-I curve. Underline indicates DCL sample.

Date	Size Class	P_M^B	α^B	β^B	I_k	[Chl] (%)
23 Jun	< 2 µm	0.36	5.75 ± 1.88	0.14 ± 0.05	0.06	1.47 (53.8)
(27 m)	2-20 µm	0.29	2.00 ± 0.34	0.21 ± 0.08	0.15	0.79 (28.8)
	20-200 µm	0.22	1.52 ± 0.13	0.51 ± 0.15	0.14	0.48 (17.5)
25 Jul	< 2 µm	0.57	15.7 ± 2.57	0.35 ± 0.05	0.04	1.71 (53.5)
(40 m)	2-20 µm	0.40	1.48 ± 0.23	**1.60 ± 4.16**	0.27	0.83 (25.9)
	20-200 µm	0.33	7.06 ± 3.88	**0.17 ± 0.09**	0.05	0.66 (20.6)
25 Sep	< 2 µm	0.67	7.21 ± 0.92	0.56 ± 0.15	0.09	0.35 (46.2)
(28 m)	2-20 µm	0.86	6.55 ± 0.41	1.12 ± 0.20	0.13	0.14 (18.0)
	20-200 µm	0.72	9.27 ± 3.24	**0.19 ± 0.11**	0.08	0.28 (35.8)

Seasonal patterns of areal production

Daily areal production calculated using measured surface PAR generally increased from May to August and decreased from August to November (Figure 3.4a). The greatest production occurred in late August (max 804 mg C m^{-2} day^{-1}) with the warmest temperatures, highest growth rates, and lowest nutrient limitation (Figure 3.3f, 3.2b, d-e). Two small peaks in production were also found in June and October that corresponded to peaks in P_M^B (Figure 3.3a). Mean monthly production (± 1 standard deviation) was highest in August (585 ± 107 mg C m^{-2} day^{-1}) and lowest in May (287 ± 61 mg C m^{-2} day^{-1}; Figure 3.4b). Mean summer production (± 1 standard deviation) from June to August was 470 ± 117 mg C m^{-2} day^{-1}, and total production from May to November was 90 g C m^{-2}. Production was not measured in January, February, March, April, and December 2017. To obtain an annual estimate of production at AW75, mean monthly winter production was assumed to be 200 mg C m^{-2} day^{-1} (see Figure 2c from Fahnenstiel et al., 2010), which is similar to the rates observed at the beginning and end of our study period. Using this estimate for winter production, annual production at AW75 was approximately 120 g C m^{-2} $year^{-1}$.

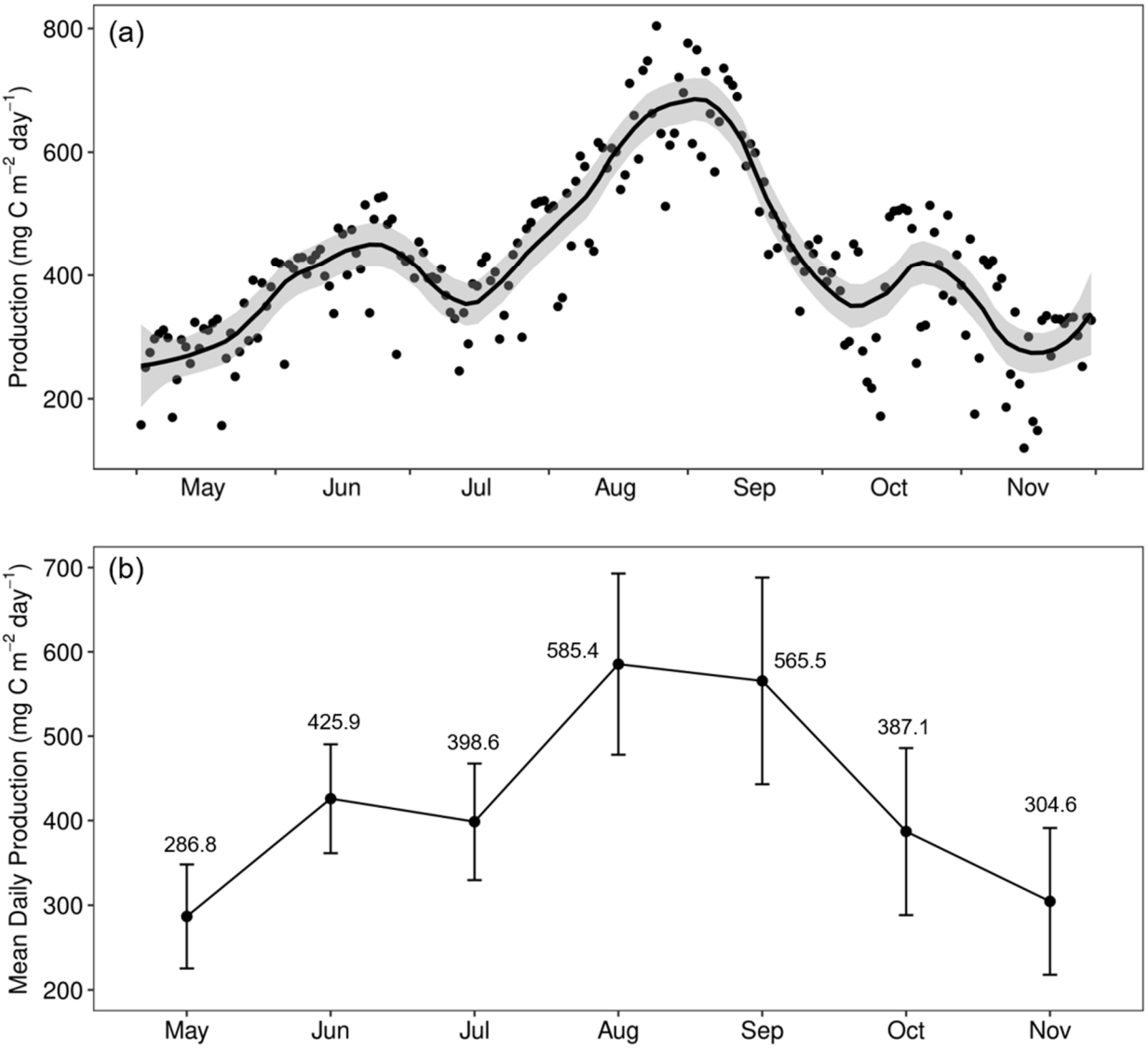

Figure 3.4. Seasonal variation in (a) daily areal production (Loess smoothing line ± 95% CI) and (b) monthly mean daily areal production (± 1 SD), both calculated using measured PAR from May to November. Daily areal production for days not sampled was calculated using interpolated P-I parameters, k_{PAR}, and chlorophyll.

Drivers of seasonal variation

Throughout most of the season, the greatest variation in production was due to variation in biomass and P-I parameters (Figure 3.5a). The effects of surface irradiance and light attenuation on areal production were greatest in May and November during deep mixing periods (Figure 3.5b). The peaks in areal production in late August and October (Figure 3.4a) appeared to due to high biomass and P-I parameters, while the peak in production in late June appeared to be due to a peak in P-I parameters, chlorophyll, and surface irradiance (Figures 3.5a-b). Higher production during November mixing than May maxing appeared to be due to higher chlorophyll and P-I parameters in November (Figure 3.5a, 3.3a-b, 3.2a, 3.1b). The mean variance in areal production due to light attenuation, chlorophyll, surface irradiance, and P-I parameters was 20.3%, 22.6%, 25.0%, and 36.4%, respectively (Figure 3.5a, b). The variance due to the combined effect of all four variables was 25.8%, lower than variance due to P-I parameters, suggesting temporal variation in the four variables had a counteractive effect on areal photosynthesis.

Seasonal variation due to chlorophyll appeared to counteract P-I parameter variation during the stratified period, as positive departures from the mean due to P-I parameters generally corresponded to negative departures from the mean due to chlorophyll (Figure 3.5a). In other words, higher P-I parameters were associated with lower chlorophyll concentrations, and vice versa. Mean percent departure for P-I parameters was greater than that of chlorophyll, however, suggesting environmental variables had a greater effect on P-I parameters. Variation due to underwater irradiance appeared to counteract surface irradiance except prior to stratification (Figure 3.5b), so high irradiance during stratification was associated with decreased underwater irradiance.

Since most production occurred within the epilimnion, regression analyses between epilimnetic conditions and P-I parameters, growth rates, and areal production were performed. Areal production, growth rates, P_M^B, and I_k were all significantly positively related to temperature but no other physical or chemical variables (Table 3.5). P_M^B was also significantly positively related to k_{PAR}, but α^B was not related to any nutrient or physical variable measured (Table 3.5). Production was also significantly positively related to epilimnetic growth rates (F statistic = 23.7, $p < 0.001$, $R^2 = 0.73$), meaning temperature and growth rates were the only two variables measured in this study that were related to areal production.

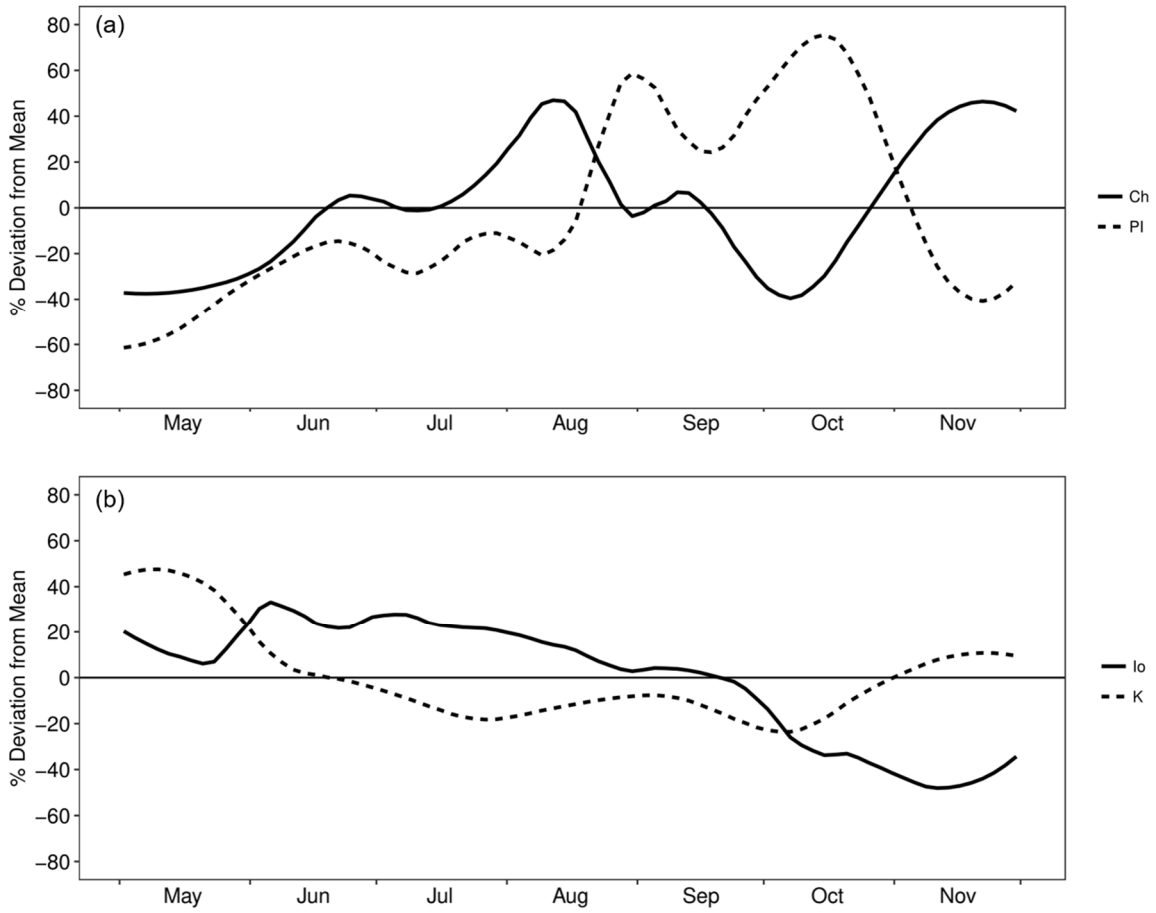

Figure 3.5. Seasonal variation in daily areal production estimates due to variation in chlorophyll (Ch), P-I parameters (PI), surface irradiance (I_o), and water clarity (k). Percent deviation from seasonal mean production was calculated by holding three variables constant and allowing the parameter of interest to vary as observed empirically.

Table 3.5. Linear regressions between environmental parameters and epilimnetic P_M^B (mg C mg chl^{-1} hr^{-1}), α^B (mg C mg chl^{-1} mol photons^{-1} m^2), I_k (mol photons m^{-2} hr^{-1}), areal production (mg C m^{-2} day^{-1}), and growth estimates (day^{-1}). Linear r^2 is presented in parentheses and the direction of relationship is indicated with + or –. F-test of overall significance was used to evaluate each relationship and bold indicates significant linear regressions where $p < 0.05$.

	P_M^B	α^B	I_k	Areal Prod.	P:B
Mean I_o	- (0.09)	- (0.19)	+ (0.07)	+ (0.06)	+ (0.13)
k_{PAR}	**+ (0.56)**	+ (0.29)	+ (0.28)	+ (0.24)	+ (0.24)
Temp.	**+ (0.33)**	+ (0.06)	**+ (0.51)**	**+ (0.50)**	**+ (0.52)**
C:P	+ (0.01)	- (0.02)	+ (0.10)	- (0.03)	- (0.03)
N:P	+ (0.02)	+ (0.03)	- (0.00)	- (0.03)	- (0.06)
C:N	- (0.12)	+ (0.08)	- (0.03)	- (0.00)	- (0.07)

Discussion

Epilimnetic production

Most phytoplankton production throughout the season (61%) was found within the epilimnion and epilimnetic production was highest in August and September. In 2017, production generally increased from May to August, peaked in late August, then generally decreased from September to November. Fahnenstiel et al. (2010) found a similar seasonal pattern in production in 2007 and 2008, where mean monthly production increased from March to July, then decreased from July to December. The late summer peak in production observed in 2007, 2008, and this study was not observed prior to the mussel invasion. In the 1980s and 1990s, production rapidly increased from March to May due to upward mixing of nutrients causing a spring diatom bloom, remained highest from April through July, then decreased after July as epilimnetic nutrient limitation increased (Fahnenstiel et al., 2010). Mussels, however, have had significant effects on the size of the spring diatom bloom and reduced spring and early summer production from 1983-1987 to 2007-2008 by 78% and 22%, respectively (Fahnenstiel et al., 2010). Therefore, the current late summer peak in production appears to reflect the loss of spring and early summer production, and it now appears that peak phytoplankton production may due to the peak in temperature.

Epilimnetic nutrient ratios, growth rates, P-I parameters, and production all appeared to be related to epilimnetic temperature. Nutrient limitation generally increased as the epilimnion warmed and nutrients were depleted by production, but nutrient limitation weakened in August and September when temperatures were warmest. Phytoplankton growth rates, chlorophyll, P_M^B, and production all peaked during this time. The reduction in epilimnetic nutrient limitation in August and September was likely due to increased nutrient recycling at warmer temperatures

(Scavia, 1979), as severe weather events did not occur near Milwaukee during this time (https://www.weather.gov/mkx/events) and summer epilimnetic phosphorus dynamics in the Great Lakes are controlled by internal recycling (Scavia, 1979).

The drivers of epilimnetic nutrient recycling are detritus decay, phytoplankton and zooplankton nutrient excretion, hypolimnion loading, and external loading (Rigler, 1973), but zooplankton-driven nutrient recycling has the greatest influence on offshore epilimnetic phosphorus dynamics and the influence of zooplankton-driven nutrient recycling is strongest during times of high zooplankton abundance and grazing (Scavia and Fahnenstiel, 1987; Scavia, 1979; Scavia et al., 1988). Zooplankton grazing physically releases nutrients from algae during feeding, and zooplankton egestion and excretion regenerate consumed nutrients (Korstad, 1983). 71 to 97% of the phosphorus released by zooplankton is SRP and 75% of the nitrogen released is ammonia (Butler et al., 1969; Corner and Newel, 1967; Jawed, 1969), which can both be directly used by phytoplankton and increase photosynthetic rates.

As total zooplankton abundance and biomass in Lake Michigan generally peak in August and September with the warmest temperatures (Driscoll et al., 2015; Vanderploeg et al., 2012), the lowest epilimnetic nutrient limitation and highest production and growth estimates in August and September in this study may be associated with the period of highest zooplankton-driven nutrient recycling. Even though net phytoplankton production may be higher during late summer due to greater nutrient recycling, this may not actually correspond to an increase in net ecosystem production (Scavia, 1979), as energy is being recycled within the epilimnion by producers and consumers rather than newly fixed by producers. As zooplankton-driven nutrient recycling has been an important factor affecting phytoplankton dynamics in past studies (Scavia, 1979) and may

be important in this study, future research should focus on understanding epilimnetic zooplankton grazing and nutrient recycling in Lake Michigan.

DCL production

Our results suggest that DCL production in Lake Michigan has decreased since the quagga mussel invasion. In 1983 and 1984, the DCL accounted for an average of 30% (range 4-74%) of total water column production from June to August (Fahnenstiel and Scavia, 1987b). In 2017, the DCL accounted for an average of 17.3% (range 7-25%) of total water column production in June and July. Integrated DCL chlorophyll concentrations and the DCM concentration have declined since the mussel invasion (Pothoven and Fahnenstiel, 2013), so it would be expected that DCL production would also decrease. A decline in DCL production is a major loss of food resources for higher trophic levels and is further evidence of declining summer productivity in Lake Michigan (Fahnenstiel et al., 2010; Warner and Lesht, 2015). It should be noted, however, that we only measured production within three DCLs in one year, whereas Fahnenstiel and Scavia (1987b) measured production within 14 DCLs across two years.

The Lake Michigan DCL is highly dynamic temporally (Fahnenstiel and Scavia, 1987a), and the mechanisms controlling the DCL varied within this study. On June 23, the DCL was highest in the water column and the BAT maxima occurred within the DCL, illustrating that the DCL was associated with an increase in particle concentrations and not just higher chlorophyll content per cell due to photo-acclimation . The highest DCL growth estimate and contribution to production were also found on June 23, suggesting *in situ* growth was important during early summer. I_k was low in the DCM, however, and the BAT maxima was near the top of the DCL, suggesting photo-acclimation was important near the base of the DCL. In July, the DCL moved deeper into the water

column, growth estimates decreased, phosphorus and low-light adaptation increased, and DCL production was reduced to only 7% of total water column production. The BAT maxima were also found higher in the water column in July, so the DCL was no longer associated with increased particle concentrations. Therefore, as the DCL deepens, photo-acclimation appears to become more important than *in situ* growth in maintaining the DCL.

No DCL was measured in August or September as in past studies (Fahnenstiel and Scavia, 1987a; Pothoven and Fahnenstiel, 2013). The lack of a DCL in August and September may have been due to increased zooplankton abundance during these months, as measured in past studies (Driscoll and Bootsma, 2015; Vanderploeg et al., 2012). Fahnenstiel and Scavia (1987a) illustrated that high zooplankton abundance in the DCL in August increased the loss of phytoplankton to grazing and resulted in a relatively rapid decrease in phytoplankton abundance from 20 to 40 m. Zooplankton grazing, therefore, may explain the loss of the DCL in August in this study even though other studies measured a DCL until September (Pothoven and Fahnenstiel, 2013). Overall, the mechanisms controlling the DCL in this study are consistent with Fahnenstiel and Scavia (1987a): *in situ* growth was most important early in the season, the importance of photo-acclimation increased as the DCL moved deeper into the water column, and zooplankton grazing possibly reduced the size of the DCL in August.

The metalimnetic DO percent saturation maximum has been used in previous studies to assess the productivity of the DCL (Scofield et al., 2017). In more productive lakes, such as Lake Ontario, the DCL is found within the metalimnion due to lower water clarity, and overlap of the metalimnetic DO maximum with the DCL and BAT maximum may indicate a productive DCL, although the contribution of physical and biological processes to oxygen maxima is highly variable (Wilkinson et al., 2015). In this study, peaks in DO were found within the metalimnion during

stratification, but the DO maxima never overlapped with the DCL or BAT maxima during the presence of a DCL. This may suggest that metalimnetic DO maxima in Lake Michigan during the presence of a DCL are due to physical processes, such as the warming of gases trapped below the thermocline, rather than biological processes (Wilkinson et al., 2015). Previous work in Lake Michigan, however, has illustrated metalimnetic peaks in production during the presence of a DCL, but the vertical structure of production is highly variable within and among years (Fahnenstiel and Scavia, 1987b; Moll et al., 1984; Cuhel and Aguilar, 2014). In this study, photosynthesis experiments on October 23 revealed higher P_M^B, α^B, growth rates and production within the metalimnetic DO maximum than the epilimnion, but this was late in the season and more sampling would be needed to conclude if the metalimnetic oxygen peak usually corresponds to a productivity peak in Lake Michigan. If growth rates and production were always higher in the metalimnetic oxygen maxima, this study may have underestimated production. This highlights the importance of characterizing photosynthesis at many depths within the water column in order to obtain accurate production estimates.

DCM chlorophyll and production were dominated by picoplankton less than 2 μm. Over 50% of DCM chlorophyll in June and July was attributed to picoplankton, and nanoplankton and microplankton contributed approximately 30% and 20%, respectively. Our results are consistent with Fahnenstiel et al. (2010), who illustrated that large diatoms are now a minor component of phytoplankton carbon (< 5%) in the July DCL. Bramburger and Reavie (2016), however, found over 50% of DCL phytoplankton biomass from 2007 to 2012 was diatoms, suggesting there may be spatial, temporal, and interannual variability in DCL community composition. DCL chlorophyll size distribution in this study was remarkably similar to that of epilimnetic chlorophyll in southeastern Lake Michigan (Carrick et al., 2001), suggesting vertical similarities in summer

epilimnetic and DCL phytoplankton communities. Fahnenstiel and Carrick (1992) and Fahnenstiel and Scavia (1987a) illustrated vertical variation in phytoplankton communities in the 1980s and 1990s prior to the mussel invasion, but Bramburger and Reavie (2016) found similarities between summer epilimnetic and DCL communities from 2007 to 2012. This may suggest that the vertical variation of phytoplankton has become more homogeneous since the mussel invasion, but our DCL samples were only limited to two dates (Table 3.4), and we did not compare DCL size-fractionated chlorophyll with epilimnetic chlorophyll on the same day.

Picoplankton also displayed the highest P-I parameters within the DCL. Higher P_M^B and α^B in picoplankton may be due to smaller cells having greater P uptake abilities than larger cells and greater light harvesting abilities due to less self-shading within the thylakoid membrane (Grover, 1989). Due to these nutrient and light adaptations, picoplankton may have a competitive edge over other phytoplankton size classes within the DCL. Prior to the mussel invasion, picoplankton less than 3 μm accounted for 40-50% of epilimnetic and DCL primary production during the mid-stratification period (Fahnenstiel and Carrick, 1992). Since the mussel invasion, the relative importance of picoplankton in the phytoplankton community has increased (Carrick et al., 2015), suggesting picoplankton production should still be large contributors to primary production and our results support this hypothesis. Picoplankton dominance in the DCL has implications for higher trophic levels because picoplankton are poorly ingested by zooplankton due to their small size (Lampert, 1987), suggesting dominance of picoplankton in the DCL is associated with inefficient energy transfer to higher trophic levels.

In September, one size-fractionated experiment was conducted below the thermocline when no DCL was present. Picoplankton were still the dominant contributor to the chlorophyll concentration, but the importance of microplankton in the chlorophyll concentration increased,

nanoplankton had the highest maximum photosynthetic rate, and microplankton were the most low-light acclimated. The decrease in picoplankton and increase in microplankton importance from summer to fall is consistent with findings of Fahnenstiel and Carrick (1992) in Lake Michigan before the mussel invasion and Scofield et al. (2017) in Lake Ontario after the mussel invasion. The seasonal shift in size-fractionated phytoplankton production observed in this study may indicate higher food quality for zooplankton in late summer during the periods of highest zooplankton abundance and biomass (Vanderploeg et al., 2012).

Drivers of daily areal production, P-I parameters, & growth rates

Variation in daily areal production throughout the season was mainly due to variation in P-I parameters (Figure 3.5a-b). In May, surface irradiance and underwater irradiance were high and had a positive impact on production, while P-I parameters and chlorophyll were below the mean likely due to the influence of low temperatures. P-I parameters and chlorophyll increased from May to August following the trend in temperature, and small peaks in P-I parameters, chlorophyll, and surface irradiance in June were related to a peak in areal production. P-I parameters were highest from August to October where they were associated with the highest daily areal production but low chlorophyll, possibly due to the influence of both zooplankton grazing and nutrient recycling. During stratification, underwater irradiance decreased while surface irradiance remained high. When phytoplankton were exposed to high irradiances and temperatures during stratification, production and biomass increased thus decreasing underwater irradiance, resulting in negative feedback. In October and November, P-I parameters, surface irradiance, temperature, and C:P decreased, while chlorophyll, underwater irradiance, and daily areal production increased

likely due to the upward mixing of hypolimnetic nutrients as stratification broke down (Cuhel and Aguilar, 2003).

Temperature was the only variable significantly related to areal production, epilimnetic P-I parameters, and epilimnetic growth rates (Table 3.5). α^B was not significantly related to any environmental parameters, and P_M^B was also positively related to k_{PAR}, reflecting negative feedback between production rates and water clarity. P_M^B, I_k, and growth rates are all known to be highly dependent on temperature (Rhee and Gotham, 1981; Talling, 1957). In this study, these parameters were all positively related to temperature, which may have been due to both the direct influence of temperature on enzymatic activity and possibly the indirect influence of temperature on nutrient dynamics through zooplankton-driven nutrient recycling. Since growth rates were positively related to temperature, and production was positively related to growth rates, the significant relationship between temperature and production appears to be due to temperature's relationship with growth rates.

Surprisingly, seston stoichiometry, which agrees with physiological methods for measuring nutrient deficiency (Hecky et al, 1993), was not significantly related to P-I parameters, production, or growth rates. The lack of significant relationships with seston stoichiometry may be partially due to the fact that seston is not entirely living phytoplankton cells, but also detritus. This study revealed epilimnetic communities were nearly always phosphorus deficient from May to November; therefore, insignificant relationships with seston stoichiometry may also be due to the fact that nutrients are always limiting, and seasonal dynamics may be more strongly controlled by other environmental factors. On the seasonal scale, it appeared that temperature was the most important factor controlling phytoplankton dynamics, but occasional reductions in nutrient limitation may regulate production on weekly scales.

Production comparisons

Our mean summer production estimate of 470 mg C m^{-2} day^{-1} at AW75 was similar to the mean 2010 to 2013 summer lake-wide production estimate of 499 mg C m^{-2} day^{-1} reported by Fahnenstiel et al. (2016). Fahnenstiel et al. (2016) estimated production using remote sensing, however, which cannot estimate the sub-epilimnetic production that has historically been a large component of total water column production in Lake Michigan (Fahnenstiel and Scavia, 1987b). This study illustrated that most production during stratification now occurs within the epilimnion (mean 60%) and only 7-25% occurs within the DCL when present, so remote sensing production estimates may not underestimate production as severely as previously expected. The summer production estimate reported by Fahnenstiel et al. (2016) was not corrected for DCL production, but their estimate was remarkably similar to our measured summer production estimate which included DCL production. Assuming total water column production was similar in both study periods, the vertical limitations of remote sensing may not have severe implications for the estimation of primary production in post-dreissenid Lake Michigan.

It has been well documented that phytoplankton production has declined in Lake Michigan since the quagga mussel invasion (Fahnenstiel et al., 2010, 2016; Warner and Lesht, 2015; Yousef et al., 2014). Our mean summer production estimate (470 mg C m^{-2} day^{-1}) was lower than average 1983 to 1987 mid-stratification production (867 mg C m^{-2} day^{-1}; Fahnenstiel et al., 2010), providing further evidence of declines in phytoplankton production in Lake Michigan since the mussel invasion. Our mean summer production estimate, however, was also lower than mean 2007 to 2008 mid-stratification production (677 mg C m^{-2} day^{-1}) reported by Fahnenstiel et al., (2010), which may be due to east-west differences in the sampling sites, differences in methodology (^{13}C vs. ^{14}C, two depths vs. 6-12 depths), or further decreases in production since 2007 and 2008.

The growth and photosynthetic capabilities of Lake Michigan phytoplankton appear to have not changed since the mussel invasion. Epilimnetic phytoplankton growth estimates determined from model ^{14}C experiments and phytoplankton carbon in 1983 and 1984 ranged from 0.42 to 0.65 day^{-1} (Fahnenstiel and Scavia, 1987b), and those from our study ranged from 0.29 to 0.75 day^{-1}. DCL growth rates from 1982 to 1984 reported in Fahnenstiel and Scavia (1987a) ranged from 0.02-0.29 day^{-1}, and our growth estimates from the DCM ranged from 0.04 to 0.20 day^{-1}. Our mean DCL phytoplankton C:Chl ratios were also similar to those reported in Fahnenstiel and Scavia (1987a), which were 20 and 17, respectively. Our mean epilimnetic C:Chl during the period of the DCL (46), however, was slightly higher than mean epilimnetic C:Chl from 1982 to 1984 (37; Fahnenstiel and Scavia, 1987a). Mean epilimnetic P_M^B in this study (1.7 mg C mg chl^{-1} hr^{-1}) was similar to offshore P_M^B in 1970 (1.8 mg C mg chl^{-1} hr^{-1} ; Fee, 1972) and 1983 to 1984 (2.1 mg C mg chl^{-1} hr^{-1}; Fahnenstiel and Scavia, 1987a). Further, our mean seasonal epilimnetic α^B (6.8 mg C mg chl^{-1} mol $photons^{-1}$ m^2) was not significantly different from mean seasonal epilimnetic α^B from 1983 to 1987 (7.0 mg C mg chl^{-1} mol $photons^{-1}$ m^2; Fahnenstiel et al., 1989; Welch two sample t-test, $p = 0.10$). Our mean seasonal epilimnetic P_M^B, however, was significantly lower than mean seasonal P_M^B from 1982 to 1984 (2.5 mg C mg chl^{-1} hr^{-1}; Fahnenstiel et al., 1989; Student two sample t-test, $p < 0.01$), but these differences could be due to interannual and spatial variability in P_M^B because our mean P_M^B similar to mean P_M^B from 1970 in southwestern Lake Michigan (Fee, 1972).

The lack of obvious changes in phytoplankton physiology and growth rates since the mussel invasion was somewhat unexpected because it suggests phytoplankton are no more phosphorus limited now than they have been in the past. This contradicts our expectations because declining offshore total phosphorus concentrations (Barbiero et al., 2018; Mida et al., 2010) should result in

increased phosphorus limitation in phytoplankton, which should decrease growth rates, P_M^B, and α^B. Pothoven and Fahnenstiel (2013) observed increases in surface mixed layer (SML) and 20-60 m C:P from 1995-2000 to 2007-2011 during early (June-July) and late summer (August-September) periods in southeastern Lake Michigan, but did not report on the significance of these increases. In our study, SML C:P during the period of the DCL averaged 232, while DCL C:P averaged 198. Pothoven and Fahnenstiel (2013) reported that early summer C:P was 225 in the SML and 185 in the mid-depth region in 1995-2000, and early summer C:P was 307 in the SML and 259 in the mid-depth region in 2007-2011. Our results in 2017 are closer to C:P prior to the mussel invasion, so our data contradicts Pothoven and Fahnenstiel (2013) and suggests Lake Michigan phytoplankton have not become increasingly phosphorus limited since the mussel invasion.

It was also somewhat unexpected that we did not observe increases in DCL production and growth rates with increasing water clarity since 2000 (Barbiero et al., 2018). Greater light availability may be expected to increase DCL growth rates and production by decreasing light limitation in the DCL (Barbiero et al., 2009; Fahnenstiel et al., 1984), but growth rates were similar and decreases in production were observed. C:Chl within the DCL also did not increase over time, and higher C:Chl may be expected with greater light availability, suggesting increased light penetration has not benefited the DCL community or the shift towards picoplankton with greater phosphorus uptake and light harvesting capabilities (Grover, 1989) has negated the effect of increasing water clarity. As DCL growth rates and light harvesting capabilities have not changed, decreases in DCL production appear to be mainly due to decreases in DCL biomass caused by mussels (Pothoven and Fahnenstiel, 2013).

Conclusions

Some temporal dynamics of phytoplankton production in Lake Michigan appear to have changed in the past several decades. DCL production has decreased and most production is now found within the epilimnion despite increases in water clarity, suggesting remote sensing may not actually underestimate a large component of total water column production. DCL production and growth rates are still greatest early in the season and decrease as the DCL moves deeper into the water column. Picoplankton are the dominant producers within the DCL, but their relative importance below the thermocline decreases into the fall. Due to the loss of spring and early summer production because of mussel grazing during isothermal mixing, production now peaks in August and September with the warmest temperatures. Temperature, rather than nutrient limitation, was the most important predictor of growth rates and production, suggesting nutrients are mostly important on shorter time scales rather than seasonal time scales. Decreased nutrient limitation during periods of known high zooplankton abundance and grazing suggests zooplankton-driven nutrient recycling may have contributed to high production and growth rates in August and September. Epilimnetic and DCL C:P, phytoplankton growth rates, and photosynthetic capabilities were similar before and after the mussel invasion, suggesting decreased phytoplankton production in Lake Michigan is mainly due to decreases in biomass rather than increases in nutrient limitation.

Chapter 4: Summary and Conclusions

This study revealed spatial and temporal variation of phytoplankton production in post-dreissenid Lake Michigan. Spatial patterns in spring phytoplankton production and growth varied between years and did not appear to be controlled by any single factor likely because nutrients, light, and temperature were all suboptimal. During the summer, phosphorus limitation was lowest, and phytoplankton production and growth estimates were highest in the northern basin, which may have bottom-up effects on fisheries production. Nearshore production was higher than offshore production on two of three sampling dates, but nearshore-offshore patterns were highly dependent on upwelling frequency. Overall, the spatial distribution of production in Lake Michigan is highly variable, suggesting studies using only one or two sampling sites from one region of the lake are severely limited in scope.

Some temporal dynamics of phytoplankton production appear to have changed since the mussel invasion. Due to the loss of spring and early summer production caused by mussels, production now peaks in August and September with the warmest temperatures. The reduction in nutrient limitation during the warmest temperatures and periods of known high zooplankton abundance suggests zooplankton-driven nutrient recycling may have been partially responsible for the late summer peak in production. Temperature was the only variable significantly related to maximum photosynthetic rates, growth rates, and areal production, suggesting phosphorus is so limiting in Lake Michigan that temperature now may have a greater effect on temporal dynamics than nutrients. Most production during the stratified period now occurs in the epilimnion and DCL production only accounted for an average 17.3% of total water column production, which is 12.7% lower than the 1980s (Fahnenstiel and Scavia, 1987a). Since most production now appears to occur

within the epilimnion, remote sensing of surface waters may not dramatically underestimate phytoplankton production.

During spring isothermal mixing and in nearshore regions when upwelling was not present, our results supported the mussels as "algal fertilizers" hypothesis (Zhang et al., 2011). Ecological modeling has suggested that nutrients released by dreissenids in a well-mixed water column, such as in shallow areas and during spring isothermal mixing, have a greater positive effect on phytoplankton growth than the negative effect of dreissenid grazing. Although spring phytoplankton production and biomass have decreased (Fahnenstiel et al., 2010), we found higher spring growth estimates in 2017 compared to the 1980s, which suggests that the phosphorus excreted by mussels may be an important new source of dissolved phosphorus for spring phytoplankton, although increased light penetration may also have increased spring growth rates (Fahnenstiel et al., 2000). Higher nearshore production in the absence of upwelling also provided support for the "algal fertilizers" hypothesis. The influence of dreissenid grazing is greatest closest to shore (Yousef et al., 2014), but the highest growth estimates were found nearshore in the absence of upwelling in this study, again suggesting the influence of phosphorus excreted by mussels may exceed the impact of mussel grazing. Therefore, during spring isothermal mixing and in nearshore regions, mussels may be more important "algal fertilizers" than algal grazers.

Offshore epilimnetic and DCL C:P has not increased, and epilimnetic and DCL growth estimates have not decreased since the mussel invasion despite decreases in offshore total phosphorus concentrations (Mida et al., 2010). Together, this suggests that phytoplankton in Lake Michigan are no more phosphorus limited now than they have been in the past, and the reduction in total water column and DCL production over time appears to be due to decreases in biomass caused by mussels rather than changes to phytoplankton physiology. Therefore, in offshore regions

during stratification, mussels appear to be more important algal grazers than "algal fertilizers," which appears to be the opposite of the role of mussels nearshore and during spring mixing. During stratification in offshore regions, mussels graze phytoplankton that sink into the hypolimnion, but the phosphorus recycled by mussels is trapped within the hypolimnion (Moseley and Bootsma, 2015) and not available for production higher in the euphotic zone. As the role of mussels as grazers versus nutrient recyclers appears to vary spatially and temporally, future studies should more directly investigate the role of mussels in controlling nutrient cycling in Lake Michigan.

While this study revealed some new spatial and temporal trends in phytoplankton production in Lake Michigan, it was limited in some respects and raised new questions regarding nutrient, phytoplankton, and zooplankton dynamics in Lake Michigan. Dissolved nutrients were not reported in this study, and future studies should relate dissolved phosphorus and nitrogen concentrations to temporal variation in production. The two depths used in this study for photosynthesis experiments were also likely not enough to characterize production throughout the entire water column, so future studies should consider using continuous profiling methods, such as fast repetition rate fluorometry (FRRF) which can estimate gross primary production, to measure phytoplankton production in Lake Michigan. Continuous surface transects with FRRF may also be an interesting way to gain higher spatial resolution of phytoplankton production than was gained in this study. As zooplankton are the trophic link between primary production and the upper food web, future studies should quantify zooplankton production and relate secondary production to primary production, as this can be used to determine the trophic efficiency of the lower food web of Lake Michigan and may provide insight into mechanisms behind decreased fisheries production in Lake Michigan.

REFERENCES

Akima, H., and Gebhardt, A., 2016. akima: Interpolation of irregularly and regularly spaced data. R package version 0.6-2. https://CRAN.R-project.org/package=akima

Auer, M.T., Tomlinson, L.M., Higgins, S.N., Malkin, S.Y., Howell, E.T., Bootsma, H.A., 2010. Great Lakes *Cladophora* in the 21st century: Same algae-different ecosystem. J. Great Lakes Res. 36, 248–255. doi:10.1016/j.jglr.2010.03.001

APHA, 1998. Standard Methods for the Examination of Water and Wastewater, 20th ed. American Public Health Association, Baltimore.

Adlerstein, S.A., Rutherford, E.S., Claramunt, R.M., Clapp, D.F., Clevenger, J.A., 2008. Seasonal movements of Chinook salmon in Lake Michigan based on tag recoveries from recreational fisheries and catch rates in gill-net assessments. Trans. Am. Fish. Soc. 137, 736–750. doi:10.1577/T07-122.1

Barbiero, R.P., Lesht, B.M., Warren, G.J., 2012. Convergence of trophic state and the lower food web in Lakes Huron, Michigan and Superior. J. Great Lakes Res. 38, 368–380. doi:10.1016/j.jglr.2012.03.009

Barbiero, R.P., Bunnell, D.B., Rockwell, D.C., Tuchman, M.L., 2009. Recent increases in the large glacial-relict calanoid Limnocalanus macrurus in Lake Michigan. J. Great Lakes Res. 35, 285–292.

Barbiero, R.P., Lesht, B.M., Warren, G.J., Rudstam, L.G., Watkins, J.M., Reavie, E.D., Kovalenko, K.E., Karatayev, A.Y., 2018. A comparative examination of recent changes in nutrients and lower food web structure in Lake Michigan and Lake Huron. J. Great Lakes Res. 44, 573-589. doi:10.1016/j.jglr.2018.05.012

Barbiero, R.P., Tuchman, M.L., Warren, G.J., Rockwell, D.C., 2002. Evidence of recovery from phosphorus enrichment in Lake Michigan. Can. J. Fish. Aquat. Sci. 59, 1639–1647. doi:10.1139/f02-132

Binding, C.E., Greenberg, T.A., Watson, S.B., Rastin, S., Gould, J., 2015. Long term water clarity changes in North America's Great Lakes from multi-sensor satellite observations. Limnol. Oceanogr. 60. doi:10.1002/lno.10146

Bukata, R.P., Jerome, J.H., and Bruton, J.E., 1988. Relationship among secchi disk depth, beam attenuation coefficient, and irradiance attenuation coefficient for Great Lakes waters. J. Great Lakes Res. 14, 347-355.

Bootsma, H.A., Rowe, M.D., Brooks, C.N., Vanderploeg, H.A., 2015. Commentary: The need for model development related to *Cladophora* and nutrient management in Lake Michigan. J. Great Lakes Res. 41, 7–15. doi:10.1016/j.jglr.2015.03.023

Bootsma, H.A., 2009. Causes, consequences, and management of nuisance *Cladophora*. Project GL-00E06901. Report submitted to the Environmental Protection Agency, Great Lakes National Program Office. Chicago, IL.

Bramburger, A.J., Reavie, E.D., 2016. A comparison of phytoplankton communities of the deep chlorophyll layers and epilimnia of the Laurentian Great Lakes. J. Great Lakes Res. 42, 1016-1025. doi:10.1016/j.jglr.2016.07.004

Bunnell, D.B., Barbiero, R.P., Ludsin, S.A., Madenjian, C.P., Warren, G.J., Dolan, D.M., Brenden, T.O., Briland, R., Gorman, O.T., He, J.X., Johengen, T.H., Lantry, B.F., Lesht, B.M., Nalepa, T.F., Riley, S.C., Riseng, C.M., Treska, T.J., Tsehaye, I., Walsh, M.G., Warner, D.M., Weidel, B.C., 2014. Changing ecosystem dynamics in the Laurentian Great Lakes: Bottom-up and top-down regulation. Biosci. 64, 26–39. doi:10.1093/biosci/bit001

Bunnell, D.B., HJ, C., Madenjian, C.P., Rutherford, E.S., Vanderploeg, H.A., Barbiero, R.P., Hinchey-Malloy, E., Pothoven, S.A., Riseng, C.M., Elgin, A.K., Bootsma, H.A., Turschak, B.A., Pangle, K.L., Claramunt, R.M., Czesny, S.J., 2018. Are changes in lower trophic levels limiting prey-fish biomass and production in Lake Michigan? Report submitted to the Great Lakes Fisheries Commission, Ann Arbor, MI.

Butler, E.I., Corner, E.D.S, and Marshall, S. M., 1969. On the nutrition and metabolism of zooplankton. VI. Feeding efficiency of *Calanus* in terms of nitrogen and phosphorus. J. Mar. Biol. Assoc. U.K. 49, 977-1003.

Cai, M., Reavie, E.D., 2018. Pelagic zonation of water quality and phytoplankton in the Great Lakes. Limnology 19, 127–140. doi:10.1007/s10201-017-0526-y

Carrick, H., Barbiero, R., Tuchman, M., 2001. Variation in Lake Michigan plankton: Temporal, spatial, and historical trends. J. Great Lakes Res. 27, 467–485.

Carrick, H.J., Butts, E., Daniels, D., Fehringer, M., Frazier, C., Fahnenstiel, G.L., Pothoven, S., Vanderploeg, H.A., 2015. Variation in the abundance of pico, nano, and microplankton in Lake Michigan: Historic and basin-wide comparisons. J. Great Lakes Res. 41, 66–74. doi:10.1016/j.jglr.2015.09.009

Chapra, S.C., Dolan, D.M., 2012. Great Lakes total phosphorus revisited: 2. Mass balance modeling. J. Great Lakes Res. 38, 741–754. doi:10.1016/j.jglr.2012.10.002

Clark, R.D., Bence, J.R., Claramunt, R.M., Johnson, J.E., Gonder, D., Legler, N.D., Robillard, S.R., Dickinson, B.D., 2016. A spatially explicit assessment of changes in chinook salmon fisheries in Lakes Michigan and Huron from 1986 to 2011. North Am. J. Fish. Manag. 36, 1068–1083. doi:10.1080/02755947.2016.1185060

Corner, E., and Newel, B., 1967. On the nutrition and metabolism of zooplankton. IV. Forms of nitrogen excreted by Calanus. J. Mar. Biol. Assoc. U.K. 47, 113-120.

Crowder, L.B., McDonald, M.E., Rice, J.A., 1987. Understanding recruitment of Lake Michigan fishes: The importance of size-based interactions between fish and zooplankton. Can. J. Fish. Aquat. Sci. 44, 141–147. doi:10.1139/f87-317

Cuhel, R.L., Aguilar, C. 2014. Deeper, deeper, deeper: Functional deep chlorophyll maxima below 50 m in oligotrophicated Lake Michigan. Ocean Sciences Meeting, Honolulu, Hawaii.

Cuhel, R.L., Aguilar, C., 2013. Ecosystem transformations of the Laurentian Great Lake Michigan by nonindigenous biological invaders. Annu. Rev. Mar. Sci 5, 289–320. doi:10.1146/annurev-marine-120710-100952

Cuhel, R.L., Aguilar, C., 2003. Coastal intensive site network (CISNet): Environmental monitoring of the coastal waters of southwestern Lake Michigan. NOAA Final Report, Award NA87OA0519.

Dolan, D.M., Chapra, S.C., 2012. Great Lakes total phosphorus revisited: 1. Loading analysis and update (1994-2008). J. Great Lakes Res. 38, 730–740. doi:10.1016/j.jglr.2012.10.001

Driscoll, Z.G., Bootsma, H.A., Christiansen, E., 2015. Zooplankton trophic structure in Lake Michigan as revealed by stable carbon and nitrogen isotopes. J. Great Lakes Res. 41, 104–114. doi:10.1016/j.jglr.2015.04.012

Eadie, B.J., Schwab, D.J., Johengen, T.H., Lavrentyev, P.J., Miller, G.S., Holland, R.E., Leshkevich, G.A., Lansing, M.B., Morehead, N.R., Robbins, J.A., Hawley, N., Edgington, D.N., Van Hoof, P.L., 2002. Particle transport, nutrient cycling, and algal community structure associated with a major winter-spring sediment resuspension event in southern Lake Michigan. J. Gt. Lakes Res. 28, 324–337.

Eadie, B., Chambers, R., Gardner, W., Bell, G., 1984. Sediment trap studies in Lake Michigan: Resuspension and chemical fluxes in the southern basin. J. Great Lakes Res. 10, 307–231.

Edwards, K.F., Thomas, M.K., Klausmeier, C.A., Litchman, E., 2015. Light and growth in marine phytoplankton: Allometric, taxonomic, and environmental variation. Limnol. Oceanogr. 60, 540–552. doi:10.1002/lno.10033

Elser, J.J., Urabe, J., 1999. The stoichiometry of consumer-driven recycling: theory, observations, and consequences. Ecology 80, 735–751.

Engevold, P.M., Young, E.B., Sandgren, C.D., Berges, J.A., 2015. Pressure from top and bottom: Lower food web responses to changes in nutrient cycling and invasive species in western Lake Michigan. J. Great Lakes Res. 41, 86–94. doi:10.1016/j.jglr.2015.04.015

Erga, S., Skjoldal, H., 1990. Diel variations in photosynthetic activity of summer phytoplankton in Lindaspollene, western Norway. Mar. Ecol. Prog. Ser. 65, 73–85. doi:10.3354/meps065073

Fahnenstiel, G.L., Scavia, D., and Schelske, C.L. 1984. Nutrient-light interactions in the Lake Michigan subsurface chlorophyll layer. Verh. Internat. Verein. Limnol. 22, 440-444.

Fahnenstiel, G., Pothoven, S., Vanderploeg, H., Klarer, D., Nalepa, T., Scavia, D., 2010. Recent changes in primary production and phytoplankton in the offshore region of southeastern Lake Michigan. J. Great Lakes Res. 36, 20–29. doi:10.1016/j.jglr.2010.03.009

Fahnenstiel, G., Scavia, D., 1987a. Dynamics of Lake Michigan phytoplankton: Primary production and growth. Can. J. Fish. Aquat. Sci. 44, 499-508. doi:10.1139/f87-062

Fahnenstiel, G., Scavia, D., 1987b. Dynamics of Lake Michigan phytoplankton: The deep chlorophyll layer. J. Great Lakes Res. 13, 285–295.

Fahnenstiel, G.L., Carrick, H.J., 1992. Phototrophic picoplankton in Lakes Huron and Michigan: Abundance, distribution, composition, and contribution to biomass and production. Can. J. Fish. Aquat. Sci. 49, 379–388. doi:10.1139/f92-043

Fahnenstiel, G.L., Carrick, H.J., 1988. Primary production in Lakes Huron and Michigan: *In vitro* and *in situ* comparisons. J. Plankton Res. 10, 1273–1283. doi:10.1093/plankt/10.6.1273

Fahnenstiel, G.L., Chandler, J.F., Carrick, H.J., Scavia, D., 1989. Photosynthetic characteristics of phytoplankton communities in Lakes Huron and Michigan: P-I parameters and end-products. J. Great Lakes Res. 15, 394–407. doi:10.1016/S0380-1330(89)71495-7

Fahnenstiel, G.L., Sayers, M.J., Shuchman, R.A., Yousef, F., Pothoven, S.A., 2016. Lake-wide phytoplankton production and abundance in the Upper Great Lakes: 2010-2013. J. Great Lakes Res. 42, 619–629. doi:10.1016/j.jglr.2016.02.004

Fahnenstiel, G.L., Scavia, D., 1987. Dynamics of Lake Michigan phytoplankton: Recent changes in surface and deep communities. Can. J. Fish. Aquat. Sci. 44, 509–514. doi:10.1139/f87-063

Fahnenstiel, G.L., Stone, R.A., McCormick, M.J., Schelske, C.L., Lohrenz, S.E., 2000. Spring isothermal mixing in the Great Lakes: evidence of nutrient limitation and nutrient-light interactions in a suboptimal light environment. Can. J. Fish. Aquat. Sci. 57, 1901–1910. doi:10.1139/f00-144

Fee, E., 1972. A numerical model for the estimation of integral primary production and its application to Lake Michigan. PhD. Thesis, University of Wisconsin-Milwaukee. 194 p.

Fee, E., 1973a. A numerical model for determining integral primary production and its application to Lake Michigan. J. Fish. Res. Board Canada 30, 1447–1468.

Fee, E., 1973b. Modeling primary production in water bodies: an approach that allows for vertical inhomogeneities. J. Fish. Res. Board Canada 30, 1469-1473.

Fee, E., 1975. The importance of diurnal variation of photosynthesis vs. light curves to estimates of integral primary production. Verh. Int. Verein. Theo. Angew. Limnol. 19, 39-46.

Fee, E.J., 1990. Computer programs for calculating in situ phytoplankton photosynthesis. Can. Tech. Report Fish. Aquat. Sci. 1740, 1–27.

Gay, D.M., 1990. Usage summary for selected optimization routines. Comput. Sci. Tech. Rep. 153, 1–21.

Geider, R.J., Osborne, B.A., 1992. Algal photosynthesis: The measurement of algal gas exchange. Chapman and Hall, New York.

Geider, R.J., MacIntyre, H.L., and Kana, T.M., 1997. Dynamic model of phytoplankton growth and acclimation: Responses of the balanced growth rate and chlorophyll a : carbon ratio to light, nutrient-limitation, and temperature. Mar. Ecol. Prog. Series. 148, 187-200.

Grover, J.P., 1989. Influence of cell shape and size on algal competitive ability. J. Phycol. 25, 402–405.

Gulati, R., DeMott, W., 1997. The role of food quality for zooplankton: remarks on the state-of-the-art, perspectives and priorities. Freshw. Biol. 38, 753–768. doi:10.1046/j.1365-2427.1997.00275.x

Hama, T., Miyazaki, T., Ogawa, Y., Iwakuma, T., Takahashi, M., Otsuki, A., Ichimura, S., 1983. Measurement of photosynthetic production of a marine phytoplankton population using a stable ^{13}C isotope. Mar. Biol. 73, 31–36.

Hamidi, S.A., Bravo, H.R., Klump, J. V., Beletsky, D., Schwab, D.J., 2012. Hydrodynamic model for Green Bay, Lake Michigan. World Environ. Water Resour. Congr. 1438–1446. doi:10.1061/9780784412312.144

Harding, L.W., Fisher, T.R., Tyler, M.A., 1987. Adaptive responses of photosynthesis in phytoplankton: Specificity to time-scale of change in light. Bio. Ocean. 4, 403–437.

Harding, LW., Meeson, BW, Prezelin, BB., and BM Sweeney. 1981. Diel periodicity of photosynthesis in marine phytoplankton. Mar. Biol. 61, 95-105.

Harding, LW., Prezelin, BB, Sweeney, BM, JL Cox. 1982a. Diel oscillations of the photosynthesis-irradiance relationship in natural assemblages of phytoplankton. Mar. Biol. 67, 167-178.

Harding, LW., Prezelin, BB, Sweeney, BM, JL Cox. 1982b. Primary production as influenced by diel periodicity of phytoplankton photosynthesis. Mar. Biol. 67, 179-186.

Healy, F.P., and Hendzel., L.L., 1980. Physiological indicators of nutrient deficiency in lake phytoplankton. Can. J. Fish. Aquat. Sci. 37, 442-453.

Hecky, R.E., Smith, R.E.H., Barton, D.R., Guildford, S.J., Taylor, W.D., Charlton, M.N., Howell, T., 2004. The nearshore phosphorus shunt: a consequence of ecosystem engineering by dreissenids in the Laurentian Great Lakes. Can. J. Fish. Aquat. Sci 61, 1285–1293. doi:10.1139/F04-065

Hecky, R.E., Campbell, P., and Hendzel, L.L. 1993. The stoichiometry of carbon, nitrogen, and phosphorus in particulate matter of lakes and oceans. Limnol. Oceanogr. 38, 709-724.

Hessen, D.O., Andersen, T., Brettum, P., Faafeng, B.A., 2003. Phytoplankton contribution to sestonic mass and elemental ratios in lakes: Implications for zooplankton nutrition. Limnol. Oceanogr. 48, 1289–1296. doi:10.4319/lo.2003.48.3.1289

Jawed, M., 1969. Body nitrogen and nitrogenous excretion in *Neomysis rayii* Murdoch and *Euphausia pacifica* Hansen. Limnol. Oceanogr. 14, 748-754.

Kana, T.M., Watts, J.L., Glibert, P.M., 1985. Diel periodicity in the photosynthetic capacity of coastal and offshore phytoplankton assemblages. Mar. Ecol. Prog. Ser. 25, 131–139. doi:10.3354/meps025131

Kerfoot, W.C., Budd, J.W., Green, S.A., Cotner, J.B., Bopaiah, A., Schwab, D.J., Vanderploeg, H.A., Budd, W., 2008. Doughnut in the desert: Lake Michigan pulse in southern production Doughnut. Limnol. Oceanogr. 53, 589–604. doi:10.4319/lo.2008.53.2.0589

Kerfoot, W.C., Yousef, F., Green, S.A., Budd, J.W., Schwab, D.J., Vanderploeg, H.A., 2010. Approaching storm: Disappearing winter bloom in Lake Michigan. J. Great Lakes Res. 36, 30–41. doi:10.1016/j.jglr.2010.04.010

Klerks, P.L., Fraleigh, P.C., Lawniczak, J.E., 1996. Effects of zebra mussel (*Dreissena polymorpha*) on seston levels and sediment deposition in western Lake Erie. Can. J. Fish. Aquat. Sci. 53, 2284–2291. doi:10.1139/cjfas-53-10-2284

Klump, J.V., Brunner, S.L., Grunert, B.K., Kaster, J.L., Weckerly, K., Houghton, E.M., Kennedy, J.A., Valenta, T.J., In press. Evidence of persistent, recurring summertime hypoxia in Green Bay, Lake Michigan. J. Great Lakes Res. doi:10.1016/j.jglr.2018.07.012

Klump, J.V., Fitzgerald, S.A., Waples, J.T., 2009. Benthic biogeochemical cycling, nutrient stoichiometry, and carbon and nitrogen mass balances in a eutrophic freshwater bay. Limnol. Oceanogr. 54, 692–712. doi:10.4319/lo.2009.54.3.0692

Korstad, J., 1983. Nutrient regeneration by zooplankton in southern Lake Huron. J. Great Lakes Res. 9, 374-388.

Kult, J.M., Fry, L.M., Gronewold, A.D., Choi, W., 2014. Regionalization of hydrologic response in the Great Lakes basin: Considerations of temporal scales of analysis. J. Hydrol. 519, 2224–2237. doi:10.1016/j.jhydrol.2014.09.083

Lampert, W., 1987. Laboratory studies on zooplankton□cyanobacteria interactions Laboratory studies on zooplankton-cyanobacteria interactions. New Zeal. J. Mar. Freshw. Res. 213, 483–490. doi:10.1080/00288330.1987.9516244

Lang, G.A., Fahnenstiel, G.L., 1996. Great Lakes Primary Production Model - Methodology and Use. NOAA Technical Memorandum.

Lee, Z., Marra, J., Perry, M.J., Kahru, M., 2015. Estimating oceanic primary productivity from ocean color remote sensing: A strategic assessment. J. Mar. Syst. 149, 50–59. doi:10.1016/j.jmarsys.2014.11.015

Legendre, L.L., Demers, S., Garside, C., Haugen, E.M., Phinney, D.A., Shapiro, L.P., Therriault, J.C., and Yentsch, C.M., 1988. Circadian photosynthetic activity of natural marine phytoplankton isolated in a tank. J. Plank. Res., 10, 1-6.

Lin, P., Guo, L., 2016. Dynamic changes in the abundance and chemical speciation of dissolved and particulate phosphorus across the river-lake interface in southwest Lake Michigan. Limnol. Oceanogr. 61, 771–789. doi:10.1002/lno.10254

Lohrenz, S.E., Fahnenstiel, G.L., Millie, D.F., Schofield, O.M.E., Johengen, T., and Bergmann, T., 2004. Spring phytoplankton photoysnthesis, growth, and primary productoin and relationships to a recurrent coastal sediment plume and river inputs in southeastern Lake Michigan. J. Geo. Phys. Res. 109, 1-13.

Madenjian, C.P., Bunnell, D.B., Warner, D.M., Pothoven, S.A., Fahnenstiel, G.L., Nalepa, T.F., Vanderploeg, H.A., Tsehaye, I., Claramunt, R.M., Clark, R.D., 2015. Changes in the Lake Michigan food web following dreissenid mussel invasions: A synthesis. J. Great Lakes Res. 41, 217–231. doi:10.1016/j.jglr.2015.08.009

Malkin, S.Y., Guildford, S.J., Hecky, R.E., 2008. Modeling the growth response of *Cladophora* in a Laurentian Great Lake to the exotic invader *Dreissena* and to lake warming. Limnol. Oceanogr. 53, 1111–1124. doi:10.2307/40058223

Marko, K.M., Rutherford, E.S., Eadie, B.J., Johengen, T.H., Lansing, M.B., 2013. Delivery of nutrients and seston from the Muskegon River Watershed to near shore Lake Michigan. J. Great Lakes Res. 39, 672–681. doi:10.1016/j.jglr.2013.08.002

Marra, J., 2009. Net and gross productivity: Weighing in with ^{14}C. Aquat. Microb. Ecol. 56, 123–131. doi:10.3354/ame01306

Marra, J., Heinemann, K., Landriau, G., 1985. Observed and predicted measurements of photosynthesis in a phytoplankton culture exposed to natural irradiance. Mar. Ecol. Prog. Ser. 24, 43–50. doi:10.3354/meps024043

Menge, B.A., 2000. Top-down and bottom-up community regulation in marine rocky intertidal habitats. J. Exp. Mar. Bio. Ecol. 250, 257–289. doi:10.1016/S0022-0981(00)00200-8

Muller, P., Li, X.-P., Niyogi, K., 2001. Non-photochemical quenching. A Response to excess light energy. Plant Physiol. 125, 1558–1566. doi:10.1104/pp.125.4.1558

Millero, F. J., 2007. The marine inorganic carbon cycle. Chem. Rev. 107, 308-341.

Moll, R.A., Brahce, M.Z., Peterson, T.P., 1984. Phytoplankton dynamics within the subsurface chlorophyll maximum of Lake Michigan. J. Plankton Res. 6, 751–766.

Mosley, C., Bootsma, H., 2015. Phosphorus recycling by profunda quagga mussels (*Dreissena rostriformis bugensis*) in Lake Michigan. J. Great Lakes Res. 41, 38–48. doi:10.1016/j.jglr.2015.07.007

Nalepa, T.F., Fanslow, D.L., Lang, G.A., Mabrey, K., Rowe, M., 2014. Lake-wide benthic surveys in Lake Michigan in 1994-95, 2000, 2005, and 2010: Abundances of the amphipod *Diporeia spp*. and abundances and biomass of the mussels *Dreissena polymorpha* and *Dreissena rostriformis bugensis*. NOAA Technical Memorandum GLERL.

Nalepa, T.F., Schloesser, D.W., 2014. Quagga and Zebra Mussels. CRC Press: Boca Raton, FL.

Pauer, J.J., Anstead, A.M., Melendez, W., Taunt, K.W., Kreis, R.G., 2011. Revisiting the Great Lakes Water Quality Agreement phosphorus targets and predicting the trophic status of Lake Michigan. J. Great Lakes Res. 37, 26–32. doi:10.1016/j.jglr.2010.11.020

Petersen, B., 1980. Aquatic primary productivity and the ^{14}C-CO_2 method : A history of the productivity problem. Annu. Rev. Ecol. Syst. 11, 359–385.

Platt, T., 1975. Analysis of the importance of spatial and temporal heterogeneity in the estimation of annual production by phytoplankton in a small, enriched marine basin. J. Exp. Mar. Biol. Ecol. 18, 99-109.

Platt, T., Gallegos, C., Harrison, W., 1980. Photoinhibition of photosynthesis in natural assemblages of marine phytoplankton. J. Mar. Res. 38, 687–701.

Platt, T., Jassby, A.D., 1976. The relationship between photosynthesis and light for natural assemblages of coastal marine phytoplankton. J. Phycol. 12, 421–430.

Plattner, S., Mason, D.M., Leshkevich, G.A., Schwab, D.J., Rutherford, E.S., 2006. Classifying and forecasting coastal upwellings in Lake Michigan using satellite derived temperature images and buoy data. J. Great Lakes Res. 32, 63–76. doi:10.3394/0380-1330(2006)32[63:CAFCUI]2.0.CO;2

Pothoven, S.A., Fahnenstiel, G.L., 2015. Spatial and temporal trends in zooplankton assemblages along a nearshore to offshore transect in southeastern Lake Michigan from 2007 to 2012. J. Great Lakes Res. 41, 95–103. doi:10.1016/j.jglr.2014.09.015

Pothoven, S.A., Fahnenstiel, G.L., 2013. Recent change in summer chlorophyll *a* dynamics of southeastern Lake Michigan. J. Great Lakes Res. 39, 287–294. doi:10.1016/j.jglr.2013.02.005

Rao, Y., Schwab, D., 2007. Transport and mixing between the coastal and offshore waters in the Great Lakes: A review. J. Great Lakes Res. 33, 202–218. doi:10.3394/0380-1330(2007)33

R Core Team, 2018. R: A language and environment for statistical computing. R Foundation for Statistical Computing, Vienna, Austria. https://www.R-project.org/

Reavie, E.D., Barbiero, R.P., Allinger, L.E., Warren, G.J., 2014. Phytoplankton trends in the Great Lakes, 2001-2011. J. Great Lakes Res. 40, 618–639. doi:10.1016/j.jglr.2014.04.013

Reinke, P., Luning, K., Harding, L.W., Prezelin, B.B., Sweeney, B.M., 1981. Diel oscillations in the photosynthesis-irradiance relationship of a planktonic marine diatom. J. Phycol. 17, 389–394.

Rhee, G.Y., Gotham, I.J., 1981. The effect of environmental factors on phytoplankton growth: light and the interactions of light with nitrate limitation. Limnol. Oceanogr. 26: 649–659.

Rhee, G.Y. 1982. Effects of environmental factors and their interaction on phytoplankton growth. In Advances in Microbial Ecology. Vol. 6. Edited by K.C. Marshall. Plenum Publishing Corp., New York. pp. 33–74.

Rigler, F.H., 1973. A dynamic view of the phosphorus cycle in lakes. pg 539-572. In E.J. Griffiths, A. Beeton, J.M. Spencer, and D.T. Mitchell (ed) Environmental Phosphorus Handbook. Wiley, New York, N.Y.

Rowe, M., Obenour, D., Nalepa, T., Vanderploeg, H.A., Yousef, F., Kerfoot, W., 2015. Mapping the spatial distribution of the biomass and filter-feeding effect of invasive dreissenid mussels on the winter-spring phytoplankton bloom in Lake Michigan. Freshw. Biol. 60, 2270–2285.

Rowe, M.D., Anderson, E.J., Vanderploeg, H.A., Pothoven, S.A., Elgin, A.K., Wang, J., Yousef, F., 2017. Influence of invasive quagga mussels, phosphorus loads, and climate on spatial and temporal patterns of productivity in Lake Michigan: A biophysical modeling study. Limnol. Oceanogr. 62, 2629–2649. doi:10.1002/lno.10595

Rowe, M.D., Anderson, E.J., Wang, J., Vanderploeg, H.A., 2015. Modeling the effect of invasive quagga mussels on the spring phytoplankton bloom in Lake Michigan. J. Great Lakes Res. 41, 49–65. doi:10.1016/j.jglr.2014.12.018

Scavia, D. 1979. Examination of phosphorus cycling and control of phytoplankton dynamics in Lake Ontario with an ecological model. J. Fish. Res. Board Can. 36: 1336-1346.

Scavia, D., Fahnenstiel, G.L., 1987. Dynamics of Lake Michigan phytoplankton: Mechanisms controlling epilimnetic communities. J. Great Lakes Res. 13, 103–120.

Scavia, D., Lang, G., Kitchell, J., 1988. Dynamics of Lake Michigan plankton: A model evaluation of nutrient loading, competition, and predation. Can. J. Fish Aquat. Sci. 45, 165–177.

Schelske, C.L., Callender, E., 1970. Survey of phytoplankton productivity and nutrients in Lake Michigan and Lake Superior. Proc. 13th Conf. Great Lakes Res. Int. Assoc. Great Lakes Res., pp 93-105.

Schelske, C.L., Stoermer, E.F., 1971. Eutrophication, silica depletion, and predicted changes in algal quality in Lake Michigan. Science. 173, 423–424. doi:10.1126/science.173.3995.423

Scofield, A.E., Watkins, J.M., Weidel, B.C., Luckey, F.J., Rudstam, L.G., 2017. The deep chlorophyll layer in Lake Ontario: extent, mechanisms of formation, and abiotic predictors. J. Great Lakes Res. 43, 782–794. doi:10.1016/j.jglr.2017.04.003

Senft, W.H., 1978. Dependence of light-saturated rates of algal photosynthesis on intracellular concentrations of phosphorus. Limnol. Oceanogr. 23, 709–718. doi:10.4319/lo.1978.23.4.0709

Shuchman, R.A., Sayers, M., Fahnenstiel, G.L., Leshkevich, G., 2013. A model for determining satellite-derived primary productivity estimates for Lake Michigan. J. Great Lakes Res. 39. doi:10.1016/j.jglr.2013.05.001

Silsbe, G.M. Malkin, S.Y., 2015. phytotools: Phytoplankton production tools. R package version 1.0.https://CRAN.R-project.org/package=phytotools

Stainton, M.P., Capel, M.J., Armstrong, F.A.J., 1977. The chemical analysis of freshwater. Fish. Environ. Canada Misc. Spec. Publ. 25, pp. 166.

Steemann Nielsen, E., 1952. The use of radioactive carbon for measuring organic production in the sea. J. Cons. Int. Explor. Mer. 18, 117–140.

Sterner, R.W., Elser, J.J., Fee, E.J., Guildford, S.J., Chrzanowski, T.H., 1997. The light:nutrient ratio in lakes: The balance of energy and materials affects ecosystem structure and Process. Am. Nat. 150, 663–684. doi:10.1086/286088

Sterner, R.W., Hessen, D.O., 1994. Algal nutrient limitation and the nutrition of aquatic herbivores. Annu. Rev. Ecol. Syst 25, 1–29.

Sterner, R., and J. Elser. 2002. Ecological Stoichiometry: The biology of elements from molecules to the biosphere. Princeton University Press.

Stockwell, J.D., Johannsson, O.E., 1997. Temperature-dependent allometric models to estimate zooplankton production in temperate freshwater lakes. Can. J. Fish. Aquat. Sci. 55, 2187. doi:10.1139/f97-141e

Talling, J.F., 1957. Photosynthetic characteristics of some freshwater plankton diatoms in relation to underwater radiation. New Phytol. 56, 29–50. doi:10.1111/j.1469-8137.1957.tb07447.x

Vanderploeg, H.A., Liebig, J.R., Carmichael, W.W., Agy, M.A., Johengen, T.H., Fahnenstiel, G.L., Nalepa, T.F., 2001. Zebra mussel (*Dreissena polymorpha*) selective filtration promoted toxic *Microcystis* blooms in Saginaw Bay (Lake Huron) and Lake Erie. Can. J. Fish. Aquat. Sci. 58, 1208–1221. doi:10.1139/cjfas-58-6-1208

Vanderploeg, H.A., Liebig, J.R., Nalepa, T.F., Fahnenstiel, G.L., Pothoven, S.A., 2010. *Dreissena* and the disappearance of the spring phytoplankton bloom in Lake Michigan. J. Great Lakes Res. 36, 50–59.

Vanderploeg, H.A., Pothoven, S.A., Fahnenstiel, G.L., Cavaletto, J.F., Liebig, J.R., Stow, C.A., Nalepa, T.F., Madenjian, C.P., Bunnell, D.B., 2012. Seasonal zooplankton dynamics in Lake Michigan: Disentangling impacts of resource limitation, ecosystem engineering, and predation during a critical ecosystem transition. J. Great Lakes Res. 38, 336–352. doi:10.1016/j.jglr.2012.02.005

Vanderploeg, H.A., Pothoven, S.A., Krueger, D., Mason, D.M., Liebig, J.R., Cavaletto, J.F., Ruberg, S.A., Lang, G.A., Ptáčníková, R., 2015. Spatial and predatory interactions of visually preying nonindigenous zooplankton and fish in Lake Michigan during midsummer. J. Great Lakes Res. 41, 125–142. doi:10.1016/j.jglr.2015.10.005

Ware, D., Thomson, R., 2005. Bottom-up ecosystem trophic dynamics determine fish production in the northeast Pacific. Science 308, 1280–1284. doi:10.1126/science.1109049

Warner, D.M., Lesht, B.M., 2015. Relative importance of phosphorus, invasive mussels and climate for patterns in chlorophyll a and primary production in Lakes Michigan and Huron. Freshw. Biol. 60, 1029–1043. doi:10.1111/fwb.12569

Warren, G.J., Lesht, B.M., Barbiero, R.P., 2017. Estimation of the width of the nearshore zone in Lake Michigan using eleven years of MODIS satellite imagery. J. Great Lakes Res. doi:10.1016/j.jglr.2017.11.011

Webb, W.L., Newton, M., Starr, D., 1974. Carbon dioxide exchange of *Alnus rubra*. A mathematical model. Oecologia 17, 281–291.

Wetzel, R., 2001. Limnology: Lake and river ecosystems, Third. ed. Academic Press, San Diego.

Wilkinson, G.M., Cole, J.J., Pace, M.L., Johnson, R.A., Kleinhans, M.J., 2015. Physical and biological contributions to metalimnetic oxygen maxima in lakes. Limnol. Oceanogr. 60, 242–251. doi:10.1002/lno.10022

Williams, P.J.L.B., Lefèvre, D., 2008. An assessment of the measurement of phytoplankton respiration rates from dark ^{14}C incubations. Limnol. Oceanogr. Methods 6, 1–11.

Withers, J.L., Sesterhenn, T.M., Foley, C.J., Troy, C.D., Höök, T.O., 2015. Diets and growth potential of early stage larval yellow perch and alewife in a nearshore region of southeastern Lake Michigan. J. Great Lakes Res. 41, 197–209. doi:10.1016/j.jglr.2015.08.003

Yousef, F., Kerfoot, W.C., Shuchman, R., Fahnenstiel, G., 2014. Bio-optical properties and primary production of Lake Michigan: Insights from 13-years of SeaWiFS imagery. J. Great Lakes Res. 40, 317–324. doi:10.1016/j.jglr.2014.02.018

Yousef, F., Shuchman, R., Sayers, M., Fahnenstiel, G., Henareh, A., 2017. Water clarity of the upper Great Lakes: Tracking changes between 1998–2012. J. Great Lakes Res. 43, 239–247. doi:10.1016/j.jglr.2016.12.002

Yurista, P.M., Kelly, J.R., Cotter, A.M., Miller, S.E., Van Alstine, J.D., 2015. Lake Michigan: Nearshore variability and a nearshore-offshore distinction in water quality. J. Great Lakes Res. 41, 111–122. doi:10.1016/j.jglr.2014.12.010

Zhang, H., Culver, D.A., Boegman, L., 2011. Dreissenids in Lake Erie: An algal filter or a fertilizer? Aquat. Invasions 6, 175–194. doi:10.3391/ai.2011.6.2.07

APPENDIX A: Photosynthesis-irradiance curve parameters

Table 1. Spring 2016 Lake Guardian survey photosynthetic parameters (± SE). Italics indicate manual parameter calculation because model fitting error was significant.

Site	Depth	Time	P_M^B	P_S^B	α^B	β^B	I_k	I_b
MI17	2	11:56	*0.88*	-	*3.07*	-	*0.28*	-
	50		0.93	1.00 ± 0.04	6.23 ± 0.77	0.08 ± 0.02	0.15	12.4
MI23	2	05:22	0.96	-	11.8 ± 0.84	-	0.08 ± 0.01	-
	51		1.39	1.54 ± 0.05	14.6 ± 1.85	0.29 ± 0.04	0.10	4.88
MI34	2	12:21	1.05	-	8.03 ± 1.89	-	0.13 ± 0.03	-
	78		1.51	-	9.84 ± 0.79	-	0.15 ± 0.01	-
MI47	2	14:52	1.24	-	9.84 ± 0.97	-	0.13 ± 0.01	-
	35		1.49	-	5.36 ± 2.45	-	0.28 ± 0.14	-
MI-N	2	20:33	1.41	-	8.90 ± 1.11	-	0.16 ± 0.02	-
	19		2.06	-	12.1 ± 0.92	-	0.17 ± 0.01	-

Table 2. Spring 2017 Lake Guardian survey 2 and 35 m integrated photosynthetic parameters (± SE). Incubator irradiance too low to simulate photoinhibition in these experiments.

Site	Time	P_M^B	α^B	I_k
MI11	19:39	0.65	8.36 ± 0.98	0.08 ± 0.01
MI23	05:53	0.77	4.87 ± 0.50	0.16 ± 0.02
MI34	13:05	1.42	1.69 ± 0.26	0.84 ± 0.24
MI41	02:30	1.41	2.09 ± 0.92	0.68 ± 0.44
GB1	19:48	1.16	1.41 ± 0.11	0.82 ± 0.13
MI52	03:00	0.72	3.95 ± 0.73	0.18 ± 0.05

Table 3. Summer 2017 Lake Guardian survey photosynthetic parameters (± SE). Bold indicates insignificant β parameter, but visible photoinhibition in the P-I curve. Italics indicate manual parameter calculation because model fitting error was significant.

Site	Depth	Time	P_M^B	P_S^B	α^B	β^B	I_k	I_b
MI11	5	17:55	0.99	**1.46 ± 0.39**	2.38 ± 0.35	**0.29 ± 0.20**	0.42	**3.37**
	37		0.53	0.63 ± 0.03	6.25 ± 0.42	0.28 ± 0.03	0.08	1.89
MI23	5	13:38	1.89	-	3.09 ± 0.37	-	0.61 ± 0.10	-
	39		0.73	0.98 ± 0.15	5.35 ± 0.73	0.45 ± 0.15	0.14	1.60
MI34	5	19:12	1.07	1.25 ± 0.09	3.09 ± 0.30	0.11 ± 0.05	0.35	9.51
	46		0.53	0.63 ± 0.06	7.64 ± 1.04	0.31 ± 0.07	0.07	1.74
MI41	5	08:07	1.06	1.27 ± 0.15	3.32 ± 0.35	0.15 ± 0.08	0.32	7.23
	34		0.50	**0.58 ± 0.10**	6.97 ± 2.00	**0.22 ± 0.10**	0.07	**2.32**
GB1	5	01:03	1.07	1.34 ± 0.10	3.81 ± 0.41	0.22 ± 0.06	0.28	4.78
MI52	5	10:55	1.26	1.44 ± 0.10	3.70 ± 0.40	0.11 ± 0.05	0.34	11.6
	15		1.37	1.52 ± 0.07	4.10 ± 0.20	0.09 ± 0.03	0.33	15.5

Table 4. 75 m depth northern basin site photosynthetic parameters (± SE). Bold indicates insignificant β parameter, but visible photoinhibition in the P-I curve.

Date	Depth	P_M^B	P_S^B	α^B	β^B	I_k	I_b
DC75							
01 Jun	5	0.35	-	3.42 ± 0.11	-	0.10 ± 0.10	-
	35	0.56	0.63 ± 0.04	7.77 ± 1.27	0.18 ± 0.04	0.07	3.12
30 Jun	5	0.93	1.00 ± 0.08	6.60 ± 0.96	0.08 ± 0.04	0.14	11.2
	21	0.39	0.41 ± 0.03	12.6 ± 4.38	0.09 ± 0.03	0.03	4.43
08 Aug	8	1.46	1.79 ± 0.12	4.33 ± 0.31	0.22 ± 0.06	0.34	6.74
	19	0.94	1.13 ± 0.18	6.50 ± 1.13	0.30 ± 0.13	0.14	3.15
MT75							
13 Jun	5	0.94	-	4.84 ± 0.76	-	0.19 ± 0.03	-
	32	0.56	**0.59 ± 0.05**	5.65 ± 1.50	**0.05 ± 0.03**	0.10	**10.8**
18 Jul	5	1.11	1.27 ± 0.10	2.89 ± 0.21	0.09 ± 0.04	0.38	12.5
	22	0.87	**0.97 ± 0.09**	3.26 ± 0.52	**0.08 ± 0.04**	0.27	**11.3**
05 Oct	5	1.87	-	8.11 ± 0.78	-	0.23 ± 0.03	-
	16	2.46	-	13.9 ± 3.92	-	0.18 ± 0.06	-

Table 5. Nearshore-offshore transect photosynthetic parameters (± SE). Bold indicates insignificant β parameter, but visible photoinhibition in the P-I curve. Italics indicate manual parameter calculation because model fitting error was significant.

Site	Depth	P_M^B	P_S^B	α^B	β^B	I_k	I_b
Jul 11							
KB15	5	2.73	-	8.79 ± 0.51	-	0.31± 0.02	-
KB45	5	1.47	-	4.41 ± 0.65	-	0.33 ± 0.06	-
	22	0.43	**0.48 ± 0.08**	4.12 ± 1.75	**0.09 ± 0.06**	0.11	**4.62**
KB75	5	1.19	-	5.35 ± 0.76	-	0.22 ± 0.03	-
	30	0.40	0.44 ± 0.02	6.70 ± 1.05	0.12 ± 0.02	0.06	3.32
12 Sep							
KB15	5	6.57	-	12.1 ± 0.63	-	0.55 ± 0.04	-
KB45	5	2.11	2.50 ± 0.20	4.67 ± 0.34	0.18 ± 0.08	0.45	11.5
	36	1.84	2.16 ± 0.33	19.1 ± 6.28	0.71 ± 0.34	0.10	6.28
KB75	5	*1.75*	-	*10.7*	-	*0.16*	-
	38	1.39	1.63 ± 0.16	16.1 ± 3.28	0.62 ± 0.18	0.09	2.23
09 Oct							
KB15	6	2.96	-	19.04 ± 4.76	-	0.16 ± 0.04	-
KB45	5	2.12	-	5.13 ± 1.23	-	0.41 ± 0.11	-
	17	1.95	2.10 ± 0.11	13.0 ± 1.83	0.18 ± 0.07	0.15	10.7
KB75	5	3.84	-	14.6 ± 3.38	-	0.26 ± 0.07	-
	10	2.82	-	13.1 ± 1.79	-	0.22 ± 0.03	-

Table 6. AW75 seasonal photosynthetic parameters (± SE). Bold indicates insignificant β parameter, but visible photoinhibition visible in the P-I curve. Italics indicate manual parameter calculation because model fitting error was significant.

Date	Depth	P_M^B	P_S^B	α^B	β^B	I_k	I_b
11 May	5	0.45	-	1.89 ± 0.57	-	0.24	-
	35	0.87	-	5.29 ± 1.24	-	0.16	-
26 May	5	0.85	-	5.64 ± 0.63	-	0.15 ± 0.02	-
	35	0.88	0.90 ± 0.02	5.69 ± 0.16	0.02 ± 0.01	0.16	50.2
08 June	5	1.25	-	5.86 ± 0.59	-	0.21± 0.02	-
	26	0.66	0.72 ± 0.05	7.73 ± 1.54	0.15 ± 0.04	0.09	4.36
23 June	5	1.96	-	6.74 ± 0.80	-	0.29 ± 0.04	-
	27*	0.33	0.41	3.93	0.23	0.08	1.40
11 July	5	1.19	-	5.35 ± 0.76	-	0.22 ± 0.03	-
	30	0.40	0.44 ± 0.02	6.70 ± 1.05	0.12 ± 0.02	0.06	3.32
25 July	5	1.57	-	4.45 ± 0.32	-	0.35 ± 0.03	-
	40*	0.67	0.85	10.2	0.64	0.05	0.75
16 Aug	5	1.47	-	3.23 ± 0.32	-	0.46 ± 0.05	-
	25	0.88	1.07 ± 0.10	5.25 ± 0.61	0.24 ± 0.07	0.17	3.66
29 Aug	5	3.13	-	8.85 ± 0.50	-	0.35 ± 0.02	-
	22	1.91	2.55 ± 0.21	12.3 ± 1.57	1.00 ± 0.21	0.16	1.92
12 Sep	5	*1.75*	-	*10.7*	-	*0.16*	-
	38	1.39	1.63 ± 0.16	16.1 ± 3.28	0.62 ± 0.18	0.09	2.23
25 Sep	5	2.63	-	7.14 ± 0.90	-	0.37 ± 0.05	-
	28*	0.74	0.95	7.84	0.53	0.09	1.37
09 Oct	5	3.84	-	14.6 ± 3.38	-	0.26 ± 0.07	-
	10	2.82	-	13.1 ± 1.79	-	0.22 ± 0.03	-
23 Oct	5	1.62	**1.99 ± 0.27**	7.21 ± 1.44	**0.36 ± 0.19**	0.23	**4.49**
	16	2.70	3.27 ± 0.24	22.5 ± 3.03	1.08 ± 0.24	0.12	2.50
13 Nov	5	0.75	0.81 ± 0.06	6.11 ± 1.47	0.09 ± 0.04	0.12	8.19
	25	0.95	1.03 ± 0.04	8.93 ± 0.98	0.16 ± 0.03	0.11	6.06

APPENDIX B: Nutrient Parameters

Table 1. Nutrient parameters reported in this study. No data indicates sample processing error.

Experiment	Chl. ($mg\ m^{-3}$)	Temp. (ºC)	DIC ($\mu mol\ L^{-1}$)	Seston C:N	Seston C:P	Seston N:P	Phyto. C:Chl	$\delta^{13}C$
MI17_3_26_2016_2M	0.52	3.25	2182.7	16.2	267.1	16.5	102.4	-27.5
MI17_3_26_2016_50M	0.48	3.21	2181.4		157.1		49.0	-24.6
MI23_3_27_2016_2M	0.79	3.42	2197.2	10.5	137.6	13.1	32.1	-26.7
MI23_3_27_2016_51M	0.57	3.42	2194.0	17.0	187.4	11.0	47.9	-28.0
MI34_3_27_2016_2M	0.62	3.50	2192.4	11.9	107.8	9.0	35.8	-26.2
MI34_3_27_2016_78M	0.56	3.49	2198.6	13.5	125.5	9.3	45.6	-26.5
MI47_3_28_2016_2M	0.59	3.47	2193.9					
MI47_3_28_2016_35M	0.55	3.42	2194.0					
MINOR_3_28_2016_2M	0.44	2.19	2115.1	11.7	83.3	7.1	53.3	-26.3
MINOR_3_28_2016_19M	0.40	2.21	2188.3	8.4	147.0	17.5	77.3	-27.7
MI11_3_26_17_2M	1.03	3.73	2183.3	11.2	117.3	10.5	24.3	-28.9
MI23_3_27_17_2M	1.03	2.95	2186.0	8.5	192.3	22.6	26.5	-29.3
MI34_3_27_17_2M	0.72	2.88	2186.1	8.8	126.4	14.4	30.1	-28.6
MI41_3_28_17_2M	0.72	3.50	2189.4	7.2	123.7	17.2	39.0	-28.0
GB1_3_28_17_2M	0.60	1.58	2192.8	10.7	205.6	19.2	40.0	-29.9
MI52_3_29_17_2M	0.72	1.47	2193.1	11.1	172.7	15.6	31.2	-28.4
KB75_5_11_17_5M	0.77	4.71	2159.1					
KB75_5_11_17_35M	0.77	4.11	2160.0	19.3	201.4	10.4	39.0	-29.1
KB75_5_26_17_5M	0.82	6.43	2153.5	6.1	193.3	31.8	36.1	-32.4
KB75_5_26_17_35M	0.84	6.22	2154.7	11.3	134.9	12.0	28.1	-29.8
DC75_6_1_17_5M	0.67	8.67	2144.7	7.4	162.7	21.9	59.5	-32.1
DC75_6_1_17_35M	1.03	4.42	2152.5	14.4	188.3	13.1	26.8	-31.3

Experiment	Chl. (mg m^{-3})	Temp. (ºC)	DIC (µmol L^{-1})	Seston C:N	Seston C:P	Seston N:P	Phyto. C:Chl	$\delta^{13}C$
KB75_6_8_17_5M	0.72	9.79	2143.4	8.1	196.3	24.2	60.6	-29.5
KB75_6_8_17_26M	1.83	6.70	2146.4	13.3	153.9	11.6	20.5	-29.9
MT75_6_13_17_5M	1.15	9.76	2163.6	8.0	139.4	17.4	36.6	-29.4
MT75_6_13_17_32M	1.37	8.07	2165.6	10.5	137.9	13.1	28.5	-33.2
KB75_6_23_17_5M	1.05	16.0	2112.5	7.3	223.2	30.7	61.3	-27.9
KB75_6_23_17_27M	2.74	6.03	2138.9	8.3	183.9	22.1	19.2	-30.3
DC75_6_30_17_5M	1.60	10.1	2143.1	9.3	268.4	29.0	52.3	-29.8
DC75_6_30_17_21M	1.60	4.50	2149.6	9.7	172.6	17.8	30.4	-30.7
KB15_7_11_17_5M	4.01	10.5	2104.7	11.1	229.8	20.8	38.3	-25.6
KB45_7_11_17_5M	1.37	15.7	2112.3	8.5	121.2	14.2	39.6	-25.1
KB45_7_11_17_22M	2.86	6.19	2141.0	9.1	171.6	18.9	21.7	-31.3
KB75_7_11_17_5M	0.91	18.4	2105.1	13.0	224.0	17.2	42.4	-27.7
KB75_7_11_17_30M	2.74	5.60	2141.6	7.9	201.8	25.5	19.0	-30.8
MT75_7_18_17_5M	1.20	18.1	2128.3	11.4	263.2	23.0	54.4	-31.8
MT75_7_18_17_22M	2.70	12.4	2134.7	7.7	112.9	14.7	33.3	-29.3
KB75_7_25_17_5M	1.15	19.9	2093.6	10.5	247.3	23.5	35.6	-29.2
KB75_7_25_17_40M	3.20	5.47	2139.6	8.5	209.4	24.7	21.9	-30.8
MI11_8_2_17_5M	1.10	23.4	2129.0	9.8	212.3	21.8	45.8	-26.9
MI11_8_2_17_37M	1.53	5.36	2180.7	15.9	176.2	11.1	36.9	-28.9
MI23_8_3_17_MEP	1.05	21.9	2120.6	9.6	273.9	28.4	48.9	-26.2
MI23_8_3_17_39M	1.40	5.01	2181.3	18.0	220.1	12.2	41.4	-29.8
MI34_8_5_17_5M	1.37	19.2	2122.3	9.6	274.7	28.6	43.3	-26.9
MI34_8_5_17_46M	2.28	4.76	2177.7	17.0	175.1	10.3	22.9	-29.9
MI41_8_6_17_MEP	1.94	19.0	2121.2	9.2	222.2	24.1	29.0	-27.7
MI41_8_6_17_34M	3.66	5.36	2165.6	6.6	182.0	27.6	26.5	-29.0
DC75_8_6_17_MEP	1.67	18.8	2121.5	10.1	240.7	23.8	33.9	-27.8
DC75_8_6_17_19M	1.58	10.6	2159.1	10.7	229.1	21.5	42.1	-28.1
GB1_8_7_17_5M	2.17	19.1	2121.1	10.6	181.2	17.2	26.9	-27.2

Experiment	Chl. (mg m^{-3})	Temp. (ºC)	DIC (µmol L^{-1})	Seston C:N	Seston C:P	Seston N:P	Phyto. C:Chl	$\delta^{13}C$
MI52_8_7_17_5M	2.06	18.8	2121.4	10.1	209.0	20.6	30.2	-26.8
MI52_8_7_17_15M	2.01	18.8	2150.5	8.7	257.7	29.5	31.4	-26.7
KB75_8_16_17_5M	2.06	21.3	2056.1	8.4	199.6	23.7	29.8	-26.1
KB75_8_16_17_25M	1.83	7.70	2082.4	9.8	168.7	17.3	37.2	-28.9
KB75_8_29_17_5M	1.07	20.1	2074.6	8.5	166.1	19.6	47.7	-26.7
KB75_8_29_17_22M	1.17	8.62	2103.2	8.5	167.3	19.7	67.2	-28.2
KB15_9_12_17_5M	2.28	18.3	2082.1	9.0	116.4	13.0	34.1	-25.4
KB45_9_12_17_5M	2.28	18.6	2057.5	10.5	193.5	18.4	29.6	-27.2
KB45_9_12_17_36M	0.62	6.47	2132.0	29.7	153.2	5.2	67.9	-27.2
KB75_9_12_17_5M	1.60	18.9	2046.6	8.4	192.9	22.9	39.8	-28.6
KB75_9_12_17_38M	0.94	5.91	2126.5	10.9	150.0	13.7	41.7	-27.6
KB75_9_25_17_5M	1.14	21.6	2038.0	9.9	292.1	29.6	67.7	-26.7
KB75_9_25_17_28M	0.77	5.82	2105.7	10.0	133.0	13.3	50.5	-28.4
MT75_10_5_17_5M	1.11	17.9	2123.7	9.0	273.7	30.4	68.4	-27.6
MT75_10_5_17_16M	0.85	17.8	2123.7	9.1	259.1	28.5	86.3	-28.0
KB15_10_9_17_6M	0.38	7.08	2138.9		94.5		95.4	-27.5
KB45_10_9_17_5M	0.92	9.93	2111.5	9.3	150.0	16.2	68.8	-28.5
KB45_10_9_17_17M	0.68	7.01	2136.0	7.6	133.6	17.7	82.6	-29.0
KB75_10_9_17_5M	0.89	14.8	2089.2	7.4	215.4	29.1	78.8	-27.4
KB75_10_9_17_10M	1.00	14.3	2092.2	9.5	202.9	21.3	69.5	-28.1
KB75_10_23_17_5M	1.48	12.0	2102.7	8.6	186.5	21.8	52.9	
KB75_10_23_17_16M	0.87	10.6	2105.8	8.6	167.1	19.4	95.1	-26.3
KB75_11_13_17_5M	1.94	6.09	2153.7	14.9			25.4	-29.0
KB75_11_13_17_25M	0.55	5.33	2149.5	11.6	214.7	18.6	27.3	-28.0